



Konrad Moser, BSc

2D Numerical Simulations of Dam Failure

MASTERARBEIT

zur Erlangung des akademischen Grades

Diplom-Ingenieur

Masterstudium Bauingenieurwissenschaften - Geotechnik und Wasserbau

eingereicht an der

Technischen Universität Graz

Betreuer

Univ.-Prof. Dipl.-Ing. Dr.techn. Gerald Zenz

Institut für Wasserbau und Wasserwirtschaft

Zweitbetreuer

Dipl. Ing. Clemens Dorfmann

EIDESSTATTLICHE ERKLÄRUNG

AFFIDAVIT

Ich erkläre an Eides statt, dass ich die vorliegende Arbeit selbstständig verfasst, andere als die angegebenen Quellen/Hilfsmittel nicht benutzt, und die den benutzten Quellen wörtlich und inhaltlich entnommenen Stellen als solche kenntlich gemacht habe. Das in TUGRAZonline hochgeladene Textdokument ist mit der vorliegenden Masterarbeit identisch.

I declare that I have authored this thesis independently, that I have not used other than the declared sources/resources, and that I have explicitly indicated all material which has been quoted either literally or by content from the sources used. The text document uploaded to TUGRAZonline is identical to the present master's thesis.

Datum / Date

Unterschrift / Signature

Abstract

For various functions, dams are built for the retention of water. During the design, the construction and the operation of a dam, usually much attention is paid to the security of the dam.

Nevertheless, cases in history show, that dam breaks e.g. caused by overtopping can lead to danger for humans and enormous damages.

Hence, knowledge and investigation in means of the type of the dam break as well as the flood wave propagation are necessary, in order to be able to evacuate affected areas in such exceptional cases.

In this work, two cases regarding the erosional breaching process and one case concerning the water propagation are numerically analysed.

In the first case, a laboratory test case, in which the failure of homogenous, sandy dams are modeled, is simulated numerically with a 2D free surface flow computation with Telemac-2D in coupled mode with the sediment-transport module Sisyphe. The results then are compared to the measured data from the laboratory. The sediment transport is implemented with the approach of Meyer-Peter and Müller. In a sensitivity analysis, the effects of the different parameters are tested.

In the second case, the findings of the first case are applied in a real case of a water storage for snow production. In the same method, the breaching process of the dam is simulated with Finite Elements and Finite Volumes. As results, the outflow hydrographs of the different simulations are compared with the hydrograph of the breach program Deich.

The flood wave propagation of the same storage is simulated in the third case. Two different scenarios are treated, one is causing a secondary dam break of another reservoir. The results from the FE- and FV simulations are compared with a computation done with the 2D-numerical program Basement.

Kurzfassung

Dammbauwerke werden für unterschiedliche Aufgaben für das Rückhalten von Wasser gebaut. Hierbei wird gewöhnlich sowohl in der Planung, in der Ausführung und im Betrieb größter Wert auf Sicherheit gelegt.

Im Lauf der Geschichte haben aber Fälle gezeigt, dass in Ausnahmesituationen durch Überströmen verursachte Dammversagen zu Gefahren für Menschen und zu erheblichen Sachschäden führen können.

Also sind Wissen und Forschung bezüglich der Art und der Zeitdauer eines Dammbruches nötig, um in solchen Ausnahmefällen über Verbindungsmechanismen entsprechende Flutwellenwarnungen ausgeben zu können.

In dieser Arbeit werden zwei Fälle von erosivem Dammversagen sowie ein Fall der Flutwellenausbreitung numerisch untersucht.

Im ersten Fall wird ein bereits vorhandener Laborversuch, in welchem das Versagen eines Homogendammes aus sandigem Material modelliert wird, numerisch mit einer 2D Oberflächen- Abflussberechnung mit dem Programm Telemac-2D in gekoppeltem Modus mit dem Sediment-Transportmodul Sisyphe simuliert.

Die Ergebnisse werden dann mit den Messdaten aus dem Laborversuch verglichen. Der Sedimenttransport ist mit dem Ansatz von Meyer-Peter-Müller implementiert. In einer Sensitivitätsanalyse werden die Effekte der unterschiedlichen Parameter gegenüber gestellt.

Im zweiten Fall werden die Erkenntnisse aus dem ersten Fall an einem Damm eines Beschneigungsteiches angewandt. Auf dieselbe Weise wird der Vorgang der Breschenbildung mit Finiten Elementen und Finiten Volumen simuliert. Als Ergebnis werden die Ausfluss- Hydrographen der verschiedenen Simulationen mit dem Hydrographen des Breschenmodells Deich verglichen.

Zusätzlich wird die Flutwellenausbreitung desselben Reservoirs im dritten Fall simuliert. Zwei verschiedene Szenarien werden dabei behandelt, bei einem davon entsteht ein Sekundärdammbruch eines unterhalb gelegenen Speichers. Die Ergebnisse der FE- und FV Simulationen werden mit denen des 2D-numerischen Programmes Basement verglichen.

Acknowledgement

I would like to express my gratitude as shown in Table 1.

Table 1: *Acknowledgement*

	General Support	Guidance through Project	Supervision	Motivation	Understanding	Diversion to maintain personal balance
Prof. Dr.tech. DI Zenz	x	x	x	x	x	
DI Dorfmann	x	x	x	x	x	
Johanna	x			x	x	x
Mother and all my family	x				x	x
Friends	x				x	x

This thesis is dedicated to You, the interested reader.

Contents

Abstract	i
Kurzfassung	ii
Acknowledgement	iii
Nomenclatur	vii
1 Introduction - Topic and Target of this Work	2
2 Thematic Basics	4
2.1 Analysis of Earth Dam Failures	4
2.2 Modelling with Telemac-2D and Sisyphe	8
2.2.1 Theory of 2D-Modelling	8
2.2.2 Telemac-2D	12
2.2.3 Sisyphe	13
2.2.4 The Modification of the Meyer-Peter-Müller Formula by Wiberg and Smith	13
2.2.5 Talmon's Approach for the Transverse Deviation Effect	15
3 The Modelling of a Laboratory Test Case	18
3.1 Presentation of Case 1 - Experiment Done by Coleman et al.	18
3.2 The Numerical Model in Telemac-2D and Sisyphe	20
3.2.1 The Mesh	20
3.2.2 The Boundary Conditions	21
3.2.3 The Steering Files and the Fortran-Subroutine	22

3.3	Sensitivity Analysis for the Hydrodynamic Modelling	25
3.3.1	Default Hydrodynamic Parameters	25
3.3.2	Overview of the Hydrodynamic Sensitivity Analysis	29
3.3.3	Variation of the Roughness	29
3.3.4	Variation of Roughness on Lateral Boundaries	30
3.3.5	Variation of the Turbulence Models	30
3.3.6	Variation of the Type of Advection for Velocities	30
3.3.7	Variation: Finite Volume Method	32
3.4	Sedimentary Modelling	35
3.4.1	Default Sedimentary Parameters	35
3.4.2	Overview of the Sedimentary Sensitivity Analysis	35
3.4.3	Variation of the Friction Angle (Sim. B, C)	36
3.4.4	Formulas for Slope Effect and Deviation (Sim. D, E, F)	38
3.4.5	Sediment Slide (Sim. G)	39
3.4.6	Porosity (Sim. I)	40
3.4.7	Modified Meyer-Peter-Müller Formula (Sim. H)	41
3.4.8	Talmon's β -Value (Sim. J)	43
3.4.9	Finite Volume Method	44
3.4.10	Results for All Time Steps	48
3.4.11	Cross Section of the Dam and Discharge	52
3.5	Discussion of the Results	54
3.5.1	Hydrodynamic Factors	54
3.5.2	Sedimentary Factors	54
3.5.3	Cross Sections and Discharge	54
3.6	Computation time	55
4	Simulation of the Breaching Process of the Dam of a Snowmaking Reservoir	56
4.1	Introduction to the Snowmaking-Reservoir	56
4.2	The Calculation of the Dam Break Hydrograph	58
4.2.1	The Numerical Model	58

4.2.2	Calculation	59
4.2.3	Results	60
4.3	Discussion of the Results	64
4.4	Computation time	65
5	Simulation of a Flood Wave Propagation	66
5.1	The Numerical Model	69
5.1.1	Boundary Conditions and the Mesh	69
5.2	Scenario A	72
5.2.1	Results from Scenario A - Water Depths	72
5.2.2	Results from Scenario A - Stream Power	74
5.3	Scenario B	76
5.3.1	Results from Scenario B - Water Depths	77
5.3.2	Results from Scenario B - Stream Power	79
5.3.3	Results from Scenario B - Flood Wave Evolution	79
5.4	Discussion of the Results	81
5.5	Computation Times	81
6	Summary	83
7	Outlook	85
	Bibliography	i
	List of Figures	iii
	List of Tables	vi
	Appendix	vii
7.1	Laboratory Test Case Steering Files	vii
7.1.1	<i>Telemac-2D CAS-file for Sim. M</i>	vii
7.1.2	<i>Sisyphé CAS-file for Sim. M</i>	x
7.2	Flood Wave Propagation Steering Files	xii

7.2.1	<i>Telemac-2D CAS-file for FE, Scenario A</i>	xii
7.3	Excerpt from the Fortran Subroutines Defining the Modification of thend the Implementation of Van Rijn's Approach for Transverse De- viation	xiv

Nomenclature

d_k	Characteristic grain diameter
d_{50}	Grain diameter at 50% passage
g	Gravity
h	Water depth
k_{st}	Strickler's roughness
q	Discharge in x
$q_{b,k*}$	Transport capacity for sediments
r	Discharge in y
u	Velocity in x
v	Velocity in y
z_b	Bottom elevation
γ_s	Specific weight of the sediment
γ_w	Specific weight of water
Θ	Shields parameter
Θ_c	Critical Shields parameter
μ	Correction factor of the grain shear stress
ρ_s	Density of the sediment
ρ_w	Density of water
σ_g	Standard deviation of the grain distribution
τ_0, τ_b	Bottom shear stress
φ	Friction angle

1 Introduction - Topic and Target of this Work

Throughout history, humans have been trying to control their environment and have been using the available conditions for different applications. The element water is specially characterized as origin of all life on earth on one hand and as versatile element for generation of electricity and storage of water on the other hand. For both purposes, often dams are required to create reservoirs for storing the water. As great the advantages of dams and thereby of storing water are, are the connected risks in case of shortages of control.

Generally, at a dam project, it is tried to reach a maximum of security. During the process of the construction of a new dam, throughout all periods, the dam safety is of essential interest. In the design of a dam, usually conservative approaches are applied and safety installing like membranes or bottom outlets are used in the planning. During the construction, an on-site supervision is controlling the quality and the correct fulfillment of the project and for the monitoring in the operation time, various equipment is installed in order to guarantee a safe use of the dam.

Still, there always remains a small residual risk in every case.

As further described in chapter 2, the failure of earth fill dams can lead to enormous floods and thus endanger human life. As [Lammerer](#) has shown, most danger in connection with dam breaks comes from small earth dams with less control. The most important causes for earth dam failure are overtopping and quality problems like piping. The importance of the knowledge of what happens in case of a dam failure consequently is important for people living downstream of a dam, for local governments as they have the responsibility for their citizens as well as for operators of dams.

The possibilities of how to find out, how a dam may break and how a flood wave might find its way downstream, were limited in the past. Laboratory test cases usually are very expensive in means of time and costs and for larger areas are hardly feasible. Usual approaches of calculating water depths on single cross sections soon find their limits in more complex problems.

In the last decades, a new method was developed on how these problems could be solved. The numerical two-dimensional simulation of water flows with the method of Finite Elements gives the possibility to compute discharges over larger areas and

thereby provides the important information on where, how much and how fast water is flowing in case of flooding, caused by dam failure or other reasons. However, the accuracy of these methods is still not definitely proved, as a numerical simulation will always stay an approximation to reality, but it will never be able to completely reproduce all influences and characteristics of reality. That is the reason for the first case of the present work. By trying to reproduce the results measured in a laboratory test case of a dam failure caused by overtopping, it will be tried, how close the numerical solution can get to the measurement data. Thereby, many different factors of the numerical model will be changed and the according effect will be documented.

In the second part, these findings will be applied in a real case at a water storage made for the production of artificial snow in a skiing area. The assumed dam is made of uniform sand and without any membrane. Moreover, no bottom outlet and no inflow into the dam is modelled.

Usually, the discharge curves for such dam breaks are made with semi-empiric approaches which have rather limited possibilities in picturing the breaking-process of a dam. In the present work, it will be tried to simulate this process by using a – also semi-empiric – sediment transport formula integrated into the 2D simulation. The outflow hydrograph then will be compared with a hydrograph generated with a different program by the Austrian engineering office “Ingenieurbüro Moser GmbH Co Kg”.

In the third and final part, the free-surface flow of a dam break will be simulated for two different scenarios.

All these simulations are done with the open source program Telemac-2D and the appropriate module for sediment transport Sisyphe. Nowadays, most of the engineering offices use proprietary software for their calculations of free surface flows. One aim of this work is to prove, that open source software packages as Telemac-2D are able to generate excellent solutions. Due to the open-source character of Telemac-2D it allows a very high flexibility, e.g. the implementation of new/different approaches in subroutines is possible.

Open Source software in general is characterized by its free available source code, hence everybody is able to get very detailed information on how the program works or even is able to program own sequences and participate in the development of the program. For example, during this work, a modification of the sediment transport formula of Meyer-Peter-Müller was implemented in Sisyphe, that would not have been possible with a proprietary software. Another advantage is the cost-free disposability of the program.

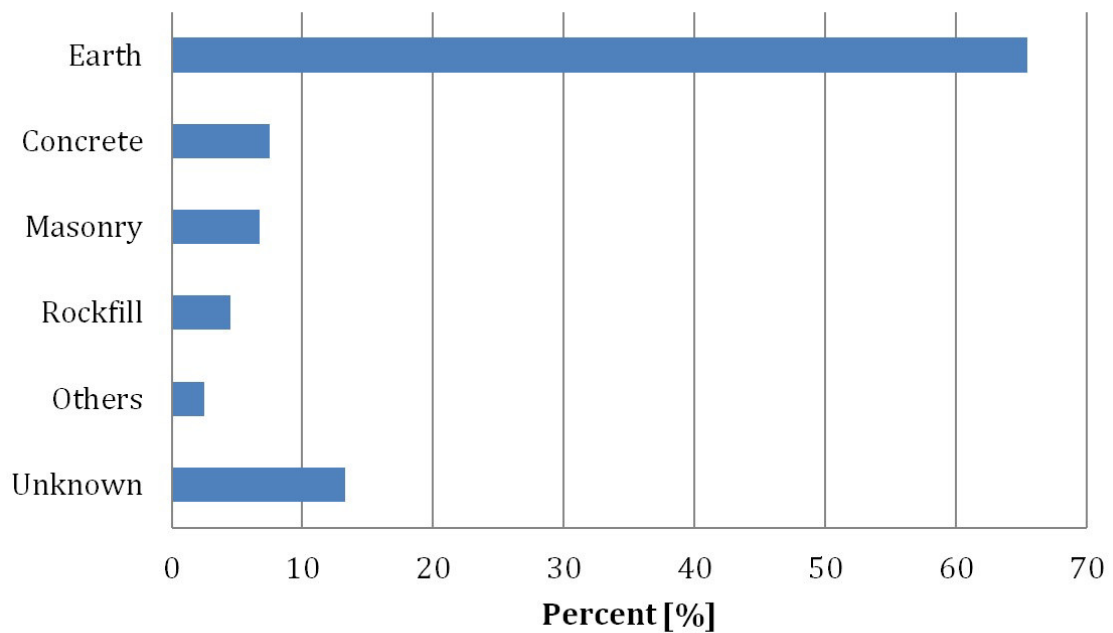
The idea for the topic of this thesis was developed at the 12th international benchmark workshop on numerical analysis of dams by the International Commission on Large Dams (ICOLD) in October 2013 in Graz. One topic of this workshop was the simulation of the dam break as well as the estimation of the consequences of a hypothetical dam.

2 Thematic Basics

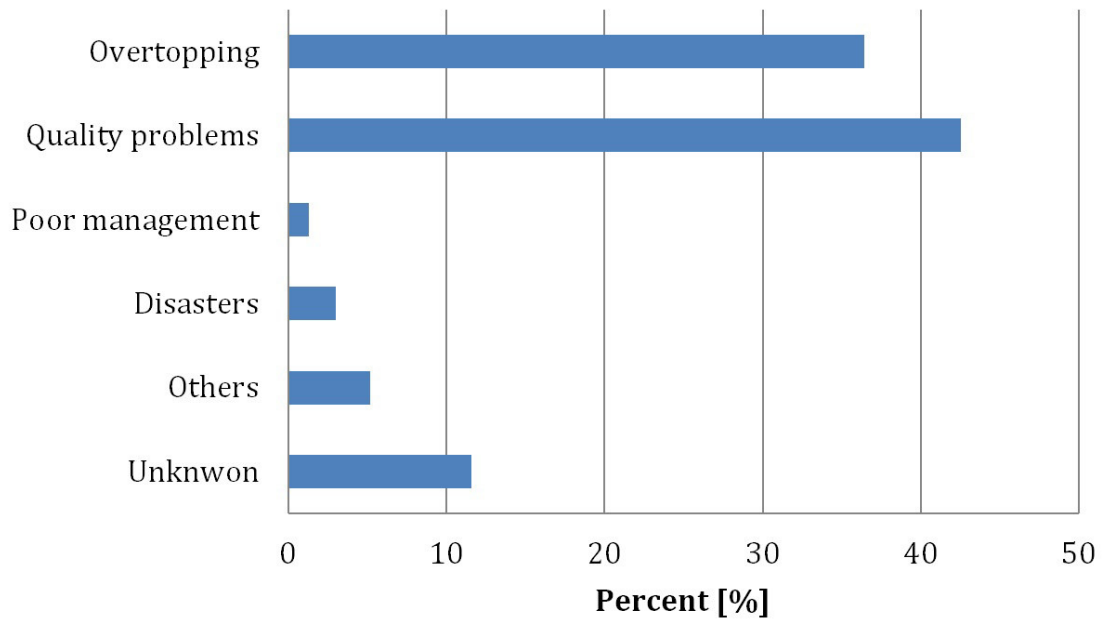
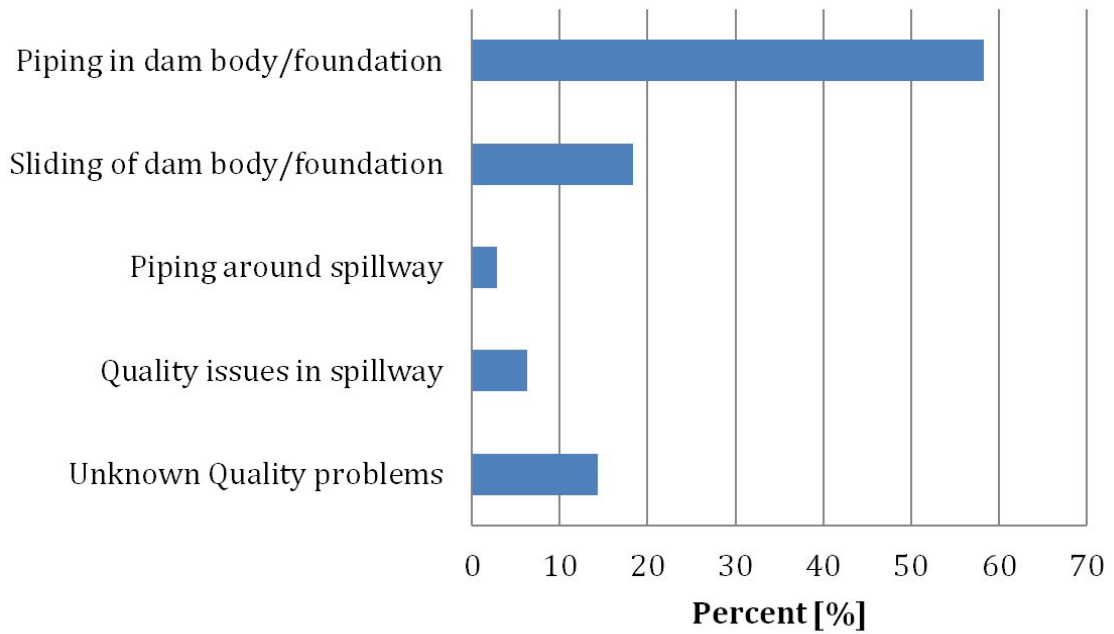
2.1 Analysis of Earth Dam Failures

To demonstrate the importance of investigation in dam failure caused by overtopping, as it is done in this work, a statistical analysis of earth dam failures and the according damages will be presented. [Zhang et al.](#) published an evaluation of a database in 2007, based on 593 failures of earth dams from more than fifty countries, excluding China.

Figure 2.1: *Dam Failure: Dam Types (Zhang et al.)*



From an evaluation of more than 900 dam failures, more than 65% were earth fill dams. Especially, smaller earth dams with either a height less than 15 meters or a “small” capacity statistically break more often than larger dams. Most failures happen in the first 5 years of operation.

Figure 2.2: Percentages of causes for earth dam failures (*Zhang et al.*)**Figure 2.3:** Subcauses of Quality Problems (*Zhang et al.*)

As shown in Figure 2.2, the main causes for earth dam failures are quality problems and overtopping. If quality problems are divided into sub-categories (Figure 2.3), overtopping becomes the largest initiator of dam failures. According to the U.S. Association of State Dam Safety Officials, about 70% of all dam failures in the U.S. between 1975 and 2001 were caused by overtopping. Therefore, two possible situations are responsible: An insufficient spillway capacity or an extreme flood exceeding design criteria. Both scenarios mean a too small capacity of the spillway and accordingly water starts to run off over the crest of the dam and causes the external erosion. In Table 2.1, some embankment failures are listed, including the according loss of life (Chanson).

Table 2.1: *Examples of embankment dam failures (Chanson)*

Dam	Construction date	Date of accident	Description of failure	Loss of life
Blackbrook dam, UK	1795-1797	1799	Collapse caused by dam settlement and spillway inadequacy	None
South Fork (Johnstown) dam, USA	1839	May 1889	Overtopping and break of earth dam caused by spillway inadequacy	over 2,000
Bilberry dam, UK	1843	5 Feb. 1852	Failure of earth dam caused by poor construction quality	81
Dale Dyke dam, UK	1863	11 March 1864	Earth embankment failure attributed to poor construction work. Surge wave volume 0.9 Mm ³	150
Habra dam, Algeria	1873	Dec. 1881	Break of masonry gravity dam caused by inadequate spillway capacity leading to overturning. Note that the storm rainfall of 165 mm in one night lead to an estimated runoff of about three times the reservoir capacity	209
Dolgarrog dams, UK	1911/1910s	1925	Sequential failure of two earth dams following undermining of the upper structure	25
Belci dam, Romania	1958-1962	1991	Dam overtopping and breach (caused by a failure of gate mechanism)	97
Teton dam, USA	1976	5 June 1976	Dam failure caused by cracks and piping in the embankment near completion.	11
Tous dam, Spain	1977	1982	Dam break (following an overtopping; collapse caused by an electrical failure)	None
Lake Ha! Ha! dam, Canada	–	July 1996	Dam overtopping caused by extreme rainfalls (18-22 July) in the Saguenay region	None
Zeyzoun (or Zayyaoun) dam, Syria	1996	4 June 2002	Embankment dam cracks, releasing about 71 Mm ³ of water. A 3.3-m high wall of water rushed through the villages submerging over 80 km ² . The final breach was 80-m wide	22
Glashütte dam, Germany	1953	12 Aug. 2002	Embankment dam overtopping during very large flood because of inadequate spillway capacity	None

Figure 2.4: *Example of a dam failure caused by Overtopping: Glashütte dam, Germany, 2002 (Chanson)*



2.2 Modelling with Telemac-2D and Sisyphe

2.2.1 Theory of 2D-Modelling

Basis for all numerical simulations of free surface flow are the conservation equations of mass, momentum and energy. From these conservation equations the Navier Stokes Equations arise, which form a system of partial differential equations. This system then usually is solved using the Finite Elements Method or the Finite Volume Method, as it cannot be solved analytically.

To reduce the computational effort, it is possible to use a depth-averaged system of equations. This means, for every node from the mesh, only one depth-averaged velocity is calculated, although in reality the velocities vary along the depth. This simplification then is used in the so-called shallow water equations. Three assumptions have to be made as requirement for their use:

- Velocity and momentum in vertical direction are insignificant.
- The vertical distribution of pressure is hydrostatic.
- Wave length is much larger than the water depth.

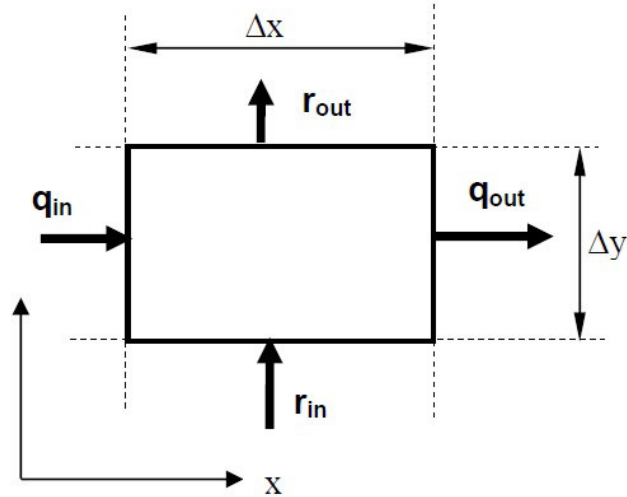
The Shallow water equations are (Minor [2005]):

$$\frac{\partial h}{\partial t} + \frac{\partial q}{\partial x} + \frac{\partial r}{\partial y} = 0 \quad \text{Mass Conservation} \quad (2.1)$$

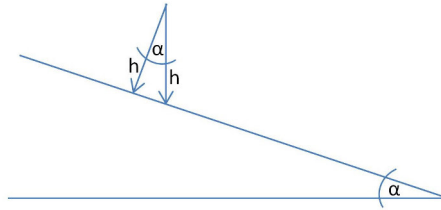
$$\frac{\partial r}{\partial t} + \frac{\partial}{\partial x} * (qv) + \frac{\partial}{\partial y} * (rv + \frac{g}{2}h^2) + gh \frac{\partial z_b}{\partial y} + \frac{\tau_{by}}{\rho} = 0 \quad \text{Momentum X} \quad (2.2)$$

$$\frac{\partial q}{\partial t} + \frac{\partial}{\partial x} * (qu + \frac{g}{2} * h^2) + \frac{\partial}{\partial y} * (ru) + gh \frac{\partial z_b}{\partial x} + \frac{\tau_{bx}}{\rho} = 0 \quad \text{Momentum Y} \quad (2.3)$$

Figure 2.5: Discharges in the shallow water equations according to their direction (Minor [2005])



The shallow water equations are primarily meant for rather flat and shallow flow conditions, as simulations of flooding normally are. The use in cases with highly non-steady flow with steep slopes generally is not advisable, but within this work it will be tested, how appropriate the results are. Mathematically, $\sin(\alpha)$ is set equal to $\tan(\alpha)$, as shown in Figure 2.6. Thus, as bigger the slope (α) is, the bigger becomes the error due to the use of these equations.

Figure 2.6: *Error of the shallow water equations*

For $\alpha \ll 1$:

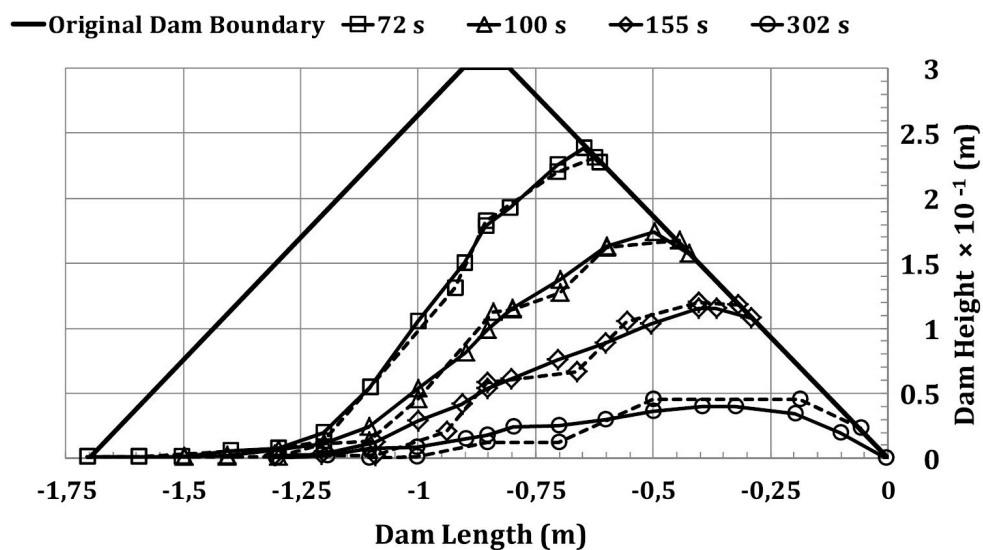
$$h * \cos(\alpha) = h$$

$$\cos(\alpha) = 1$$

$$\tan(\alpha) = \frac{\sin(\alpha)}{\cos(\alpha)}$$

$$\tan(\alpha) = \sin(\alpha)$$

Sabbagh-Yazdi and Jamshidi [2013] corrected the shallow water equations by accounting for the slope and by developing a hydrodynamic FV-model (EBS) and also simulated the laboratory case of Coleman et al. (see Chapter 3) with their model. They obtained very well fitting results with their simulation, as shown in Figure 2.7. Nevertheless, in this work will be shown, how well the results of the uncorrected shallow water equations will fit to those from a laboratory test.

Figure 2.7: *Comparison of Sabbagh-Yazdi's results*

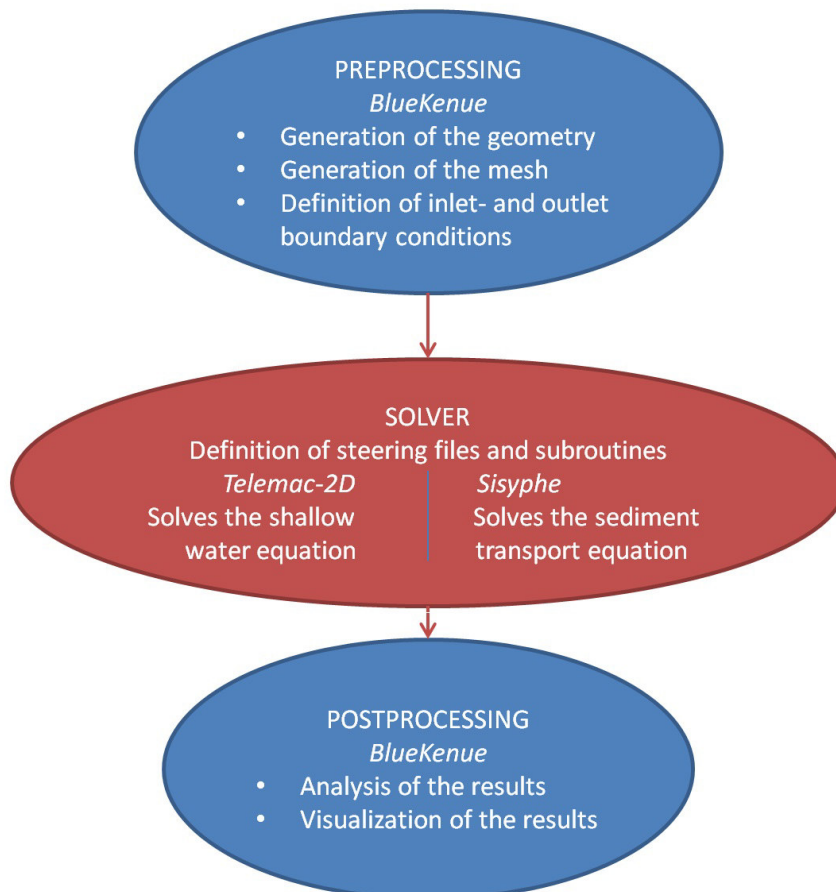
A numerical free surface flow simulation always consists of three components: A preprocessor, a solver and a postprocessor.

During the pre-processing, a discretization of the geometry in a calculation-mesh is generated. It can either be regular (structured) or unstructured. While structured meshes facilitate the calculation, an unstructured mesh allows more complicated geometries. Moreover, the boundary conditions including all other input-files, such as hydrographs, definitions of the rigid bottom etc. are defined. The pre-processing in the present work was done with the free available program “BlueKenue” (<http://www.nrc-cnrc.gc.ca>).

The solver is the “heart” of every simulation. It has to solve the before mentioned equations of flow for every node. Telemac-2D was used in this work as solver.

In the post-processing, the results get edited and prepared. BlueKenue was also used for the post-processing of the handled cases.

Figure 2.8: *Components of numerical simulations*



2.2.2 Telemac-2D

Telemac-2D (<http://www.opentelemac.org/>) is an open-source solver for depth-averaged free surface flow equations as described above. It was developed by the National Hydraulics and Environment Laboratory of the Research and Development Directorate of the French Electricity Board (EDF-RD), in collaboration with research institutes.

Telemac-2D is mainly used for free-surface maritime or river hydraulics. It is able to take into account the following phenomena:

- Propagation of long waves, including non-linear effects,
- Friction on the bed,
- The effect of the Coriolis force,
- The effects of meteorological phenomena such as atmospheric pressure, rain or evaporation and wind,
- Turbulence,
- Supercritical and subcritical flows,
- Influence of horizontal temperature and salinity gradients on density,
- Cartesian or spherical coordinates for large domains,
- Dry areas in the computational field: tidal flats and flood-plains,
- Entrainment and diffusion of a tracer by currents, including creation and decay terms,
- Particle tracking and computation of Lagrangian drifts,
- Treatment of singularities: weirs, dikes, culverts, etc.,
- Dyke breaching,
- Inclusion of the drag forces created by vertical structures,
- Inclusion of porosity phenomena,
- Inclusion of wave-induced currents (by link-ups with the Artemins and Tomawac modules),
- Coupling with sediment transport,
- Coupling with water quality tools.

(cp. [Telemac-2D \[2013\]](#))

2.2.3 Sisyphe

Sisyphe is the sediment-transport module of the hydroinformatics finite element and finite volume system Telemac-Mascaret (Open Source Modelling Suite Telemac-Mascaret). Sediment transport is split into bed load and suspended load calculation, the user is able to choose which phenomena shall be computed. The calculations are done for every node of the mesh. For the bed load transport, various classical sediment transport formulas as Meyer-Peter-Müller or Van Rijn are available, whereas for the suspended load an additional transport equation has to be solved. For the bed evolution, the Exner-equation is solved.

The necessary variables like the velocity or water depths are obtained whether by coupling with one of the hydrodynamic modules of the Telemac system like Telemac-2D or they can get imposed in the model. Variables like the grain diameters or the density have to be defined by the user. The particle size distribution is entered via the definition of a finite number of grain classes. Sisyphe is applicable for cohesive and non-cohesive sediments.

The following effects can also be included in the calculation:

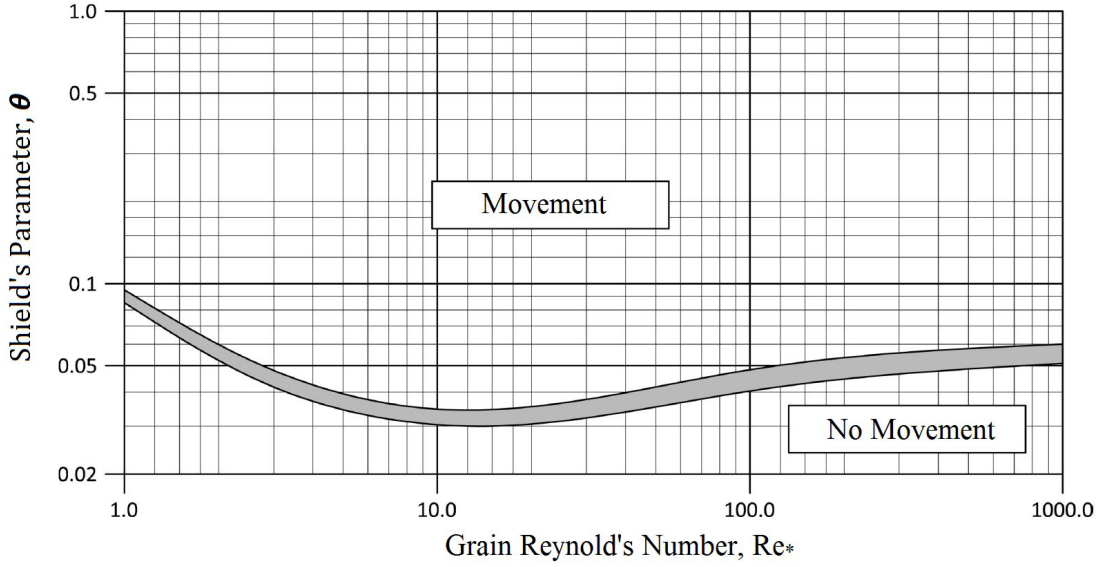
- Sediment slide
- Effect of bottom slope
- Effect of transverse deviation
- Rigid beds
- Secondary currents
- Slope failure
- Effect of consolidation for cohesive sediments

(cp. [Sisyphe \[2014\]](#))

2.2.4 The Modification of the Meyer-Peter-Müller Formula by Wiberg and Smith

The critical Shields parameter is one of the input parameters for the calculation of the sediment transport rate with the Meyer-Peter-Müller formula. It is based on empirical investigations and was published by Shields in 1936. The Shields Parameter together with the Grain Reynold's number has to be entered in the diagramm. If the Shields paramter is higher than the critical Shields-Parameter, erosion takes place. If the Grain Reynold's number exceeds a value of 100-500, the critical Shields parameter remains constant and according to Meyer-Peter-Müller has a value of 0.047.

Meyer, Peter and Müller (MPM) published their sediment transport formula in 1948, based on a high number of empirical experiments. According to their formula, the

Figure 2.9: Shields Diagram (*Bed-Load-Analyzer* [2013])

transport capacity is proportional to the difference of the grain's shear stress and the critical shear stress. The experiments of Meyer, Peter and Müller were done in flumes with slopes between 0.4 and 20 ‰ and grain sizes from 0.4 to 30 mm. The average velocities were between 0.37 and 2.87 m/s. The main influencing parameter of the formula was determined as the bed shear stress.

$$q_{b,k*} = \alpha * \left[\frac{\mu * \tau_0}{(\gamma_s - \gamma_w) d_k} - \Theta_c \right]^{3/2} * \gamma_s * \left[\left(\frac{\gamma_s}{\gamma_w} - 1 \right) * g * d_k^3 \right]^{1/2} \quad (2.4)$$

Originally, the authors of the formula determined $\alpha=8$. In 1989, Wiberg and Smith modified the factor α after comparing a large dataset of laboratory test cases from different investigators in order to achieve a closer approximation of the MPM function to the measured data. (2.5).

In Chapter 3, simulations will be presented using the classical MPM- formula as well as with this modification. (cp. *Bed-Load-Analyzer* [2013])

$$\alpha = 9.64 * \left[\frac{\mu \tau_0}{(\gamma_s - \gamma_w) d_k} \right]^{1/6} \quad (2.5)$$

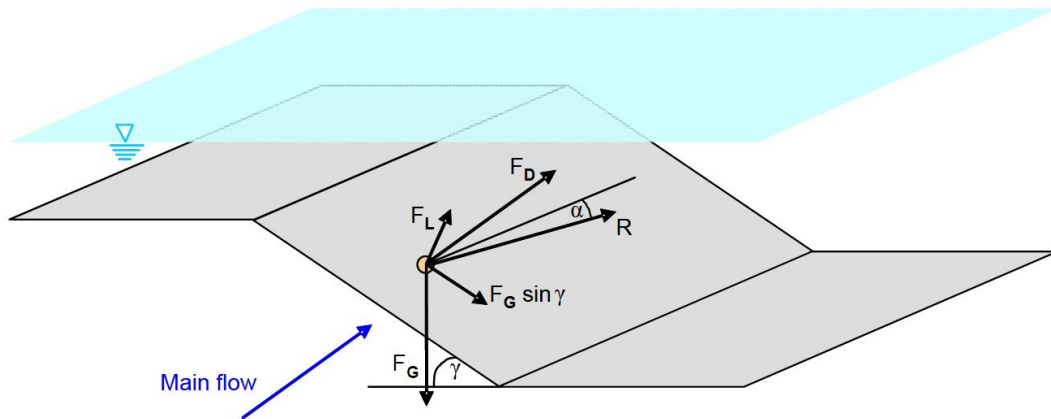
(cp. *Wiberg and Smith* [1989])

As this modification was still not available in Sisyphe, a subroutine with the implementation of this approach was programmed. The code can be found in the Appendix.

2.2.5 Talmon's Approach for the Transverse Deviation Effect

As sediments are influenced by gravity, their movement direction on an transversely inclined bed is not only dependent from the flow direction. For the determination of the sediment transport direction, a balance of forces on the grain is made. The forces are: The drag of the water in flow direction F_D , the gravity F_G and the uplifting force F_L as well as the resulting force F_R (Figure 2.10).

Figure 2.10: Forces applied on the sediment grain on a transverse sloping bed (Wiesemann et al. [2006])



Generally, the deviation of the sediment is described with (2.6), in which α is the angle between the direction of the solid transport in relation to the flow direction and δ is the angle between the direction of the bottom shear stress in relation to the flow direction.

$$\tan(\alpha) = \frac{\sin(\delta) - \frac{1}{f(\Theta)\frac{\partial z_b}{\partial y}}}{\cos(\delta) - \frac{1}{f(\Theta)\frac{\partial z_b}{\partial x}}} \quad (2.6)$$

(cp. [Talmon et al. \[1995\]](#))

$$\text{with } T = \frac{1}{f(\Theta)} \quad (2.7)$$

$$\text{the Equation can be shortened to } \tan(\alpha) = \tan(\delta) - T \frac{\partial Z_f}{\partial n} \quad (2.8)$$

$$\text{and with } T = \frac{1}{\beta\sqrt{\Theta}} \quad (2.9)$$

(cp. [Sisyphe \[2014\]](#)) β is introduced as a calibration factor.

The β -factor is an empiric value, which has a high influence on the calculation of the deviation. In Literature, different approaches for β are available:

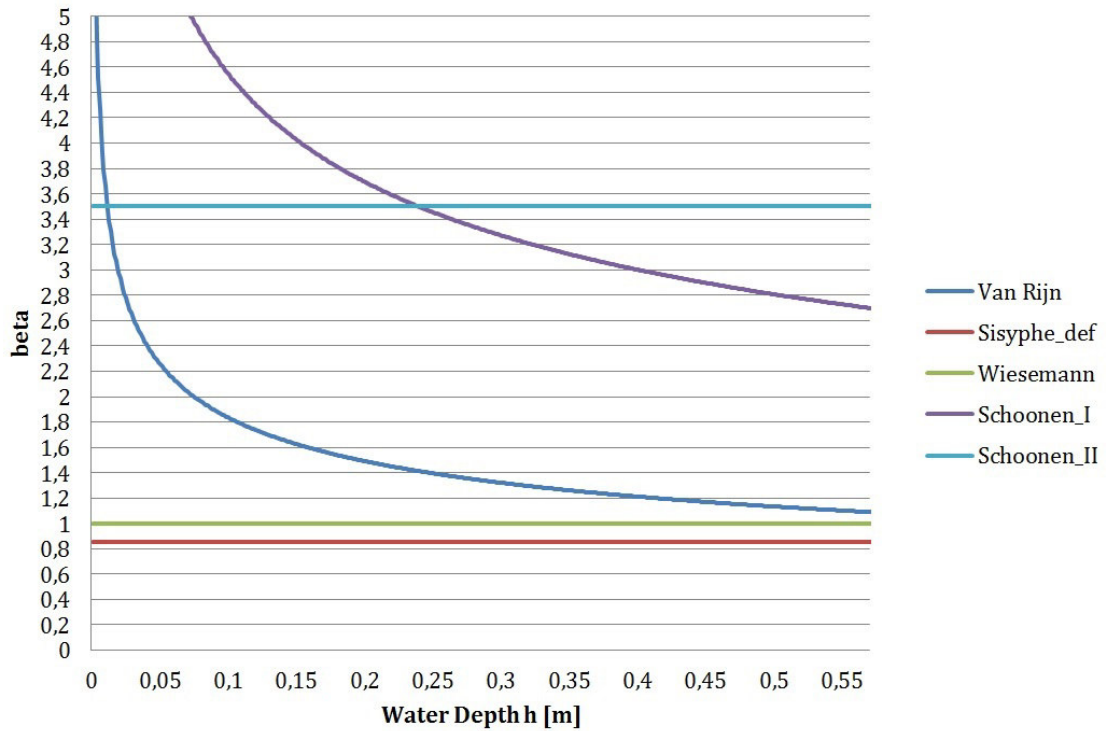
$$\begin{aligned} & \beta=0.85 \text{ ([Sisyphe \[2014\]](#) - default value)} \\ \beta &= 9 * (d_{50}/h)^{0.3} \text{ ([Talmon et al. \[1995\]](#) - Formula of Van Rijn)} \\ & \beta= 1 \text{ ([Wiesemann et al. \[2006\]](#))} \\ \beta &= 22.3 * (d_{50}/h)^{0.3} \text{ ([Schoonen \[2006\]](#))} \\ & \beta= 3.5 \text{ ([Schoonen \[2006\]](#))} \end{aligned}$$

Van Rijn's and Schoonen's first formula are varying with the water depth, while the others are using a constant value. In [Figure 2.11](#), the different formulas are compared, using a grain size $d_{50}=0.5\text{mm}$.

During this work, the values of $\beta=0,85$, $\beta=0.4$ and Van Rijn's formula were tested in [chapter 3](#).

In the steering file of Sisyphe, it is only possible to enter a constant value for β . The variable calculation with the formula of Van Rijn was implemented in a subroutine.

Figure 2.11: Various calculations of Talmon's beta



According to Figure 2.11, all approaches except those from Schoonen approximate to similar values for β with water depths larger than 0.55 m between 0.85 and 1.1. For lower depths, the variable Van Rijn formula scores very high values. Schoonen adapted his approaches for special laboratory tests and it is not known, if they are appropriate for other cases.

3 The Modelling of a Laboratory Test Case

3.1 Presentation of Case 1 - Experiment Done by Coleman et al.

In 2002, [Coleman et al. \[2002\]](#) published a paper, in which they presented laboratory tests done by Andrews and Jack. In these laboratory tests, dams with a certain geometry were constructed with a homogenous, uniform material and afterwards destroyed by overtopping the crest with water, initiating the water-flow through a pilot channel situated on the left wall (in flow direction). The upstream and downstream slopes of the dam were 1:2.7 (V:H).

The water level on the upstream boundary was constantly set to 0.3 m; additionally a flow straightener as well as a water level-probe was installed. Thus, the discharge over the dam was only influenced by the erosion process itself. The discharge then was measured via a V-notch weir downstream of the dam.

The wall on the left side was meant to form the centerline of the flume, so the intention was to simulate a symmetric flume. Therefore, the wall has to be very smooth, in order to not to create turbulence and according to that a deceleration of water, what would mean a drop of erosion in the area of the side wall. Referring to that assumption, the side walls in the numeric model were also modelled without friction.

[Coleman et al. \[2002\]](#) documented the erosion process and published the longitudinal profiles along the breach channel centerline (Figure 3.1) for medium sand for six different time-steps.

Figure 3.1: *Experimental Setup by Andrews (Coleman et al. [2002])*

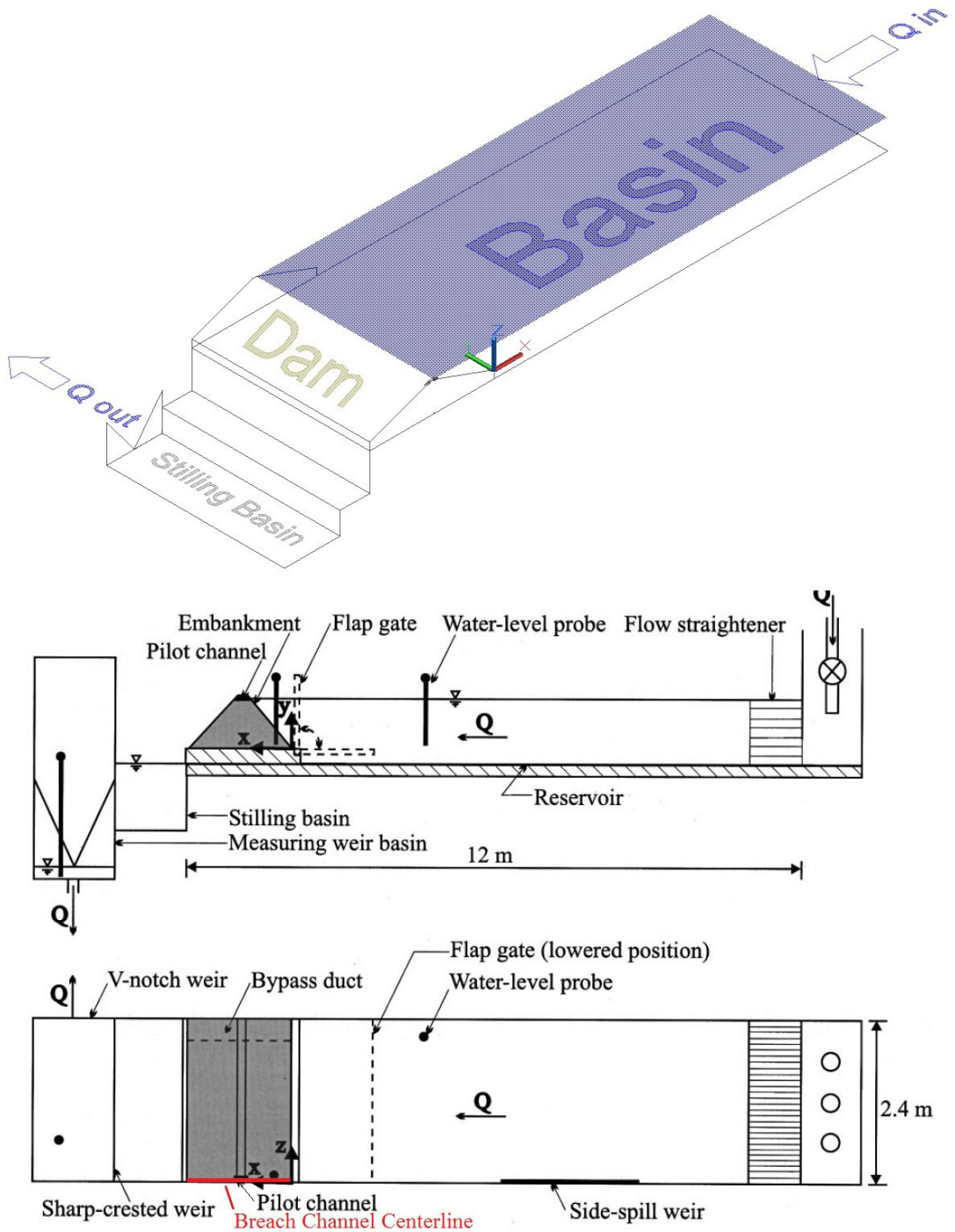
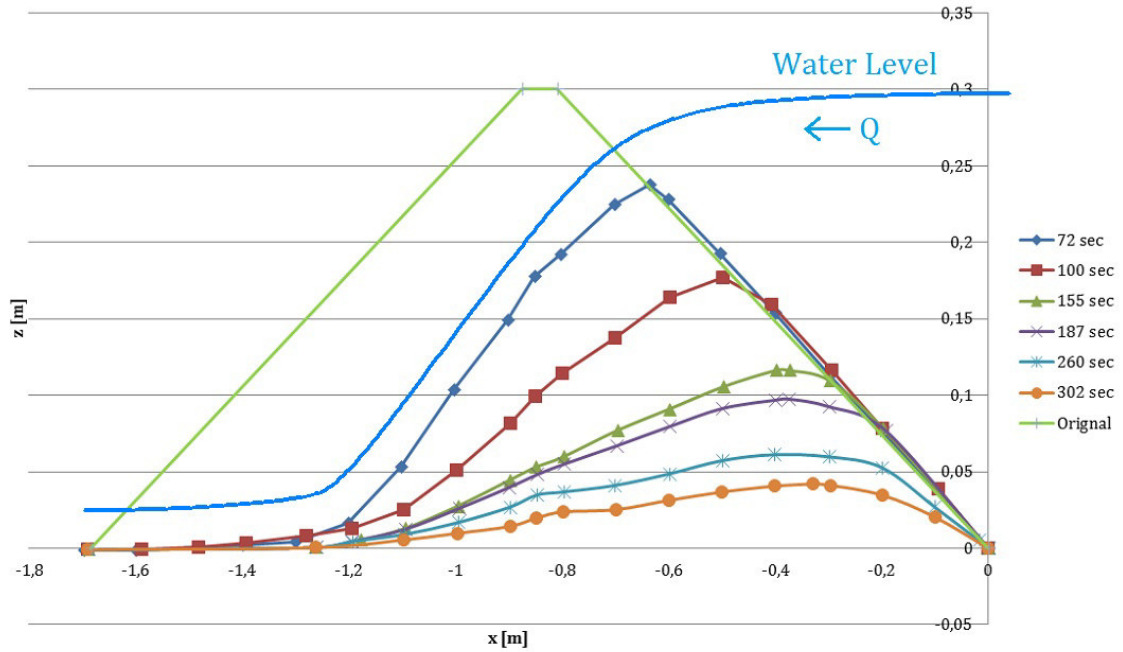


Figure 3.2: Longitudinal profiles along the developed breach channel centerline for medium sand (Coleman et al. [2002])



For the laboratory tests, the material described in Table 3.1 was used. Of course, the same parameters were used in the numerical model as well. The comparison of the erosion process was carried out with the longitudinal profiles along the breach channel as shown in Figure 3.2.

Table 3.1: Material Properties (Coleman et al. [2002])

Sediment Material	d [mm]	σ_g	ρ_s [kg/m ³]	φ [°]
Medium sand	0.5	1.6	2630	32

3.2 The Numerical Model in Telemac-2D and Sisyphe

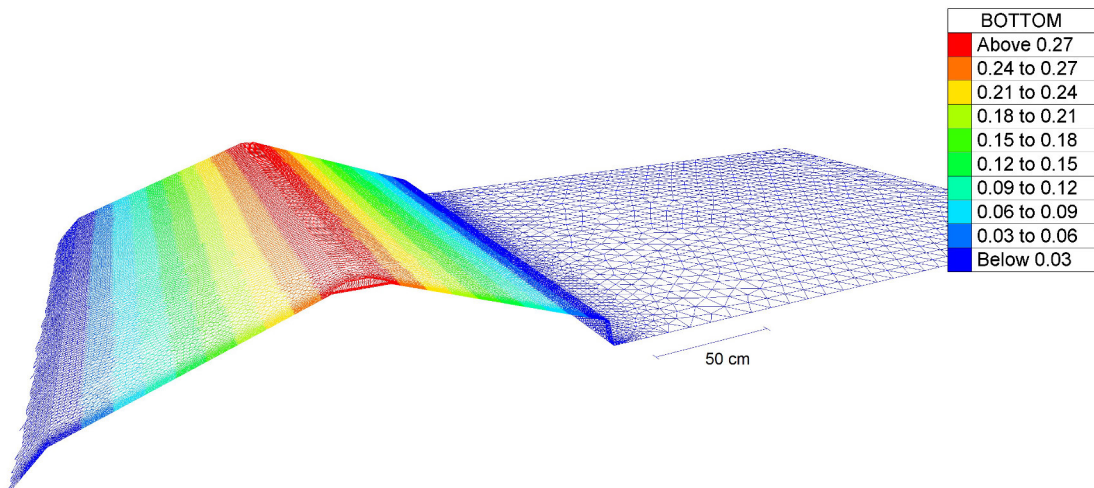
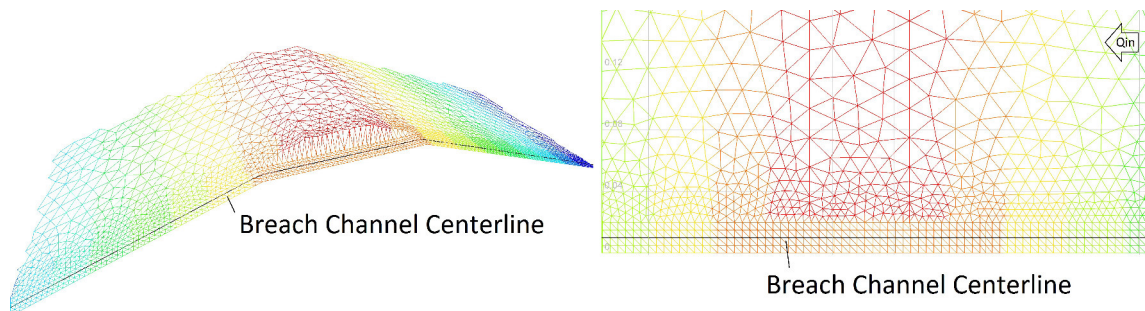
3.2.1 The Mesh

On the upstream side of the dam, the flume is only reproduced approx. to where the water level probe in the laboratory test case is placed. Downstream of the dam, the model is slightly different to the test case done by Andrews, as neither a rectangular step nor a measuring-weir is installed, and in exchange, a steep slope is modeled for guaranteeing a backwater-free outflow of water and sediments. At the end of this slope, also the downstream reservoir is represented.

Table 3.2: *Mesh Data*

Area	Default Edge Length
Channel Up/Downstream	2 cm
Dam	2 cm
Pilot Channel/ Channel Centerline	0.5 cm

The mesh with triangular elements has 20 789 nodes.

Figure 3.3: *3D-View of the Mesh***Figure 3.4:** *Mesh-Detail of the Pilot Channel, 3D and Plan View*

3.2.2 The Boundary Conditions

As the lower reservoir is also computed in the model, there is no downstream boundary condition. The upstream boundary condition is set to a constant water level

of 0.3 m (The water depth then is 0.4 m, as the bottom of the upstream reservoir is at -0.1 m due to the step next to the dam base and the origin being situated at the dam base). As it was not possible to create an open boundary which allows the eroded sediments to exit the model, a downstream basin was annexed, collecting all the water and sediments during the calculation.

3.2.3 The Steering Files and the Fortran-Subroutine

There are two steering files necessary for the calculation: One for the hydrodynamic model in Telemac-2D and one for the sedimentary calculation in Sisyphe. In the following tables, some of the keywords from the steering files are explained. The values and settings are shown and discussed in section 3.3 and section 3.4. Complete steering files are to be found in the Appendix.

Table 3.3: *Selected parameters for hydrodynamic modelling*

Keyword	Explanation
COUPLING WITH = 'SISYPHE'	Connects Telemac-2D with Sisyphé
PARALLEL PROCESSORS	Activation of parallel mode if >1
GEOMETRY FILE	Definition of the geometric input, inc. the mesh
BOUNDARY CONDITIONS FILE	Definition of boundaries, like the upstream bc, which is set to 0.3 m
FORTRAN FILE	Definition of the subroutine, e.g. for definition of the rigid bottom
TIDAL FLATS	Has to be 'YES', if dry cells turn wet during the calculation
MASS-LUMPING ON H	Stabilizing the calculation by simplifying the calculation-matrix
TYPE OF ADVECTION	Allows to choose different options for the water propagation, for velocity and water depth
SUPG OPTION	Upwinding scheme, stabilizes the calculation
TIME STEP	Definition of the time step
NUMBER OF TIME STEPS	Number of time steps * time step = Duration of the simulation
LAW OF BOTTOM FRICTION	3 = Law of Strickler
FRICTION COEFFICIENT	According to the law, e.g. k_{st} for Strickler
TURBULENCE MODEL FOR SOLID BOUNDARIES	Option for rough or smooth wall
TURBULENCE MODEL EQUATIONS	Option for Finite Volume, Finite Elements etc.

Table 3.4: *Selected parameters for sedimentologic modelling*

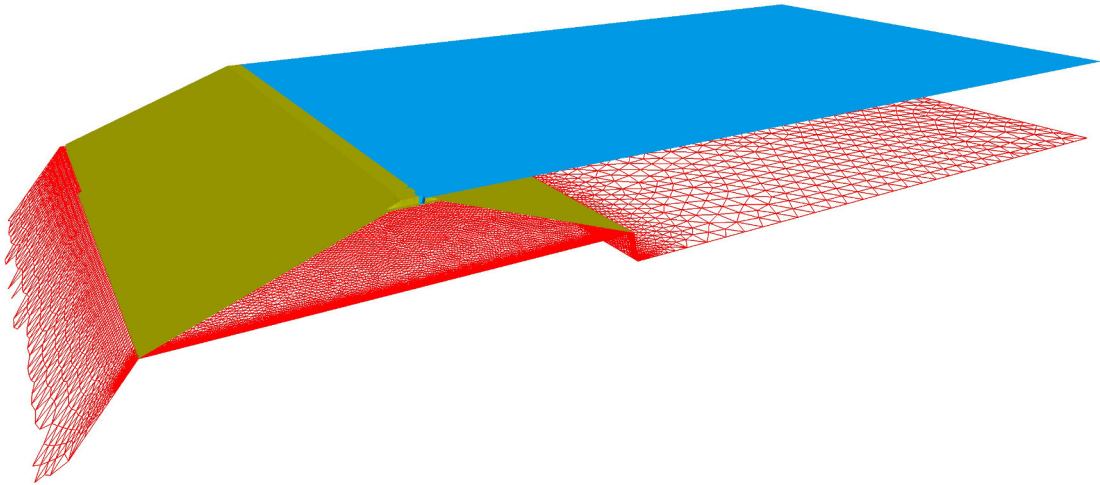
Keyword	Explanation
NUMBER OF SIZE-CLASSES OF BED MATERIAL	
SEDIMENT DENSITY	
FRICITION ANGLE OF THE SEDIMENT	Definition of the Dam Material
SEDIMENT DIAMETERS	
NON COHESIVE BED POROSITY	
SLOPE EFFECT	Increases the material transport rate
FORMULA FOR SLOPE EFFECT	Koch and Flokstra or Soulsby
FORMULA FOR DEVIATION	Enables a correction of the direction of the bed load material
SEDIMENT SLIDE	If the slope becomes bigger than the friction angle, material erodes
BED-LOAD TRANSPORT FORMULA	Several methods can be chosen, like Meyer-Peter-Müller (MPM)

For the definition of the rigid bottom, the water surface at the beginning of the calculation as well as for some modifications of the calculations, a subroutine was created.

For the initial water surface, the hydraulic model was split into 2 parts, in which upstream of the dam crest the water height was defined at 0.3 m.

According to that, the free surface at time step $t=0$ is as shown in Figure 3.5.

The rigid bed (=non-erodible bottom) is defined as the bottom itself up- and downstream of the dam, and under the dam as a planar face at $Z=0$.

Figure 3.5: *Free Surface at $t=0$ and the rigid bed (red)*

3.3 Sensitivity Analysis for the Hydrodynamic Modelling

3.3.1 Default Hydrodynamic Parameters

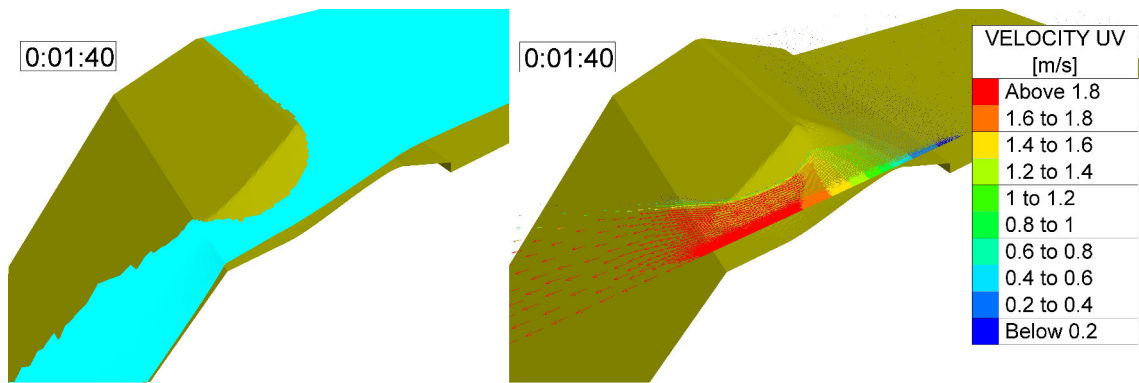
As basis for the variation study, some settings were fixed as default. To find out the influence of the different parameters, they got changed and the results then were compared in a sensitivity analysis. The first task was to receive a hydrodynamic stable simulation, which means no oscillation in the water surface should occur. Therefore, different time steps as well as stabilizing options were tested. The best stable results were achieved with a time step of 0.001 sec and the activation of “Mass Lumping on H” as well as the setting of “Supg” to 0;1 (Streamline Upwind Petrov-Galerkin). Both are stabilizing, but are also smoothening the results.

In the next step, different types of advection were tested. Although Telemac-2D suggests using the default option of the characteristics-method, the usage of other schemes led to better results.

Table 3.5: *Default hydrodynamic settings*

Keyword	Value
Strickler roughness	92 m ^{1/3} /sec
Turbulence model	Constant eddy viscosity
Velocity diffusivity	10 ⁻⁴ m ² /sec
Method	Finite Elements
Type of advection	1;5 (Velocity; depth. 1=Method of characteristics)
Mass Lumping	Yes
SUPG option	0;1
Time step	0.001 sec

The sediment transport parameters used in the sensitivity analysis are listed in Table 3.8. In Figure 3.6, the velocities as well as the water surface for the standard simulation after 100 sec are shown.

Figure 3.6: *3D-View of water surface (left) and velocities (right) after 100 sec*

As the diameter of the uniform bed material is 0.5 mm, a Strickler-roughness of $k_{st}=92 \text{ m}^{1/3}/\text{sec}$ was chosen.

$$k_{st} = \frac{26}{d_{50}^{1/6}} \approx 92 \quad (3.1)$$

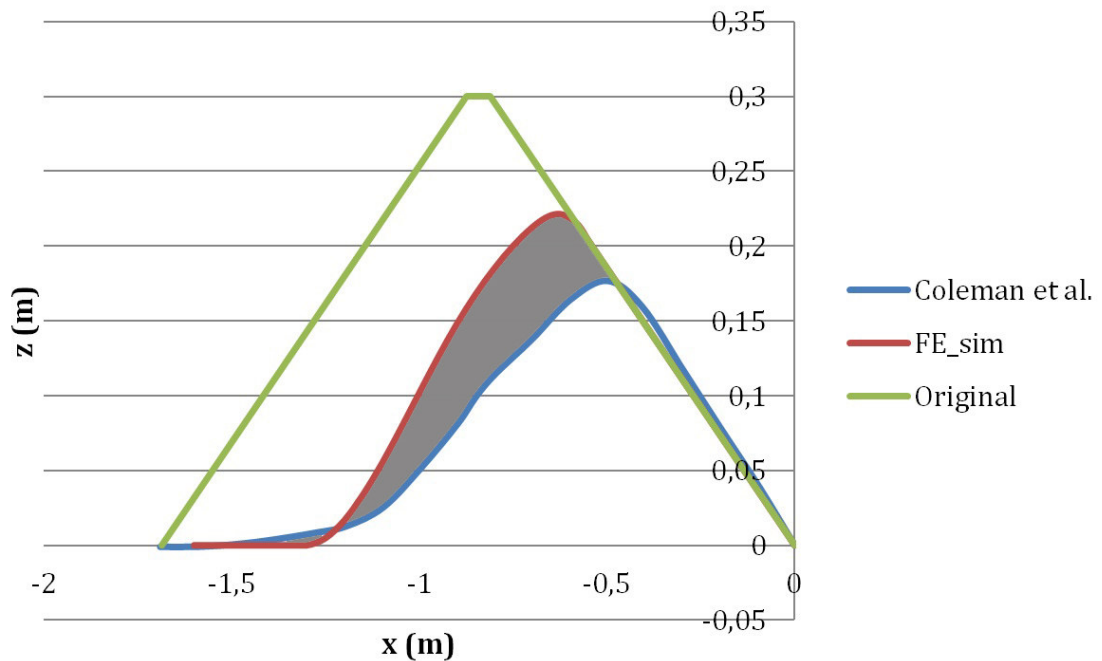
(cp. [Lehmann et al.](#))

For a better comparison of the different simulations, the non-coinciding area between the graph from the laboratory test case (Coleman) and the calculated graph is determined with (3.2).

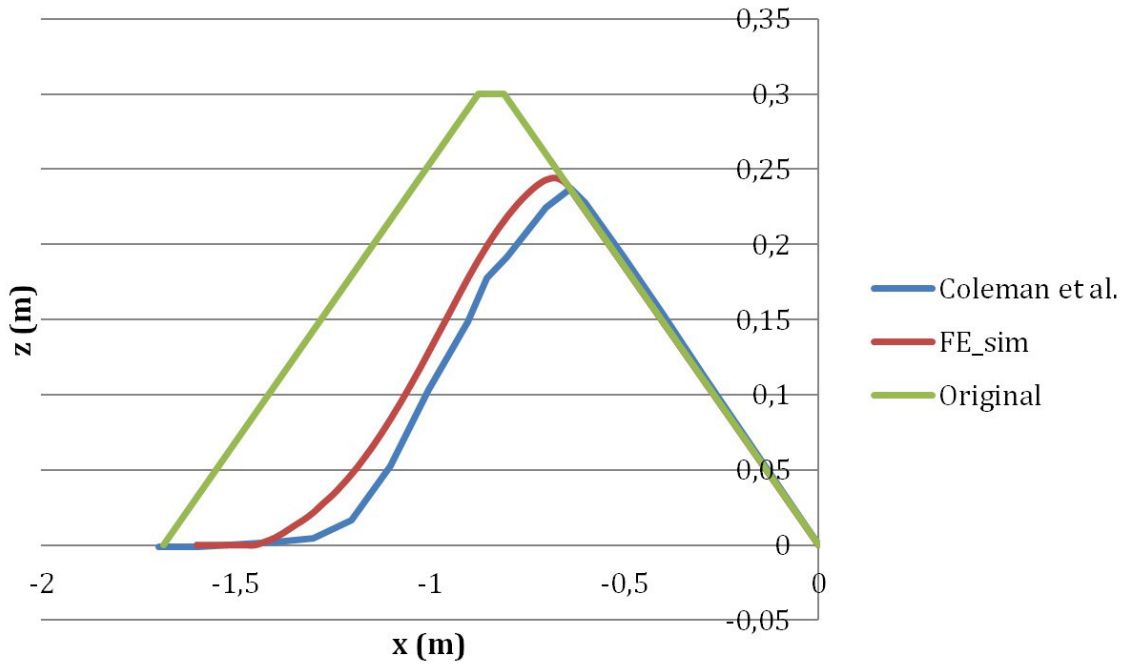
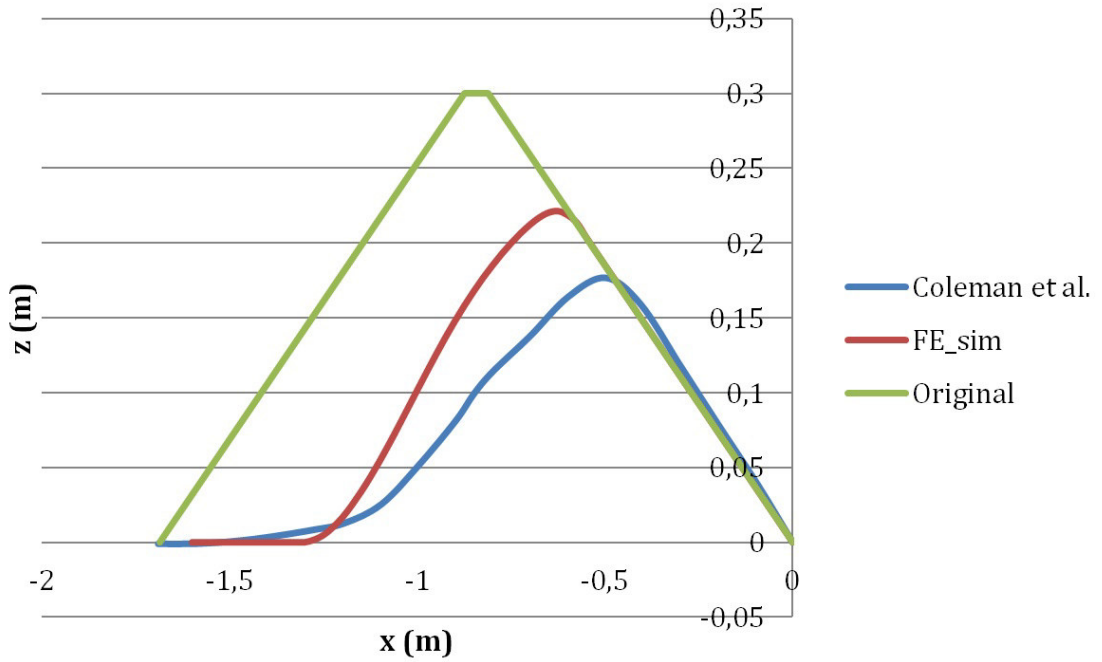
$$A_{error} = \sum abs(y_{Coleman} - y_{Simulation}) * dx \quad (3.2)$$

Of course, this simple calculation of the non-coinciding area shows only the precision of the computed results in one axis, but it is a very accurate tool to determine the quality of the approximation of the computation to the measurement data from the laboratory test case and enables a fast comparison between the different simulations. In Figure 3.7 the non-coinciding area of an example is shown.

Figure 3.7: Non-coinciding area A_{error} at an example longitudinal profile



Attention: The following graphs of the results from different simulations are super-elevated!

Figure 3.8: Results for the default hydrodynamic simulation, $t=72$ sec**Figure 3.9:** Results for the default hydrodynamic simulation, $t=100$ sec

Although Coleman et al. [2002] published the longitudinal profiles for six time steps, during the calibration phase only the profiles of the first two time steps after 72 sec and 100 sec were calculated. Subsequently, the effects of the different variations will be validated for the later time steps.

As shown in Figure 3.8, the results at $t=72$ sec qualitatively fit quite well to those from the laboratory test case. At $t=100$ sec, too less erosion occurs on top of the dam. The non-coinciding area in the first two time steps (72 sec, 100 sec) sums up to $A_{error} = 5.79 \text{ dm}^2$.

3.3.2 Overview of the Hydrodynamic Sensitivity Analysis

In Table 3.6, a selection of simulations is shown, presenting the most important parameters and the according effects caused by a variation of these parameters. A more detailed description can be found in the following sub-chapters.

Table 3.6: *Overview of hydrodynamic simulations*

Changed parameter	Value in default simulation	Used value	$A_{error} \text{ [dm}^2\text{]} \text{ (first two time steps)}$
(default)			5.79
Strickler roughness	92	70	9.44
Strickler roughness	92	110	5.08
Turbulence model	Constant eddy viscosity	k-Epsilon Model	6.23
Method	FE	FV	3.66
Type of advection (FE)	1 Method of characteristics	6 PSI scheme on non conservative equation	4.12
Velocity diffusivity	10^{-4}	10^{-6}	5.50
Velocity diffusivity	10^{-4}	0	5.50

3.3.3 Variation of the Roughness

The determination of the Strickler roughness is shown in (3.1).

As various adaptations for the conversion of a diameter to the Strickler-value are available in literatur, which are leading to higher or lower values, also $k_{st}=70$ and $k_{st}=110$ were tested. As awaited, the lowering to 70 leads to a deceleration of the

flow and accordingly less erosion occurs. The failure area then sums up to 9.44 dm². With a smoothening of $k_{st}=110$, the bed shear stress rises according to the higher velocity and more material erodes.

3.3.4 Variation of Roughness on Lateral Boundaries

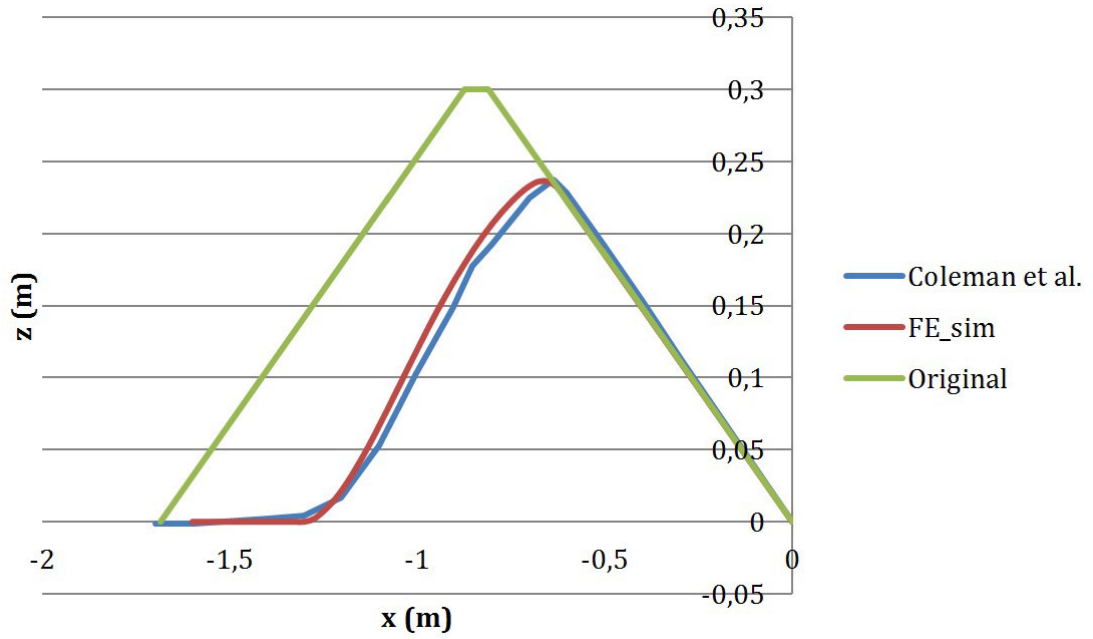
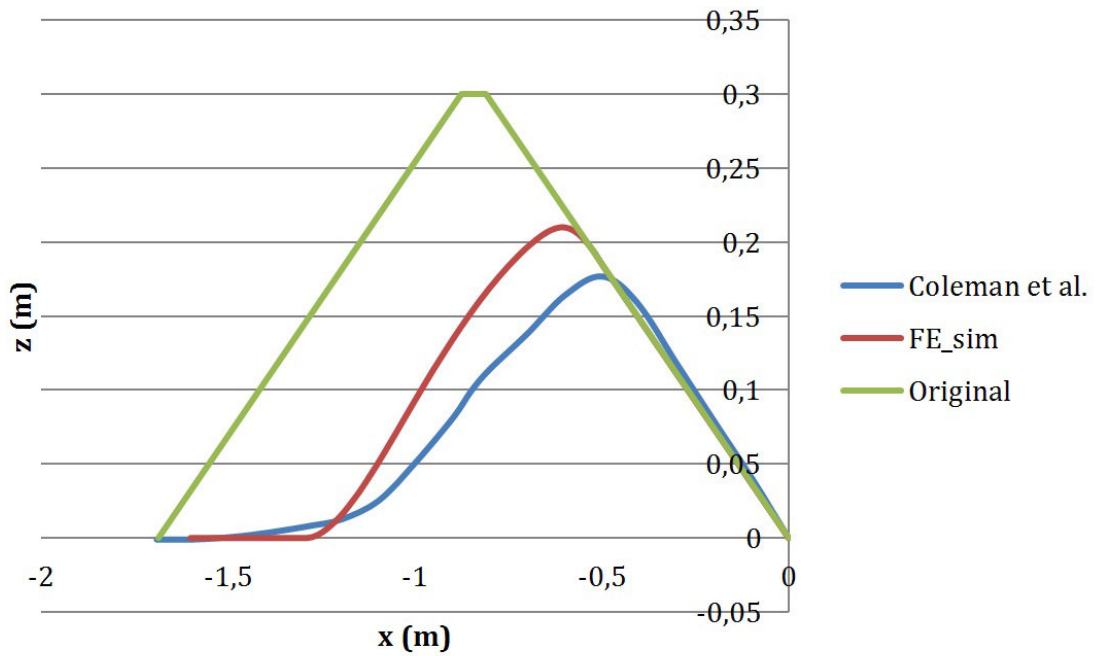
To test the influence of the roughness of the side wall next to the pilot channel, a simulation was done with a friction coefficient of 120 m^{1/3}/sec. Expectedly, the water flow next to the side wall gets decelerated and accordingly less erosion takes place. In this case, A_{error} amounts to 6.43 dm² (t=72 sec and t=100 sec).

3.3.5 Variation of the Turbulence Models

In the default simulation, a constant eddy viscosity with a velocity diffusivity of 10^{-4} is used as turbulence model. To test the influence of the turbulence model, it was changed to the k- ϵ -model. The different turbulence model led to less erosion ($A_{error} = 6.23$ dm²). In another simulation, the diffusivity was set to 10^{-6} , using the constant eddy viscosity. This way, the bottom curves from the simulation converged slightly better to those from the laboratory test case by Andrews and Coleman ($A_{error} = 5.50$ dm²).

3.3.6 Variation of the Type of Advection for Velocities

Telemac-2D also offers different methods for the advection of velocities in the FE-method. Although the characteristics-method is suggested for the calculation of velocities, the German BAW (Bundesamt f. Wasserbau, co-developer of the Telemac-Suite) recommends also the PSI (Positive Streamwise Invariant) scheme on non-conservative equation, which is less diffusive and is producing results without oscillations (source: Based on personal communication).

Figure 3.10: Results for FE-PSI Scheme, $t=72$ sec (Sim. A)**Figure 3.11:** Results for FE-PSI Scheme, $t=100$ sec (Sim. A)

3.3.7 Variation: Finite Volume Method

The implemented Finite Volume-Solver in Telemac-2D is special for its ability of shock capturing and therefore is suitable for the calculation of highly non-uniform flow, as the dam failure treated in the present study. Furthermore, the FV-Method in Telemac-2D is explicit solving, whereas FE is implicit. The Finite Volume Method was tested in the hydrodynamic test cases with different schemes (Telemac-2D provides 7 of them). The HLLC scheme, combined with a smooth side wall, generates good results.

Figure 3.12: Results for FV-HLLC Scheme, $t = 72$ sec

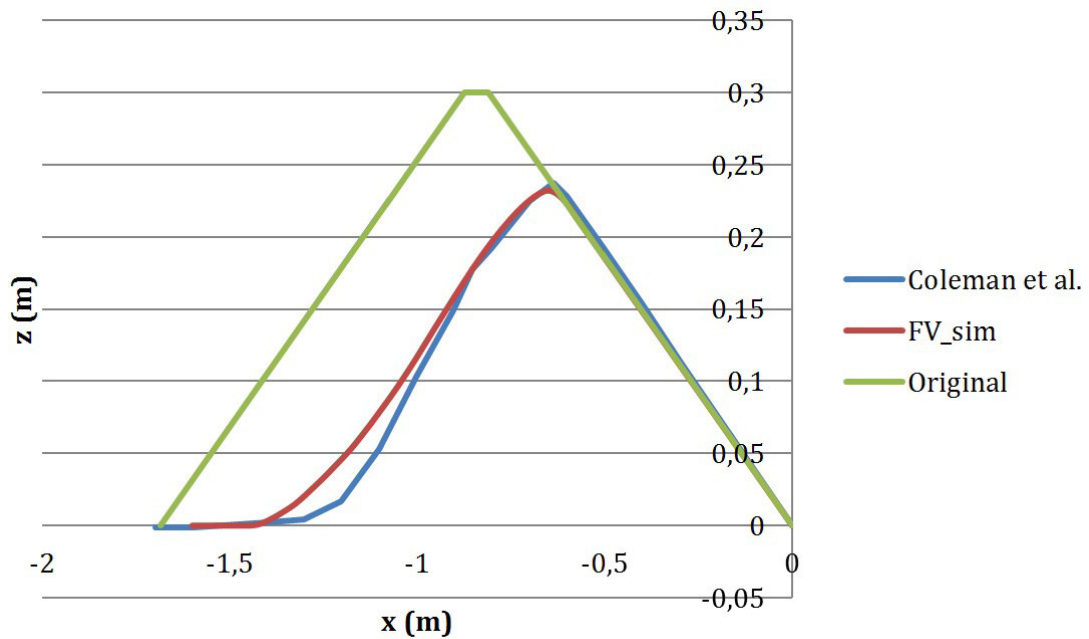
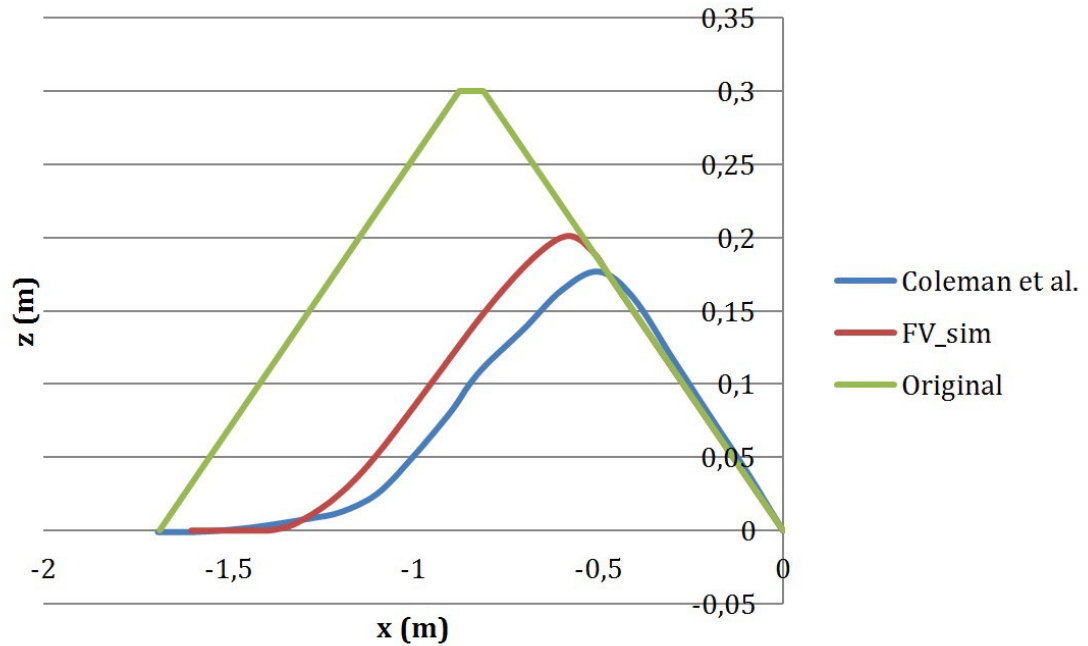


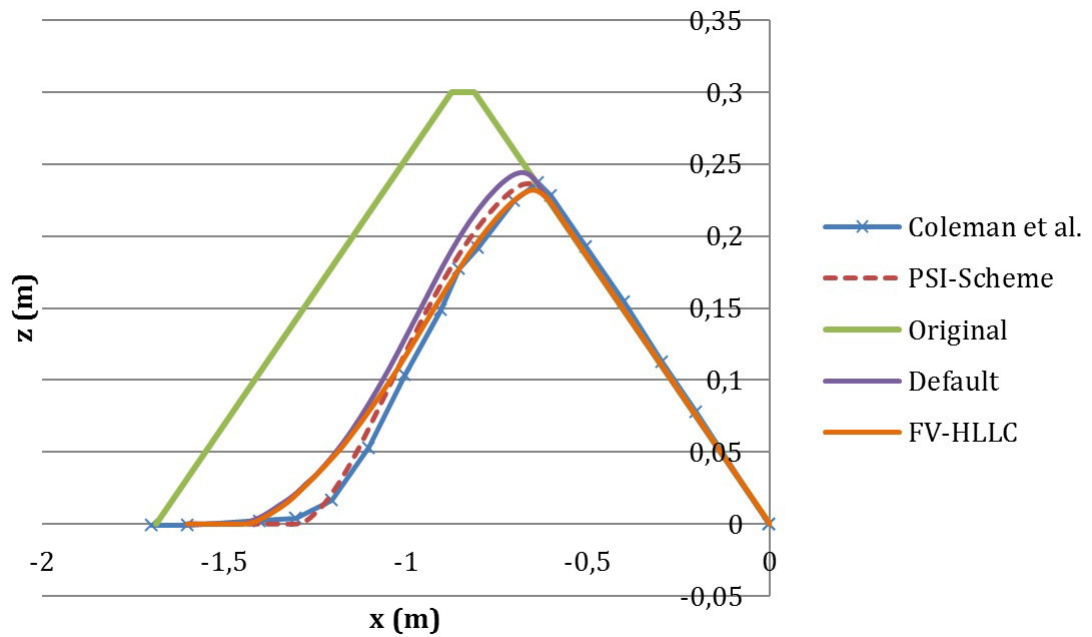
Figure 3.13: Results for FV-HLLC Scheme, $t= 100$ sec

A_{error} for the HLLC Scheme and a smooth side wall is 3.66 dm^2 ($t=72 + t=100$); in contrast, HLLC reacts much more sensitive on friction at the side wall, producing an A_{error} of 6.06 dm^2 ($t=72$ sec and $t=100$ sec).

To compare the different variants tested in this hydrodynamic analysis, the profiles at $t=72$ sec are compared in Figure 3.14. It is clearly to see, that the PSI scheme achieves the closest approximation to the laboratory data (Coleman-line). Accordingly, the PSI scheme was selected as default for the following sedimentary parameter study, together with the other chosen parameters shown in Table 3.7. Although the FV-simulation scored a lower A_{error} for both time steps, the PSI was preferred, as it fits better at $t=72$ sec. Of course, the FV-method will be tested again in the part of the sedimentary modelling.

Table 3.7: *Chosen hydrodynamic settings*

Keyword	Value
Strickler roughness	92 m ^{1/3} /sec
Turbulence model	Constant eddy viscosity
Velocity diffusivity	10 ⁻⁶ m ² /sec
Method	Finite Elements
Type of advection	6;5 (Velocity; depth. 6=PSI scheme)
Mass Lumping	Yes
SUPG option	0;1
Time step	0.001 sec

Figure 3.14: *Comparison of hydrodynamic simulations at t=100 sec*

3.4 Sedimentary Modelling

3.4.1 Default Sedimentary Parameters

The default values for the sedimentary modelling, as they were also used in the hydrodynamic simulations, are shown in Table 3.8.

The results for this standard- erosion simulation are already presented in Figure 3.10 and Figure 3.11.

Table 3.8: *Default Sedimentary Parameters*

Keyword	Value
NUMBER OF SIZE-CLASSES OF BED MATERIAL	1
SEDIMENT DENSITY	2630
FRICTION ANGLE OF THE SEDIMENT	32
SEDIMENT DIAMETERS	0.0005
NON COHESIVE BED POROSITY	Default = 0.4
SLOPE EFFECT	YES
FORMULA FOR SLOPE EFFECT	Soulsby
FORMULA FOR DEVIATION	Talmon
PARAMETER FOR DEVIATION	0.85 (=Talmon's β)
SEDIMENT SLIDE	YES
BED-LOAD TRANSPORT FORMULA	Meyer-Peter-Müller (MPM)

3.4.2 Overview of the Sedimentary Sensitivity Analysis

In Table 3.9, the different simulations done in the sedimentary analysis are presented. The varying parameters, which are different to the default simulation, are printed bold.

Table 3.9: *Overview of the Sedimentary Simulations*

Sim.	Friction Angle	Formula for Slope	Formula for Deviation	Sediment slide	Sediment Transport formula	Porosity	Talmon's beta	Method
Sim. A (default)	32°	Soulsby	Talmon	Yes	MPM	0.4	0.85	FE
Sim. B	28°	Soulsby	Talmon	Yes	MPM	0.4	0.85	FE
Sim. C	36°	Soulsby	Talmon	Yes	MPM	0.4	0.85	FE
Sim. D	32°	Koch	Koch	Yes	MPM	0.4	–	FE
Sim. E	32°	Koch	Talmon	Yes	MPM	0.4	0.85	FE
Sim. F	32°	Soulsby	Koch	Yes	MPM	0.4	–	FE
Sim. G	32°	Soulsby	Talmon	No	MPM	0.4	0.85	FE
Sim. H	32°	Soulsby	Talmon	Yes	MPM_{mod}	0.4	0.85	FE
Sim. I	32°	Soulsby	Talmon	Yes	MPM _{mod}	0.3	0.85	FE
Sim. J	32°	Soulsby	Talmon	Yes	MPM _{mod}	0.4	0.4	FE
Sim. K	32°	Soulsby	Talmon	Yes	MPM _{mod}	0.4	mod	FE
Sim. L	32°	Soulsby	Talmon	Yes	MPM _{mod}	0.4	0.4	FV
Sim. M	32°	Soulsby	Talmon	Yes	MPM _{mod}	0.4	mod	FV

3.4.3 Variation of the Friction Angle (Sim. B, C)

The first variation in the sedimentary test series was done with a variation of the friction angle of the sediment. Two arguments support the reduction of the friction angle:

- As the dam is saturated with water, the grains get uplifted by the water pressure. As this uplift pressure is not represented in the present study, a method of representation could be the decrease of the friction angle.
- As the results presented in the hydrodynamic variations all show a too steep slope from $t=100$ sec onwards, the conclusion is evident, that the friction angle does not represent the state of the sediment-material in an appropriate way.

A simulation with a friction angle of 28° improved the slope at the dam base in $t=100$ sec, but still too less material erodes.

Figure 3.15: Results for a modified friction angle of 28° , $t=72$ sec (Sim. B)

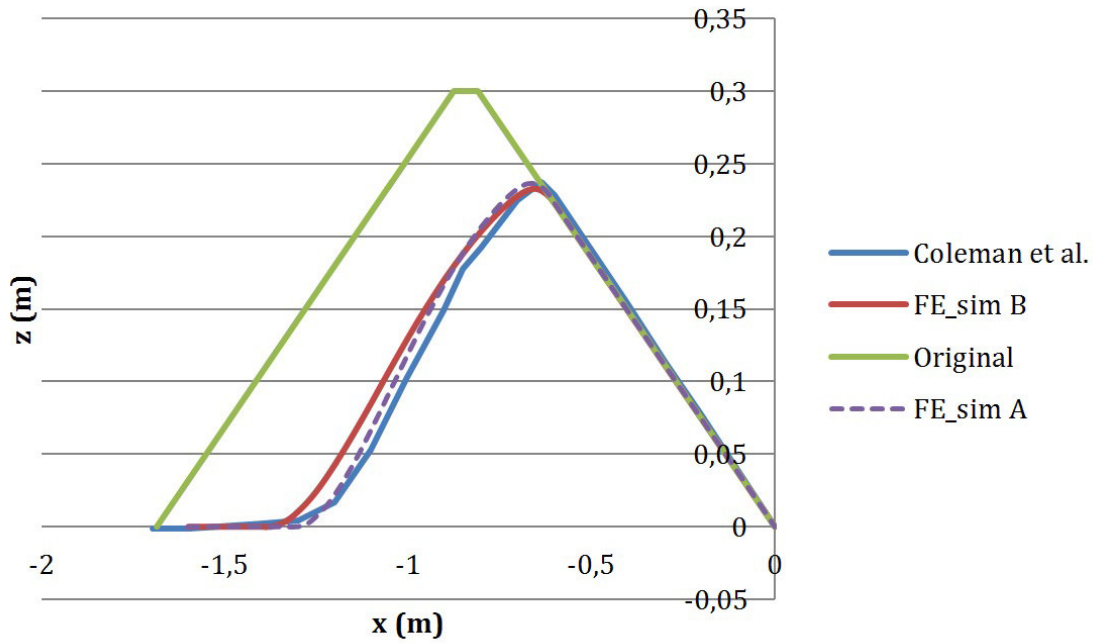
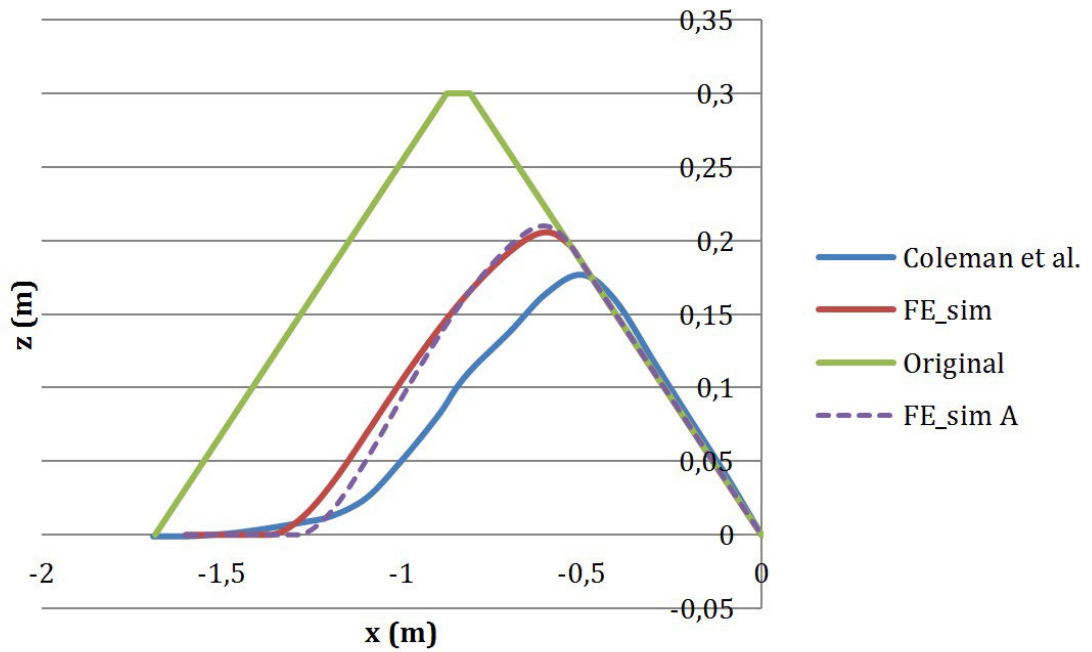


Figure 3.16: Results for a modified friction angle of 28° , $t=100$ sec (Sim. B)



3.4.4 Formulas for Slope Effect and Deviation (Sim. D, E, F)

Sisyphé provides different approaches for the calculation of the slope effect (Koch et Flokstra or Soulsby) as well as for the deviation (Koch et Flokstra or Talmon). In the simulations of the hydrodynamic sensitivity analysis, Soulsby and Talmon were used, as they worked well with the method of characteristics as advection scheme. In a series of calculations, the different combinations were tested with the PSI-scheme on non-conservative equation. For example, the combination of Koch/Talmon also achieved good results, A_{error} is even smaller than with Soulsby/Talmon. Nevertheless, in $t=72$ sec, the profiles fit better with Soulsby/Talmon, so this combination was kept.

Figure 3.17: Results for Koch/Talmon, $t=72$ sec (Sim. E)

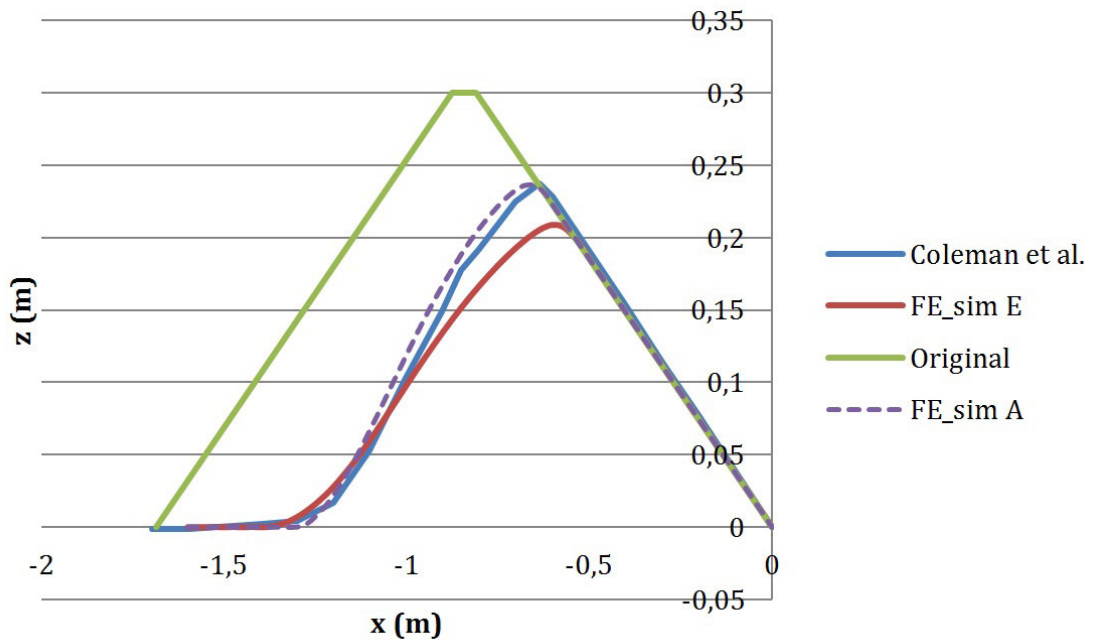
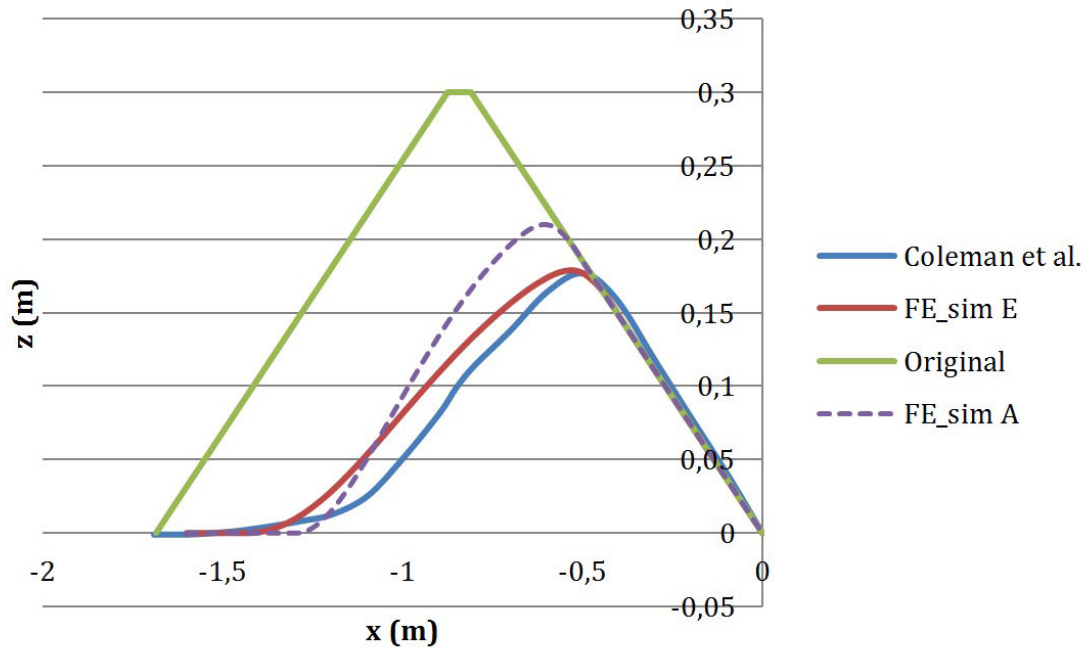


Figure 3.18: Results for Koch/Talmon, $t=100$ sec (Sim. E)

3.4.5 Sediment Slide (Sim. G)

As described before, the option called 'Sediment slide' enables material to erode, although it's not in contact with water. Therefore, the slope has to become bigger than the friction angle of the sediment. As this option is quite new in the Telemac-Suite, one simulation is done without Sediment slide, simply to test its function.

Figure 3.19: Breaching process without (left) and with (right) slide effect, $t=100$ sec

The breaching process without slide effect creates a very narrow and unnatural channel with steep side banks. On the other hand, the simulation with slide effect produces a much more realistic breach channel. Of course, the profiles of the channel axis fit much better with sediment slide.

3.4.6 Porosity (Sim. I)

As Coleman et al. [2002] do not mention any values for the porosity of the used material, the default value of 0.4 is used by Sisyphe. Sabbagh-Yazdi and Jamshidi [2013], who modeled the same test case numerically, used a porosity of 0.3 instead and achieved impressive accurate results with their FV-method. By decreasing the porosity (pore volume/total volume), the material gets more compact and due to that reason it shall be less erodible. A simulation proves the opposite of this assumption (Figure 3.20 and Figure 3.21), the reason for this behavior is not really known. However, the material tends to erode more with a lower porosity. The profiles fit better at $t=100$ sec, but in $t=72$ sec, too much erosion happens. A_{error} is reduced to 2.84 dm^2 , while in Figure 3.10 it was still 4.12 dm^2 .

Figure 3.20: Results for Porosity=0.3, $t=72$ sec (Sim. I)

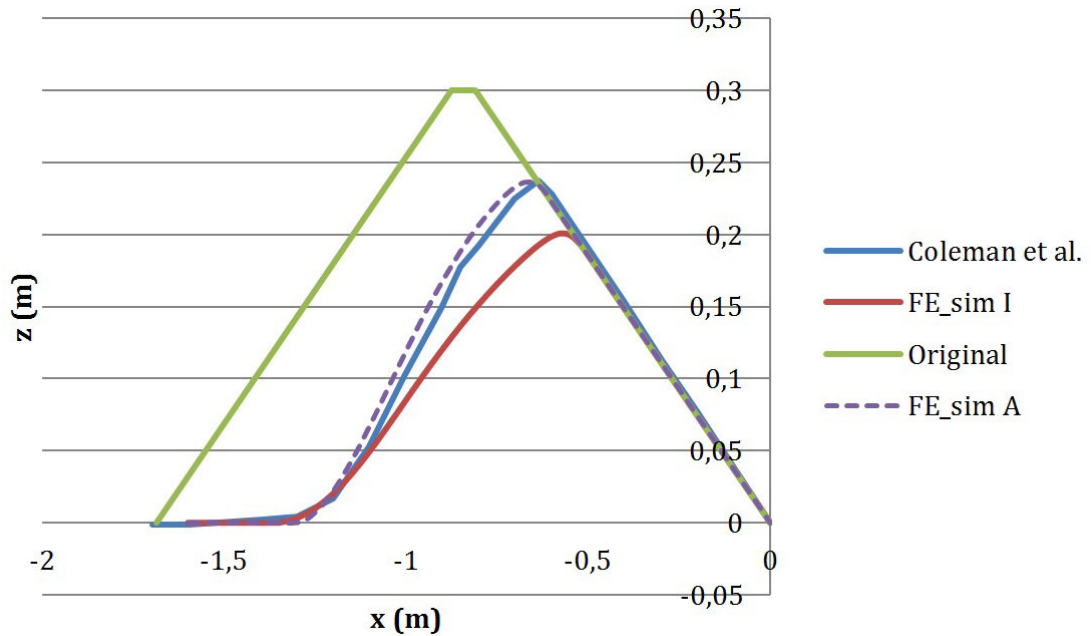
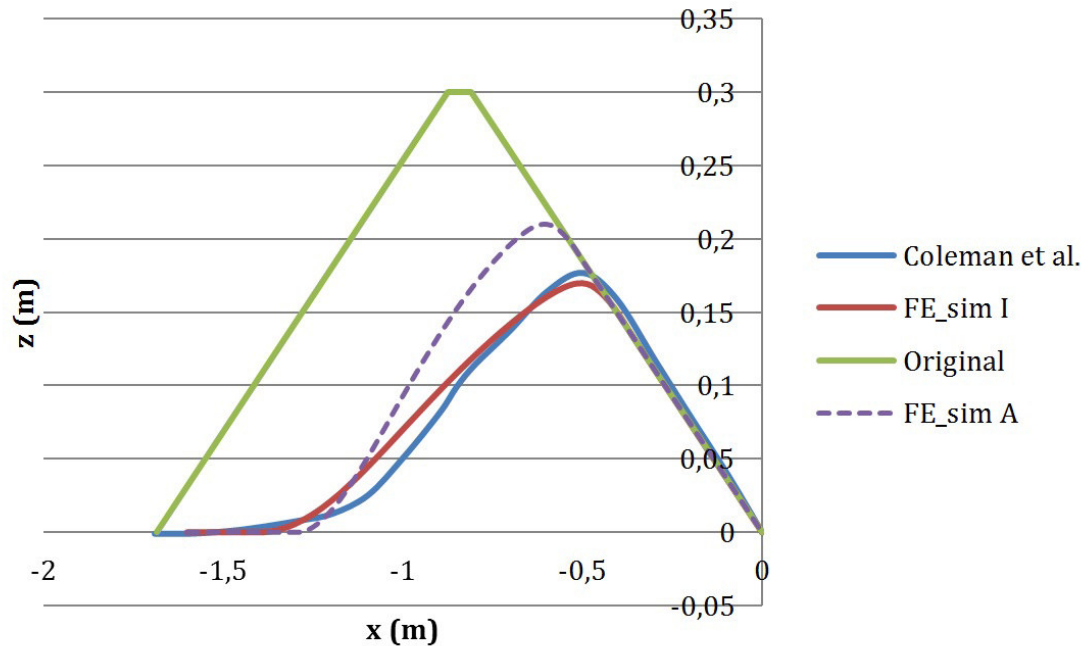
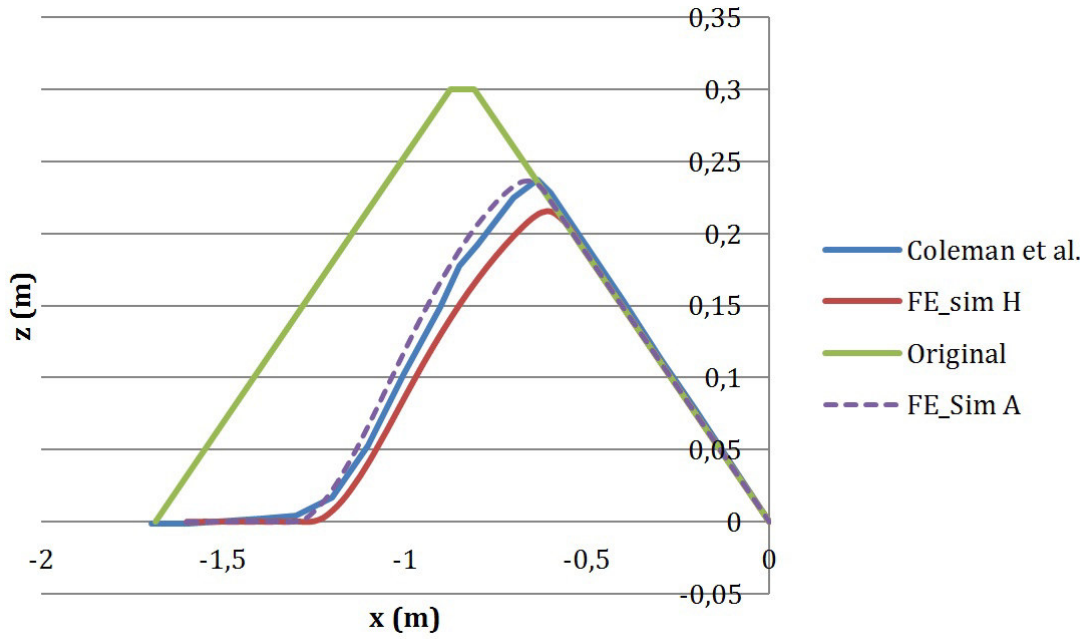
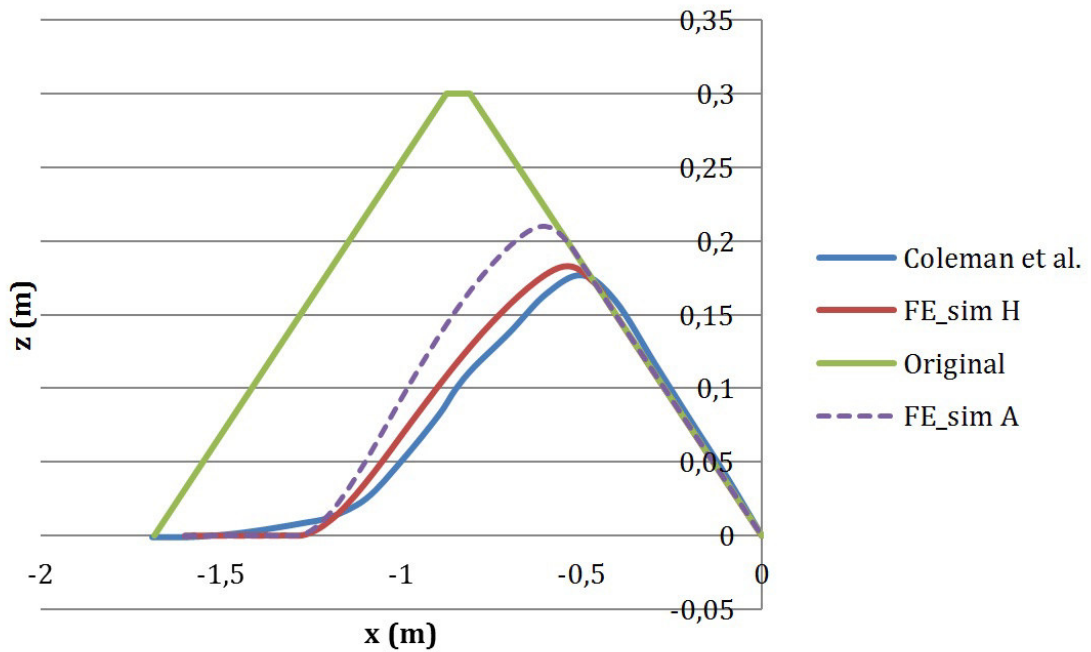


Figure 3.21: Results for Porosity=0.3, $t=100$ sec (Sim. I)

3.4.7 Modified Meyer-Peter-Müller Formula (Sim. H)

As shown in Table 3.9, the normal Meyer-Peter-Müller (MPM) Formula is used for the calculation of the sediment transport. MPM normally uses $\alpha = 8$, but as [Wiberg and Smith \[1989\]](#) argued, α can be replaced by $9.64 * (\text{Grain-Froude-Number})^{0.166}$. This modified MPM-formula was implemented in Sisyphe via a Fortran-subroutine, which can be found in the Appendix. With this modification, more material erodes than compared with the classical formula. Although in $t=72$ sec slightly too much material gets washed away on top of the crest, in $t=100$ sec the shape of the dam fits quite well to the empirical measurement data.

Figure 3.22: Results for the modified MPM-formula, $t=72$ sec (Sim. H)**Figure 3.23:** Results for the modified MPM-formula, $t=100$ sec (Sim. H)

3.4.8 Talmon's β -Value (Sim. J)

The different test cases have shown that the usage of Talmon's formula for deviation on transverse slopes leads to the best fitting results. The calculation in Sisyphe is as shown in (2.6).

Talmon et al. [1995] describes in the original paper of the derivation of the formula an alternative way of calculating β by using Van Rijn's approach (3.3).

$$\beta = 9 * \left(\frac{d_{50}}{h}\right)^{0.3} \quad (3.3)$$

Sisyphe uses a default value of $\beta = 0.85$, but Talmon et al. [1995] mentions, that for laboratory test cases, β can be reduced to its half. As in the present study, a laboratory experiment is simulated, a simulation with a reduced $\beta = 0.4$ was carried out, with the consequence of achieving better results at $t=100$ sec. At $t=72$ sec, the erosion is also raised and now is further to much, but still in an acceptable range.

Figure 3.24: Results for $\beta = 0.4$, $t=72$ sec (Sim. J)

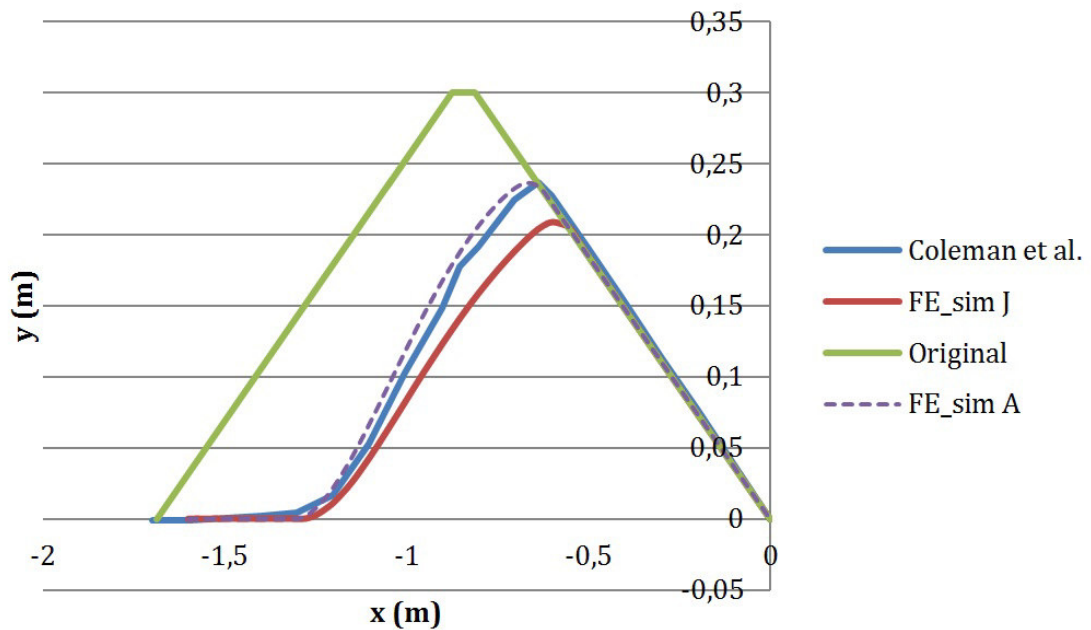
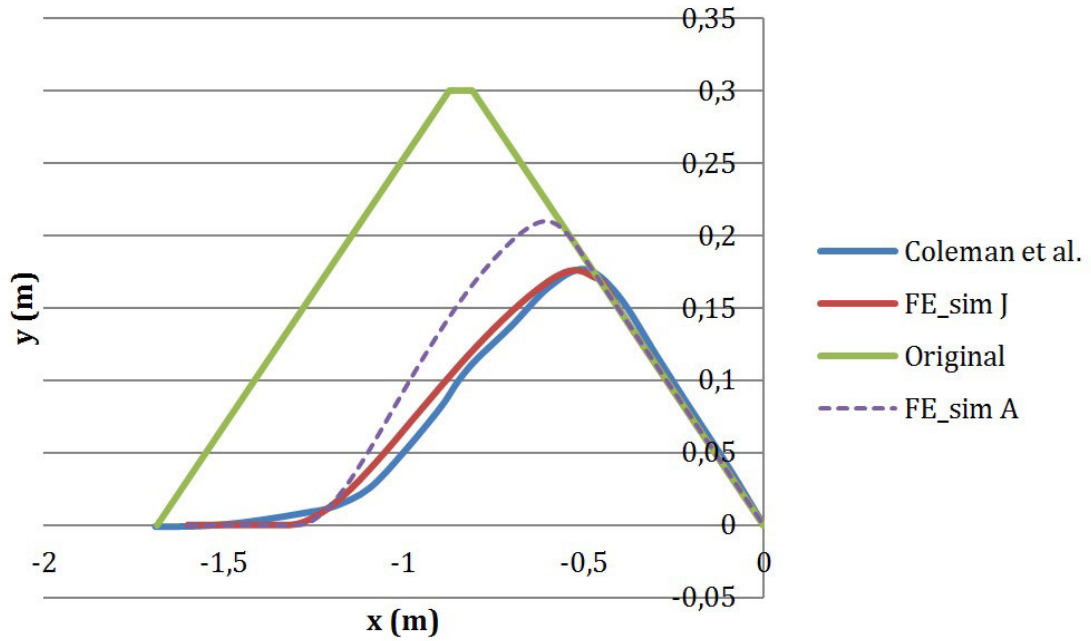
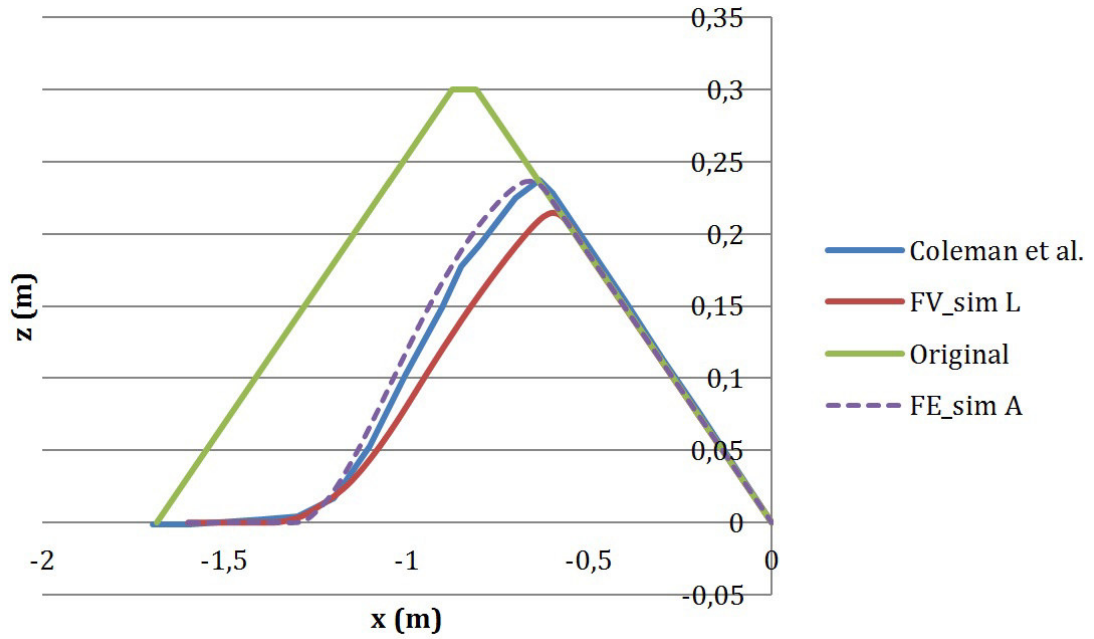
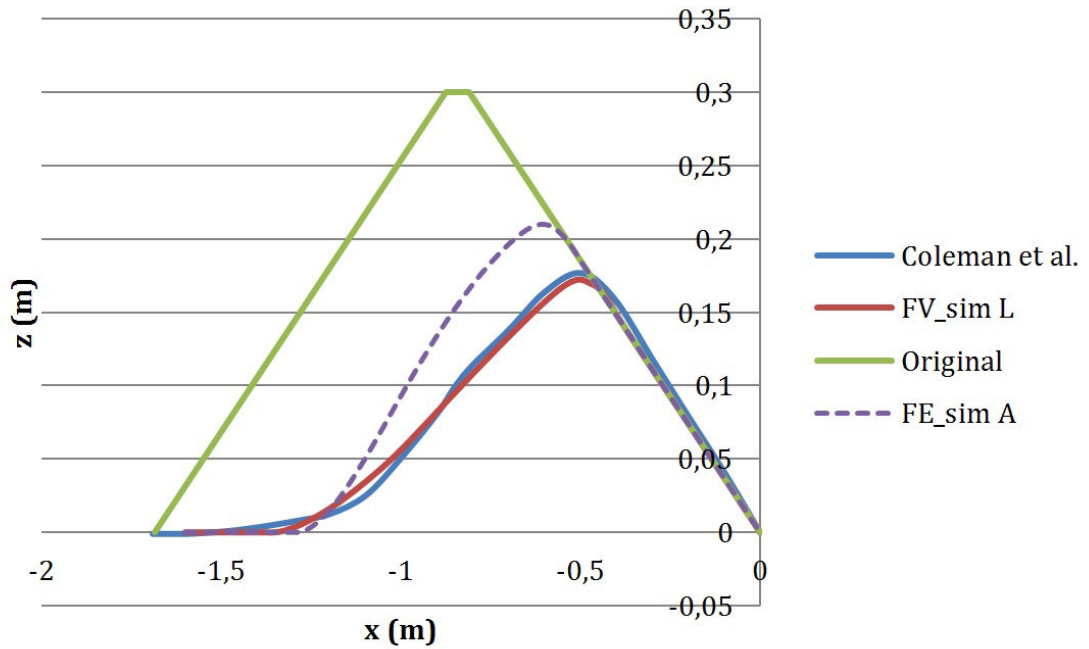


Figure 3.25: Results for $\beta = 0.4$, $t=100$ sec (Sim. J)

3.4.9 Finite Volume Method

As the hydrodynamic tests have shown, the Finite Volume Schemes like HLLC also achieve good performances. Simulation L was carried out with the same sedimentary options, like slope effect, deviation ($\beta=0.4$) etc. as the ones before, but the used hydrodynamic equations were FV-HLLC.

Figure 3.26: Results for HLLC with MPMmod, $t=72$ sec (Sim. L)**Figure 3.27:** Results for HLLC with MPMmod, $t=100$ sec (Sim. L)

With an A_{error} of 2.69 dm^2 , the FV-simulation achieves a lower value than all the FE-simulations before.

For simulation M, the variable calculation of β as presented in (3.3) was used. As the water depth is a changing value, β cannot remain constant. By implementing this variable formula and applying it in the HLLC-simulation with modified parameters, another improvement could be achieved. A_{error} sums up to an all-simulations-minimum of 2.03 dm^2 for the profiles of $72 \text{ sec} + 100 \text{ sec}$.

Figure 3.28: Results for HLLC with MPMmod and beta_mod, $t=72 \text{ sec}$ (Sim. M)

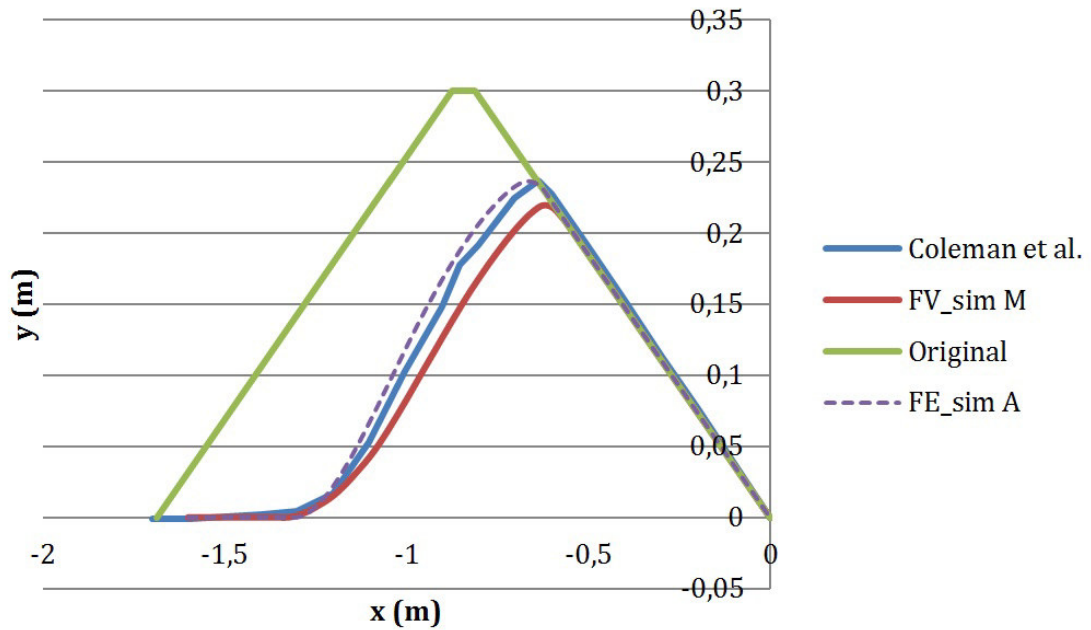
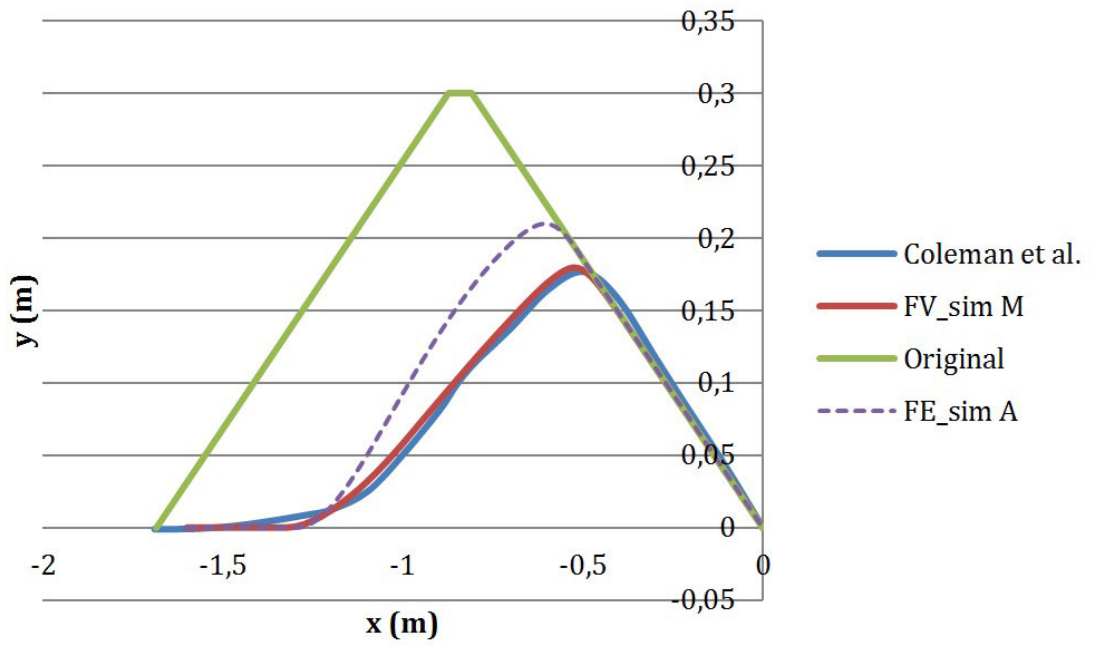
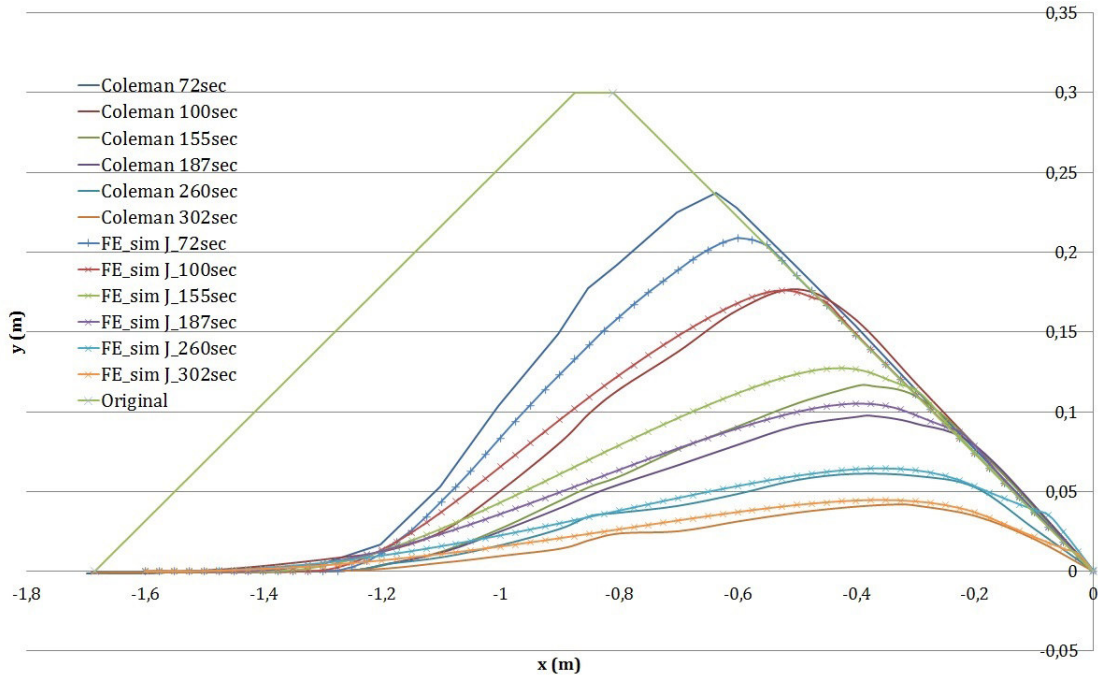


Figure 3.29: Results for HLLC with MPMmod and beta_mod, $t=100$ sec (Sim. M)

3.4.10 Results for All Time Steps

In this section the profiles of all six time steps – as it was published by Coleman et al. – will be compared to the results from the FE- and FV computations. As the FE-simulation J with the use of Talmon’s $\beta=0.4$ achieved the best fitting results, it will be shown here. The failure area A_{error} for all six time steps is 6.63 dm^2 .

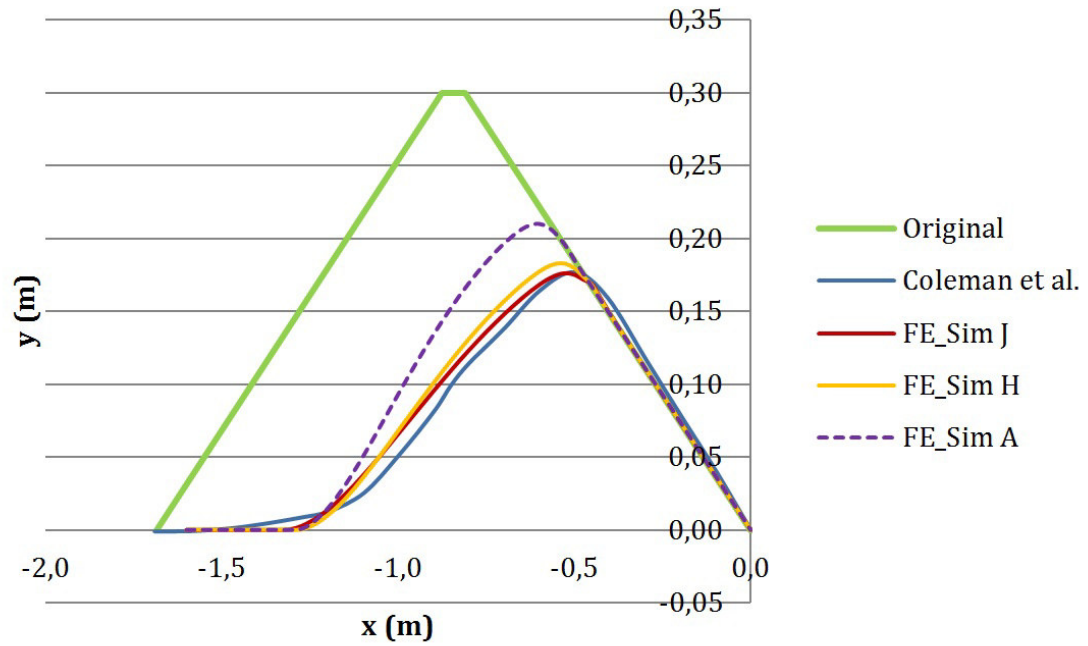
Figure 3.30: Comparison of Sim. J, all Time Steps (FE’s best)



The two most important changed factors for these results are the modified Meyer-Peter-Müller formula as well as the setting of Talmon’s β to 0.4. To clarify the influence of these two parameters, two simulations will be discussed without the appropriate factors.

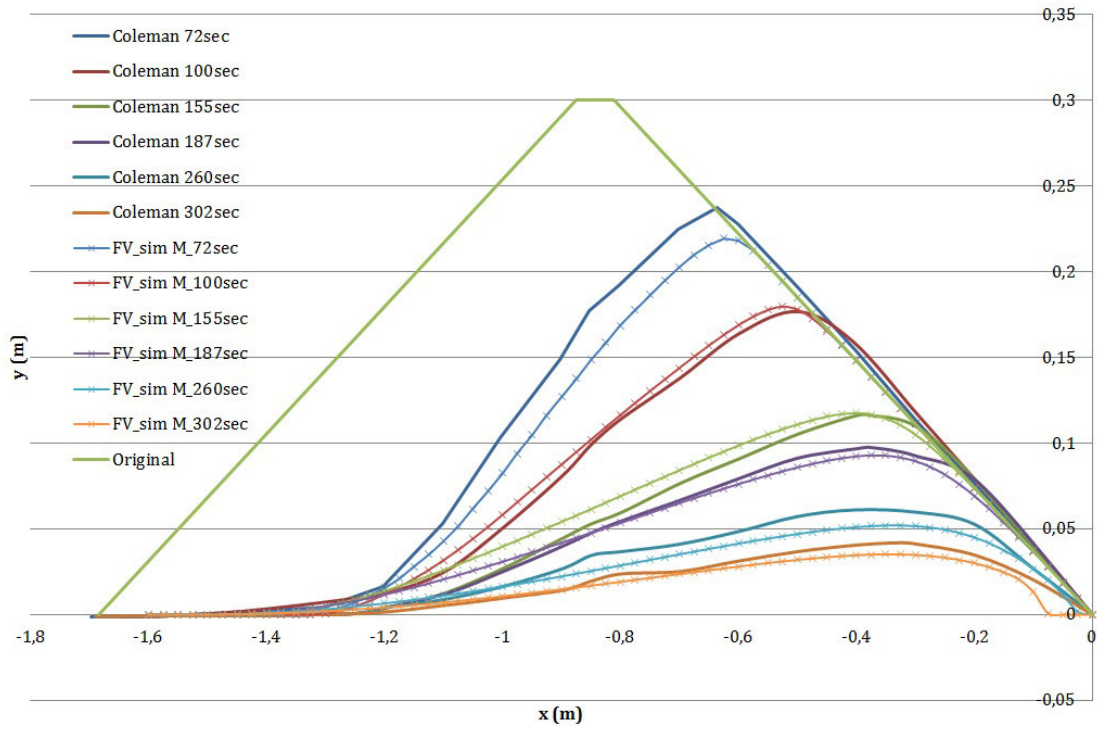
If β remains unchanged at 0.85, slightly less erosion takes place in all time steps. Thus, the profiles fit slightly better in the time steps from 100 sec onwards with $\beta = 0.4$. Only in $t=72$ sec, the failure-area is a little bit bigger than with $\beta = 0.85$. A_{error} for all time steps gets reduced from 8.30 dm^2 to 6.63 dm^2 by the change of β from 0.85 to 0.4.

If the normal Meyer-Peter-Müller formula is used instead of the modified one, the effect is much bigger. Although the results look good in $t=72$ sec, the results for the remaining time steps drift away enormously. A_{error} for all time steps then is 16.97 dm^2 . Figure 3.31 shows, that the modified MPM formula in combination with $\beta = 0.4$ (red line) generates the closest results.

Figure 3.31: Comparison of MPM versions and different beta-values at $t=100$ sec

In the FV-simulations, the use of the variable calculation of β led to the most fitting results (sim. M). In this case, A_{error} sums up to only 4.58 dm^2 for all six time steps. Special attention should be paid to the high accordance of the profiles in the later time steps. In Figure 3.33, a 3D view of different time steps of the erosion of the dam is shown.

Figure 3.32: Comparison of HLLC with modified Parameters, all Time Steps (Sim. M) FV's best

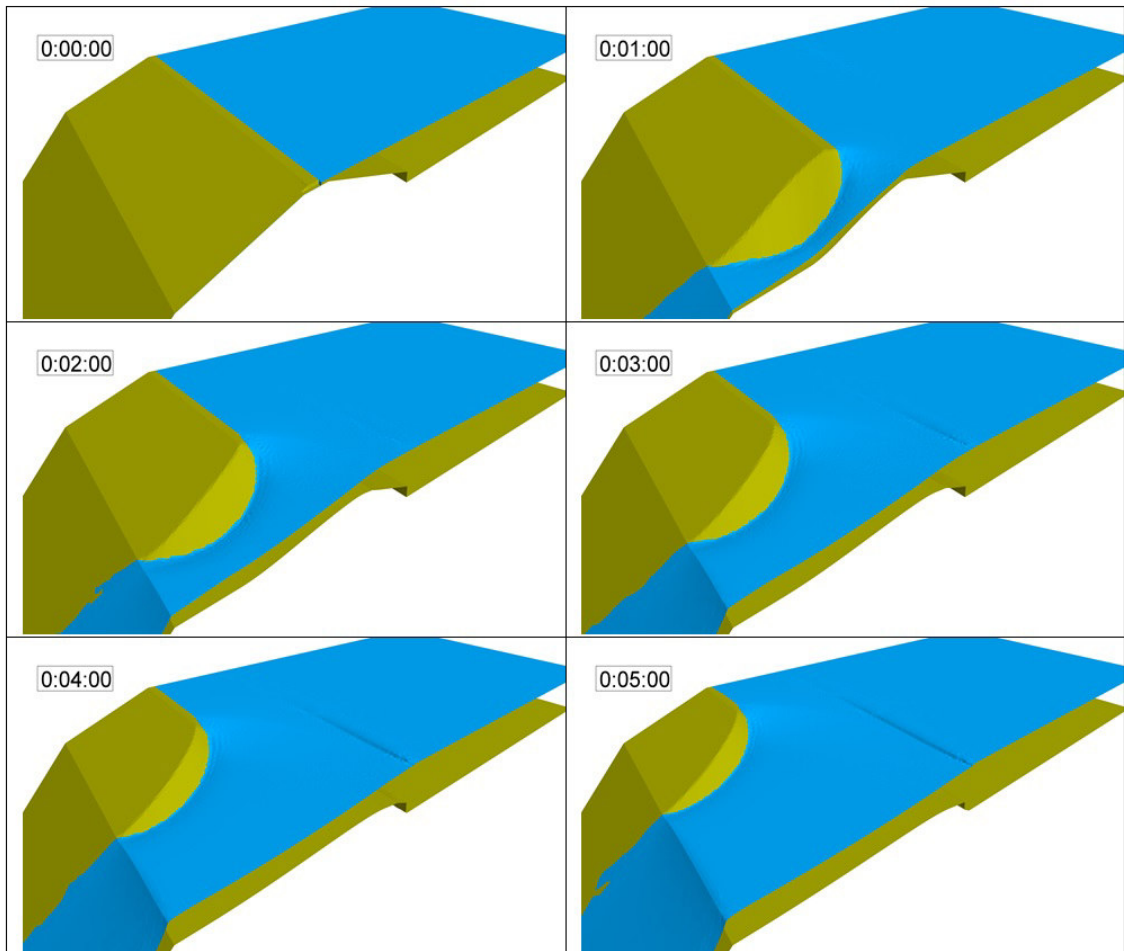


The non coinciding areas from the most important simulations are presented in table 3.10.

Table 3.10: A_{error} of important simulations

Simulation	$A_{error}(dm^2)$ (t=72 sec + t=100 sec)
Sim. A	4.12
Sim. H	2.77
Sim. J	2.69
Sim. K	2.81
Sim. L	2.22
Sim. M	2.03

The total area of the dam in its original form in this section is 25.50 dm².

Figure 3.33: *3D-View of various timesteps of the breaching process in Sim. J*

3.4.11 Cross Section of the Dam and Discharge

Figure 3.34: Channel Cross Sections, $t=72$, $t=155$, $t=260$ sec (Sim. J)

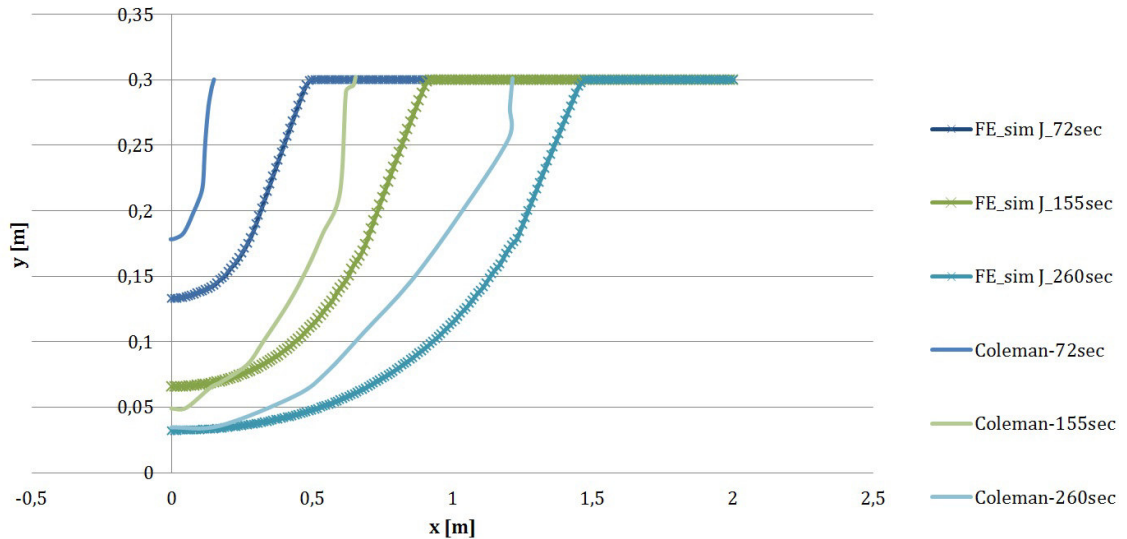
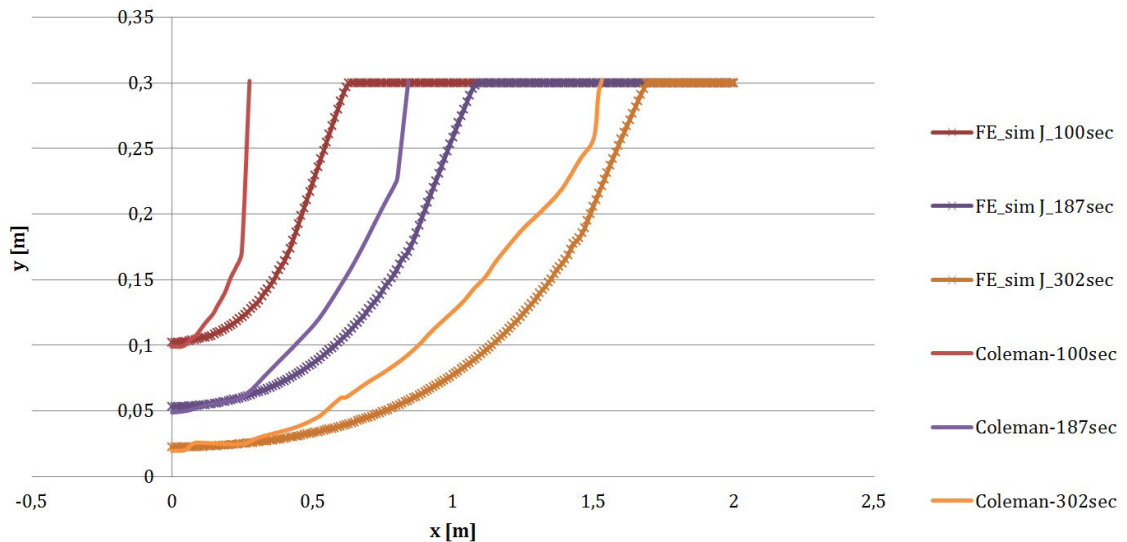


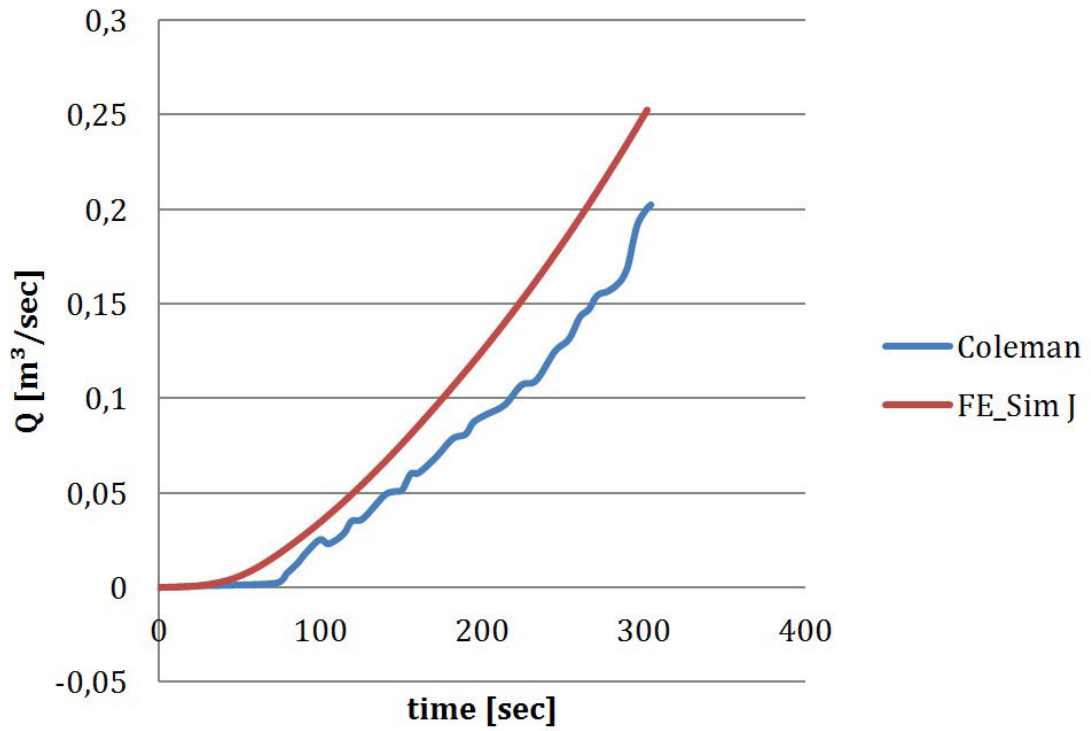
Figure 3.35: Channel Cross Sections, $t=100$, $t=187$, $t=302$ sec (Sim. J)



As shown in Figure 3.34 and Figure 3.35, the dam erodes faster in the simulation as it does in the laboratory (Coleman-data) in the cross sections of the dam. While the slopes in the cross sections from the simulation never exceed the friction angle, the slopes in the laboratory data are much steeper. As the material is sand, it is

usually without cohesion, but saturated with water, the sandy material becomes cohesive and consequently is able to resist steeper slopes. As the saturation of the embankment material was not considered in the Telemac-simulation, this effect is not represented in the results. According to that, the discharge is higher in the simulation than it is in the laboratory case (Figure 3.36).

Figure 3.36: Comparison of the discharge Q



3.5 Discussion of the Results

3.5.1 Hydrodynamic Factors

The most important hydrodynamic awareness is the difference between the computation with FE and FV. For example, if all the other influencing factors are kept equal but only FE and FV are changed, the results are changed significantly. A reason for this finding is not really identifiable, but it might be caused by the fact that FV is solving the shallow water equations explicitly. A general trend concerning the influence on erosion of FE and FV is hard to formulate, but the FV method usually generates slightly more erosion than the FE-method does.

A similar behavior is noticed at the different uses of the advection schemes in the FE-method. Three types were tested: No. 1 – Method of Characteristics, No. 6 – PSI scheme on non-conservative equation and No. 14 – Edge by edge implementation of the N distributive scheme. No. 1 is recommended in the Telemac-2D manual, but from the second time step (100 sec) onwards, in all profiles far too less erosion occurred, and even the first compared time step after 72 sec. was not that good. Scheme No. 6 managed to simulate the first time step much better, and although too less erosion happened in the later time steps, it worked better. Scheme No. 14 was calculating that slow, that no comparable results could be achieved.

A change of the turbulence model from the default eddy viscosity to the k-Epsilon model led to less erosion. Different velocity diffusivities, varying from 10^{-4} to 0, did not really influence the results.

3.5.2 Sedimentary Factors

The use of the modification of Wiberg and Smith for the Meyer-Peter-Müller formula was the most important factor for achieving the accurateness in the computed results. Without the modification, in the FE method, too less sediment was transported in all time steps from 100 sec onwards. With the use of the modification, the profiles fitted significantly better.

The second main parameter of the sedimentary variation was the changing of Talmon's β value for the deviation of grains on a transverse slope. In the FE-method, the use of a constant value of 0.4 led to the best fitting results, while in the FV-method the implementation of Van Rijns formula for β was more appropriate.

The activation of the slide effect was yielding a very realistic breach shape along the longitudinal profiles. Without it, a far too steep and narrow breach channel is produced, as only grains are allowed to erode which are directly washed away by the water.

3.5.3 Cross Sections and Discharge

Using the slide effect brings also something negative. The exact erosion of the bed material in with water saturated sand until the friction angle is reached, as it was computed in this chapter, is not really realistic, as the comparison with the measured

cross sections from the laboratory test case shows. According to the laboratory data, the side walls are able to stand steeper than the friction angle, as the sandy material becomes cohesive when it is saturated with water. This cohesion is not represented appropriately with the use of the slide effect.

Summarized, the findings of this case are:

- More erosion with Finite Volume Method than with Finite Element Method
- More accurate results with the PSI-advection scheme than with the method of characteristics
- Modification of Wiberg and Smith for Meyer-Peter-Müller formula increases approximation to the laboratory data
- Variation of Talmon's parameter for deviation (β) affects results – best results with Van Rijn's approach
- 'Slide effect' makes results more realistic

3.6 Computation time

As it is an aim of this work to compare the different methods of simulating two-dimensional water flows, also the according calculation durations shall be shown. Although many different simulations with a lot of different parameters, which are influencing the computation time, were carried out during the work for this chapter, only two groups depending the duration of the computation resulted, namely the FE and FV methods.

Table 3.11: *Computation Times*

FE	FV
173 min	249 min

(All calculations were done in parallel mode with four processors. The used computer has a Intel Core i5-3320M CPU with 2.60 GHz.)

4 Simulation of the Breaching Process of the Dam of a Snowmaking Reservoir

4.1 Introduction to the Snowmaking-Reservoir

The dependency on artificial snow in skiing regions is rising in order to guarantee the operation, which requires certain amounts of snow. Therefore, basins are needed for storing water for the snow production, like the Snowmaking-Storage, which is used for this applied case.

Figure 4.1: Example cross section of the storage

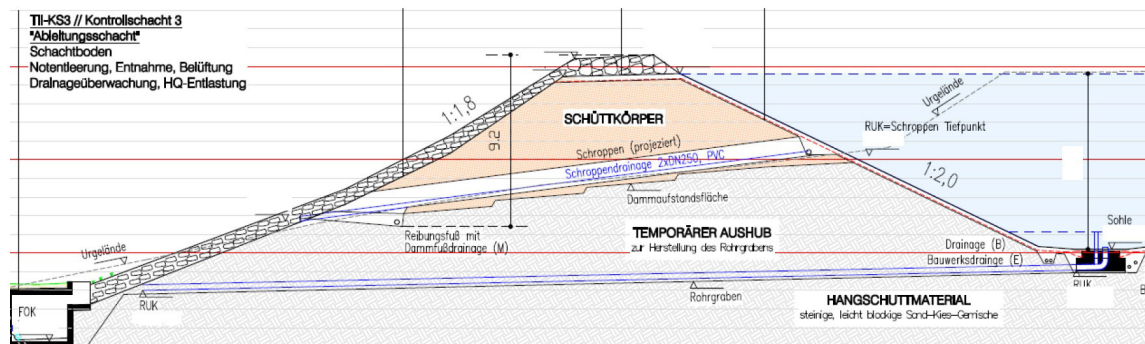


Table 4.1: *Data of the Snowmaking-Storage*

Width of the crest	3.5 m
Maximum height of the dam	approx. 11 m
Dam slope water-side	1:1.8
Exterior slope of the dam	1:1.75
Usable water volume at capacity level	approx. 30 000 m ³
Water area at capacity level	approx. 5000 m ²

In this part, the experiences of the Coleman-Case will be applied to this real case, by simulating the dam break of the above mentioned dam. As there are no measurement data for the comparison with the calculated results, they will be compared with results computed by the engineering office “Ingenieurbüro Moser GmbH Co KG”, who used the parameter model Deich (cp. [Deich \[2014\]](#)), developed by the engineering office Dr. Broich, for the calculation of the breach hydrograph and the 2D depth-averaged numerical model Basement (cp. [Basement \[2014\]](#)), developed at the ETH Zurich, for the flood wave propagation. In the following chapter, the flood calculation of the flood wave propagation is shown.

It has to be mentioned, that this simulated breaching process in Telemac-2D and Sisyphe is based on an assumption of a dam. In the real dam, for example a membrane is installed to protect the dam from erosion due to overtopping. Furthermore, the operation is controlled very detailed, in order to prevent such an overtopping-scenario. All this safety arrangements were not considered in the following simulations. In addition, in this simulation an initial pilot channel is modelled to start the erosion process, which of course does not exist in the real dam.

Table 4.2: *Dam Material for the Breach Development*

Grain diameter	5 mm
Grain density (dry)	2000 kg/m ³
Porosity	0.25
Friction angle	35 °
Strickler-roughness	63 m ^{1/3} /sec

4.2 The Calculation of the Dam Break Hydrograph

4.2.1 The Numerical Model

For the simulation of the development of the breach, the Mesh shown in Figure 4.2 was generated. It has a total number of 25492 nodes. In the area of the breach, the default edge length was reduced to 0.5 m, while it is 5 m at the border. For the definition of the initial water level and the rigid bottom, a 2D-line was drawn, which was read by the program via a subroutine. The command “inpoly” helps the user to check whether a node point is inside or outside a line. Thus, the user can easily set the initial water level of a certain region to a certain value, as the following excerpt shows:

```

OPEN(61, file = './waterline.txt', status = 'old')
DO I = 1, 33
read(61, *)XG(I), YG(I)
ENDDO
CLOSE(61)
DO I = 1, NPOIN
IF (inpoly(x(I), y(I), XG, YG, 33)) THEN
H%R(I) = 1849.61D0 - ZFU%R(I) = 0.D0
ELSE
H%R(I) = 0.D0
U%R(I) = 0.D0
ENDIF
ENDDO

```

“Waterline” is a text file containing 33 lines with coordinates of the water line. Inside the subroutine, it has the name “61”. With the function “Inpoly” it is checked, if the different node points (x(I), y(I)) are inside the read-in coordinates of the waterline (XG, YG) or not. Then, the relevant points get a water depth H defined by the desired water level minus the bottom elevation (ZF) of the certain point. In the same manner, the rigid bottom level in the area of the breach is defined, until where erosion might occur:

```

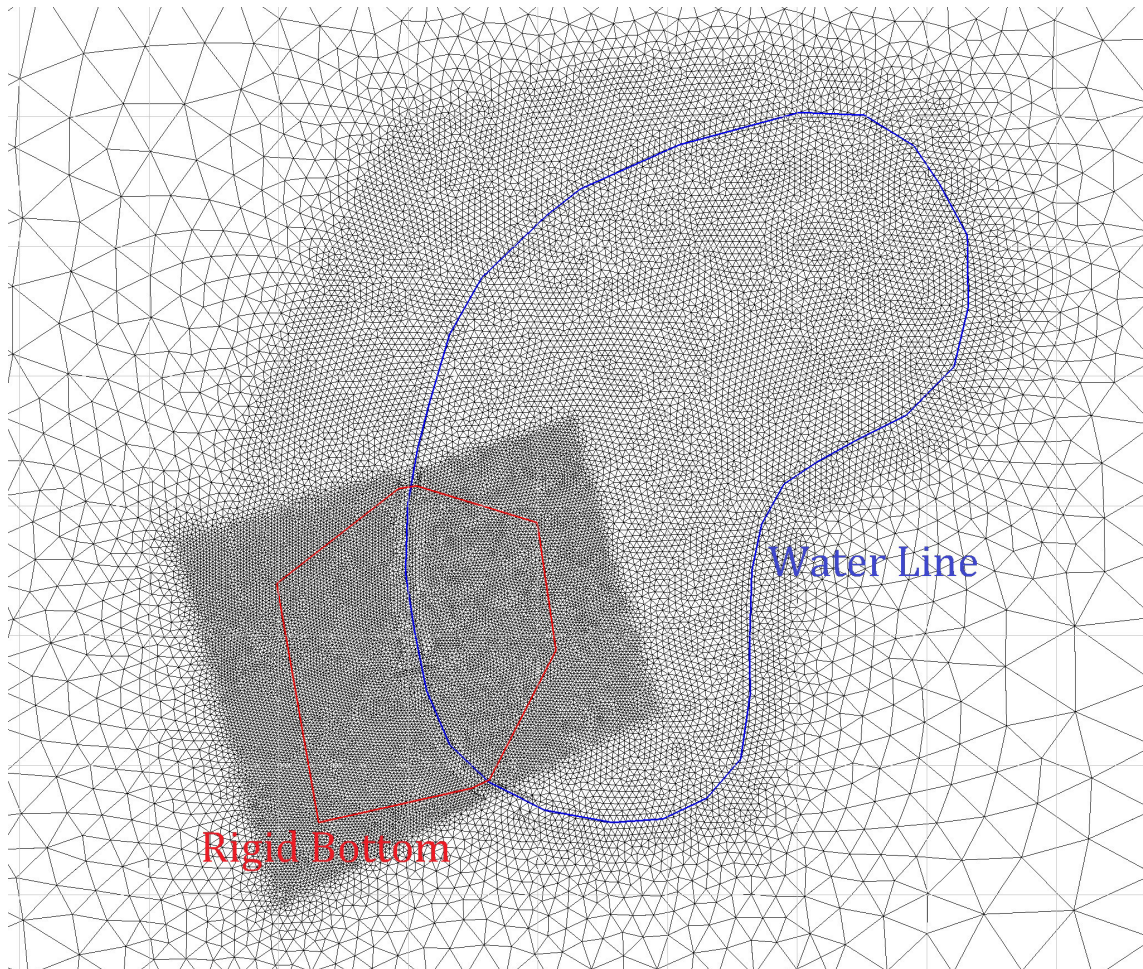
DO I = 1, NPOIN
IF (inpoly(x(I), y(I), XG, YG, 8)) THEN
ZR(I) = 1840.2D0
ELSE
ZR(I) = ZF(I) - 0.5D0
ENDIF
ENDDO

```

For all points in the area of the breach, the rigid bottom level is defined at a height of ZR=1840.2 m, which is the ground elevation of the reservoir. In all other points, the rigid bottom starts 0.5 m under the bottom level. That means, that the first

half meter of the surrounding area is erodible.

Figure 4.2: *Mesh of the Breach Simulation with waterline and rigid bottom level*



The material was the same as used in the calculation with Deich (Table 4.2). The initial breach is slightly different in the simulated model. Both have a difference in height of 0.3 m between the water-sided edge and the downstream edge with a slope towards downstream, but in the simulation model, the pilot channel becomes wider with its height, according to the materials friction angle. In the Deich-Input, the width of the initial breach channel stays constantly at 0.75 m. This modification in the numerical model was done because of the activated slide effect in Sisyphe. Without this adjustment, the slope of the side wall of the pilot channel would be much higher than the friction angle of the dam material (it would be rectangular), thus the material would slide down and the pilot channel would be closed.

4.2.2 Calculation

To illustrate the influence of the achieved modifications from the laboratory-case in chapter 3, four simulations will be presented in this chapter. The FE- and FV

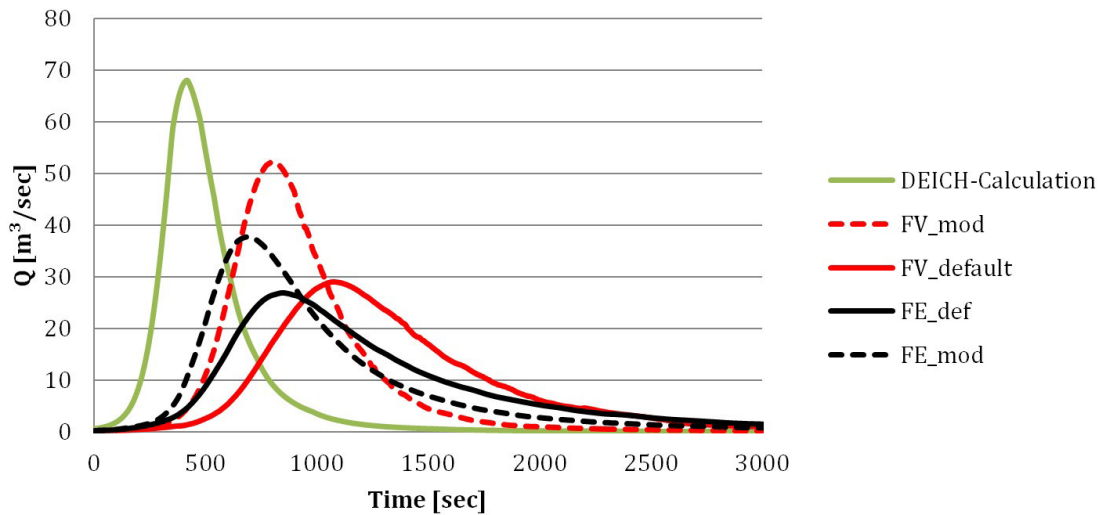
methods will be used, each of them with the modifications of the MPM-formula and Van Rijn's β -factor as well as without them.

Table 4.3: *Overview of Simulations for the Dambreak-Hydrograph*

	FV_ default	FV_ modified	FE_ default	FE_ modified
Sediment Transport formula	Classical approach of Meyer-Peter-Müller	Modified version of Meyer-Peter-Müller according to Wiberg & Smith	Classical approach of Meyer-Peter-Müller	Modified version of Meyer-Peter-Müller according to Wiberg & Smith
Deviation approach	Classical Talmon-Formula ($\beta=0.85$)	Talmon-formula with computed β with the formula of VanRijn	Classical Talmon-Formula ($\beta=0.85$)	Talmon-formula with computed β with the formula of VanRijn
Scheme	FV-HLLC	FV-HLLC	PSI scheme on non-conservative equation	PSI scheme on non-conservative equation

4.2.3 Results

Figure 4.3: *Comparison of various calculations of the Dam Break Hydrograph*



The hydrographs from the Telemac-2D simulations show, that the dam is not breaking as fast as the calculation of the Deich program assumes. Still, it creates very realistic outflow curves and again is proved that the combination of Telemac-2D and Sisyphe is able to simulate dam breaks – at least of homogenous material – in a very proper way.

Very clearly to see is the difference between the simulation with default parameters and the modified ones. The usage of the approach of [Wiberg and Smith \[1989\]](#) in the modified Meyer-Peter-Müller formula, combined with Van Rijn’s equation for β has a highly visible influence. The same effect as in the Coleman- study can be observed: The modification of the MPM-formula leads to a faster and more realistic erosion process, while the classical one seems to restrain it slightly too much.

The FV-method generally creates a faster outflow than the FE-method. Accordingly, the Finite Volume-simulation in combination with the modified parameters creates the highest peak-outflow and thus has the highest similarity with the Deich-calculation.

Furthermore it has to be mentioned, that the hydrograph curve created by Deich is also only a computed solution without the claim to be more realistic than the simulated solution.

Figure [4.4](#) shows 3D views of different time steps of the breaching process. It is clearly to see, that the outflow rises fast in the first few minutes and then is reduced slowly until the reservoir is almost empty, as described by the calculated hydrographs.

Figure 4.4: 3D-View of various timesteps from the modified FE-simulation

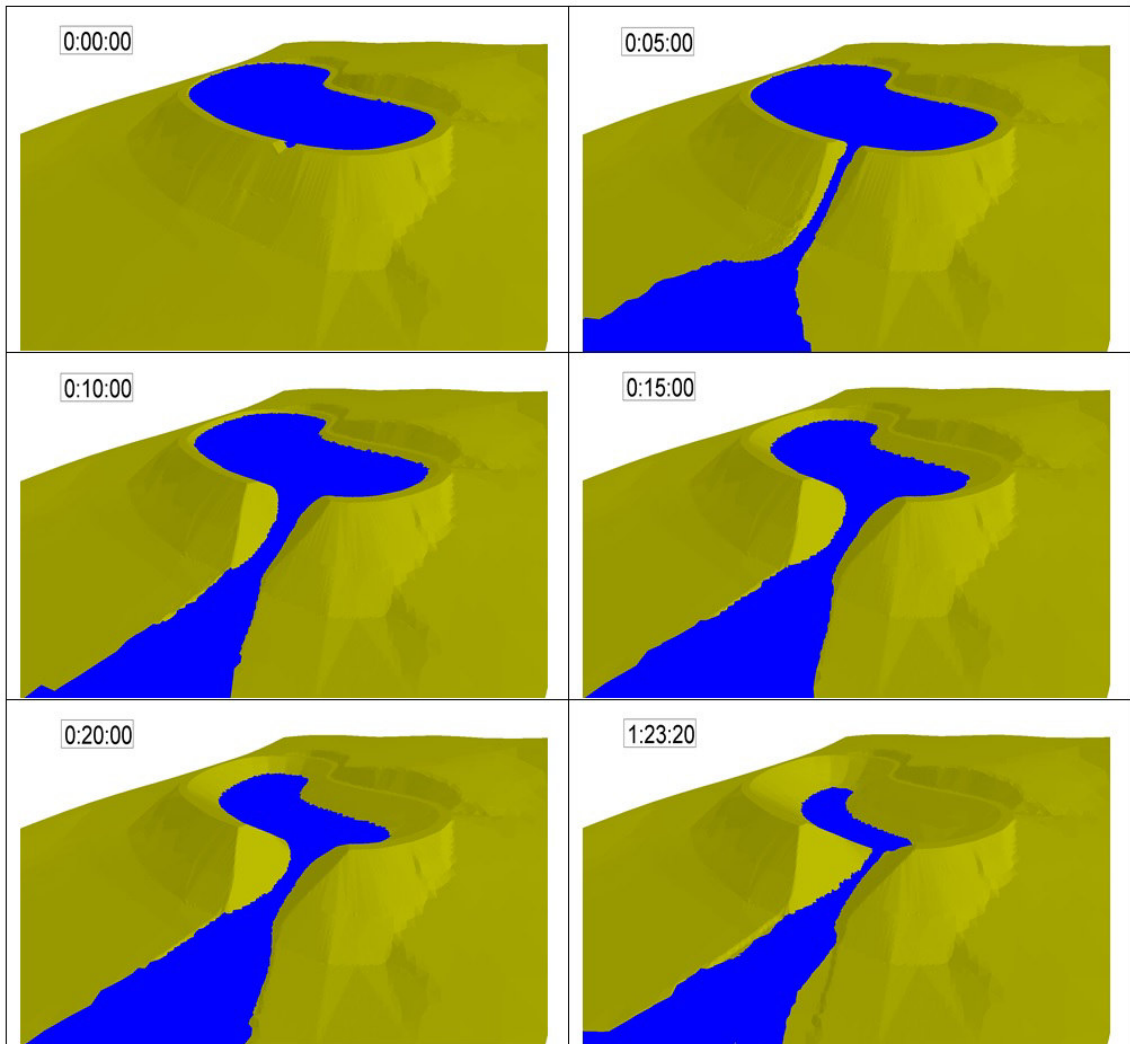


Figure 4.5: Velocity UV [m/s] at $t=10$ min

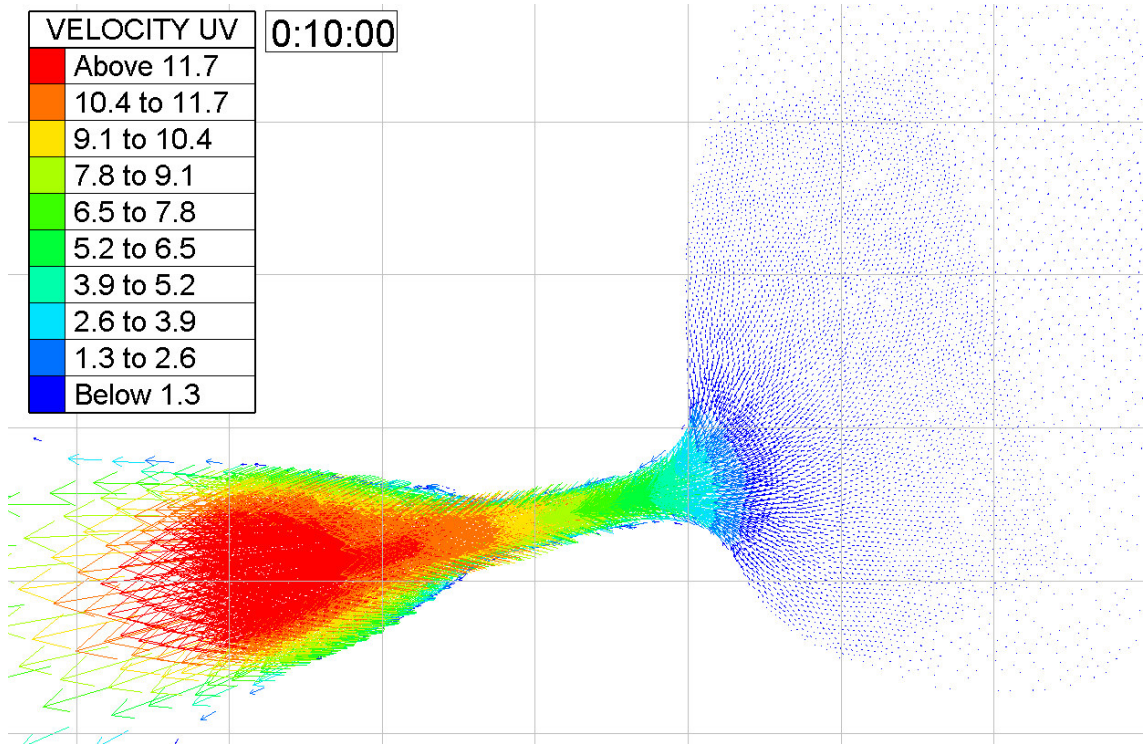
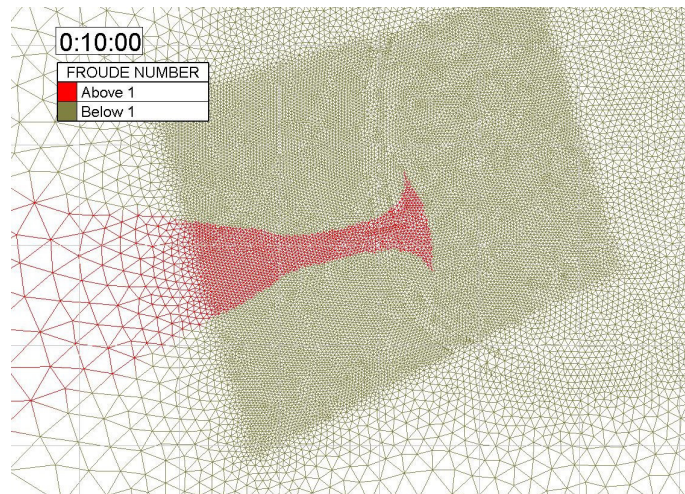


Figure 4.6: Froude-Number at $t=10$ min

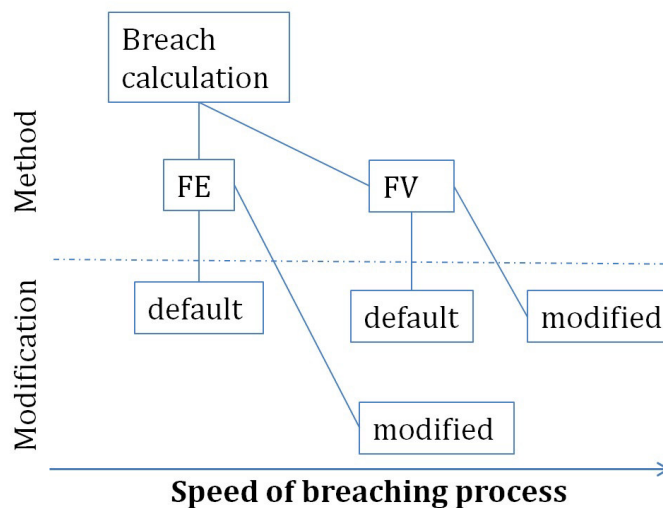


As shown in Figure 4.5, the maximum velocities during the dam break do not occur at the narrowest part of the dam break (the breach), but in the following section, where the flume is already a bit wider. This acceleration takes place according to the broadening of the cross section during supercritical flow and hence a lowering of the water depth in this area. The Froude-number is above 1 from the beginning of the breach.

4.3 Discussion of the Results

During the simulations in this chapter, most all of the awarenesses of the first chapter according the difference between FE and FV as well as the use of the modifications of the Meyer-Peter-Müller formula and Talmon’s β were confirmed. The comparison of the calculated hydrographs shows, that the FV-simulations create a higher peak outflow, which means that the breach is opening faster because of a faster erosion of the dam. The combined use of both modifications increases the velocity of the erosion process, leading to a further approximation of the computed results with Telemac-2D towards the results from the Deich-computation.

Figure 4.7: *Influence of Method and Modification on Breaching Velocity*



In Figure 4.7, the influence of FE or FV and the modification is shown. “modified” means that the modified MPM-formula and the variable calculation of Talmon’s β according to Van Rijn are activated, “default” means the classical MPM-formula and a β of 0.85.

4.4 Computation time

Table 4.4: *Computation Times*

FE_{def}	FE_{mod}	FV_{def}	FV_{mod}
138 min	142 min	126 min	117 min

(All calculations were done in parallel mode with four processors. The used computer has a Intel Core i5-3320M CPU with 2.60 GHz.)

5 Simulation of a Flood Wave Propagation

For the risk assessment of a dam, the estimation of the flood wave propagation of a possible dam break is an essential component. Therefore, science is investigating a lot in testing and comparing methods of calculating these propagations, for example the International Committee on Large Dams (ICOLD) arranged a benchmark workshop on numerical analysis of dams in 2013 ([Zenz and Goldgruber](#)), where the risk assessment of dams was one special topic.

In this chapter, the same water-storage as presented in chapter 4 will be used for the simulations of the flood wave propagation. Two different main flow directions are possible in case of a dam break of the storage, depending on the situation of the breach. If the breach is situated in the North-West, the flood wave will propagate towards the valley in the West, heading to region A. If the breach is located in the South-West, the water from the storage will flow into another reservoir, causing a secondary dam break. The water then will flow through the southern valley towards region B. To be able to compare the simulations with the reference-simulation done by “Ingenieurbüro Moser GmbH Co KG” with the program Basement, the dambreak hydrograph computed with Deich is used (see chapter 4).

To give an impression of the area, the 3D-view of the used mesh is shown in Figure 5.1. Furthermore, Figure 5.2 shows the elevation model of the region. The red line presents the main flow direction of both scenarios as the simulations will show. In Figure 5.3 the longitudinal section of flow line (red line in Figure 5.2) is shown.

Figure 5.1: *3D-View of the Mesh*

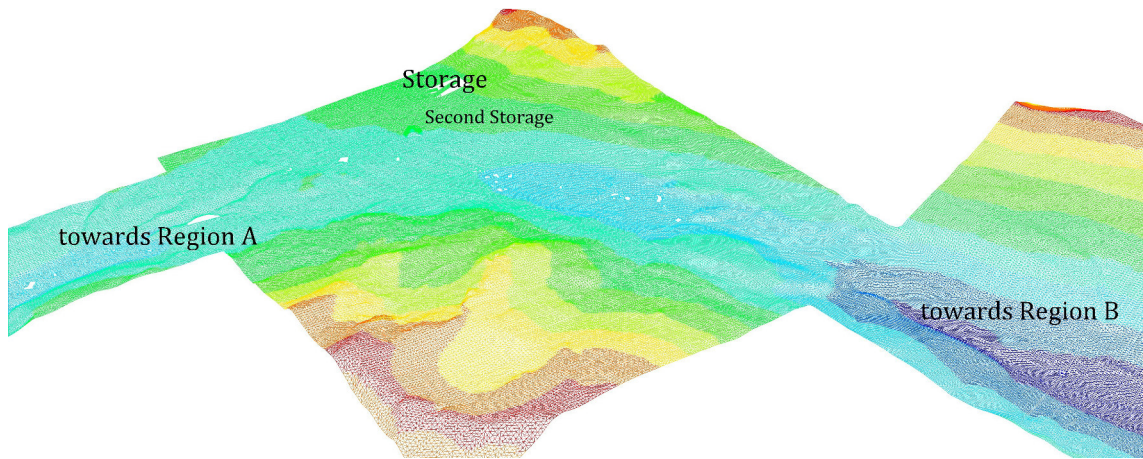


Figure 5.2: *Elevation model of the region*

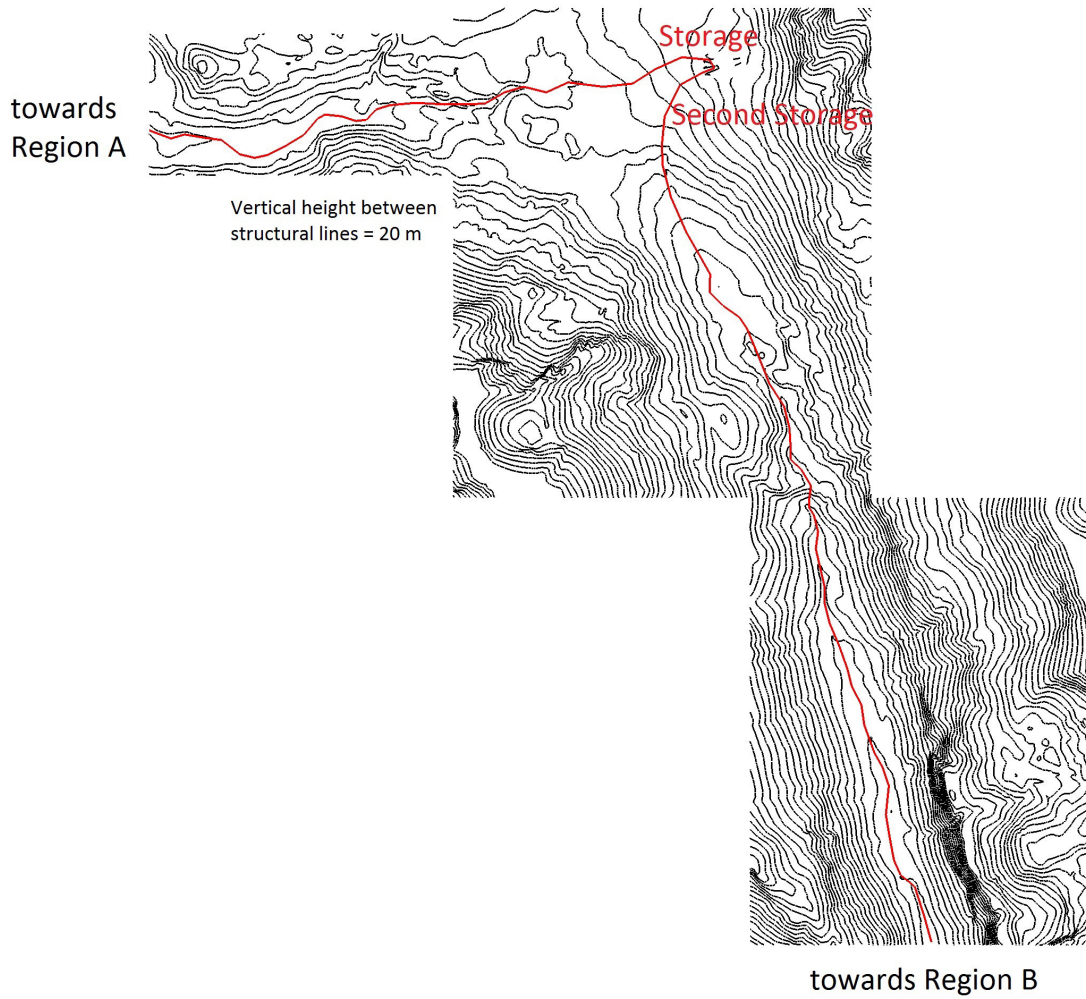
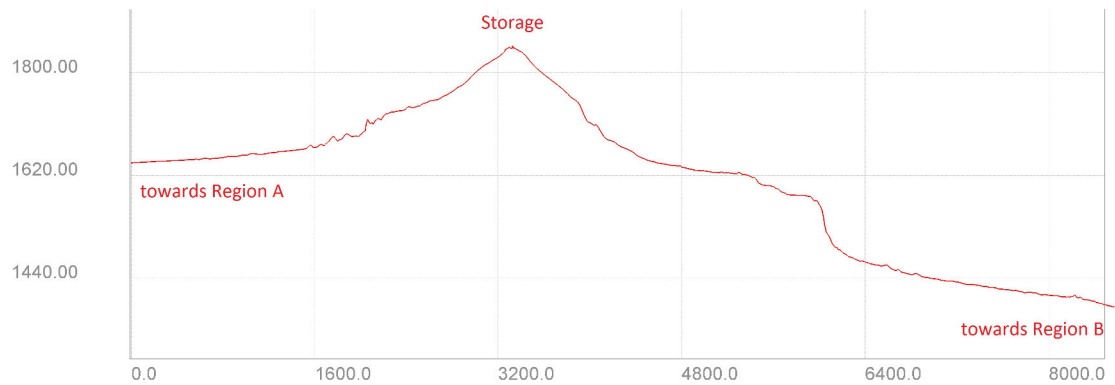


Figure 5.3: *Longitudinal section of the bottom elevations along the main flow directions*



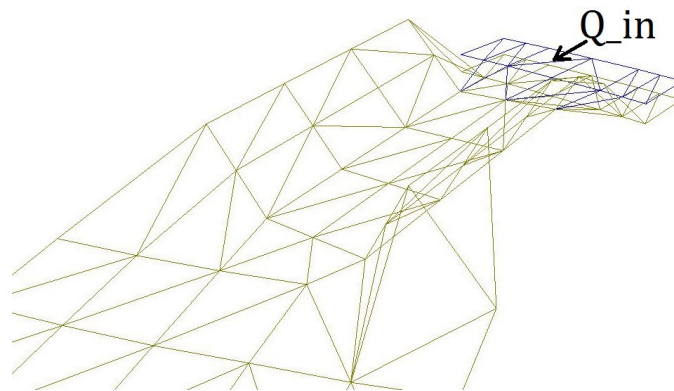
5.1 The Numerical Model

5.1.1 Boundary Conditions and the Mesh

If water enters at a dry boundary condition in the hydrodynamic model, it is not possible that only a discharge is given by the user. One further information has to be added, like the according water depth or the adequate energy slope. During this project, it was tried to enter the discharge curve together with a calculated water depth. The calculation of the inlet water depths according to the discharge was done with the open-source software “Bed Load Analyzer” ([Bed-Load-Analyzer \[2013\]](#)), which is developed by the Institute of Hydraulic Engineering and Water Resources Management at Graz University of Technology. During the checking of the inflow, a discharge at the boundary different to the entered one due to an unknown error in the program was observed.

Thus, a new method of entering the discharge was used, by creating a small pond at the very beginning of the inlet. Hence, the water does not have to enter in a dry boundary condition and it can be computed by Telemac-2D. The outflow from the pond into the terrain then happens as the outflow from a lake into a flume at critical depth, as the inlet channel is steep enough for super critical flow.

Figure 5.4: *3D View of the inlet channel for Scenario A with inlet-basin at $t=0$ sec*



To start the simulation with a prescribed water level in the before mentioned inlet ponds, a previous result file with an appropriate water level was connected to the simulation. By using the keyword “Previous Computation file” in the Telemac-2D steering file, it is possible to start a computation with initial values, as in this case an initial water level was added. Of course, it would be also possible to define the initial water level in a subroutine, as it was done in Coleman’s laboratory case. For both simulations, also the same mesh as in the Basement-calculation was used. It was already provided by “Ingenieurbüro Moser GmbH Co KG”, including the measurement-data for the heights of the terrain. It is a regular mesh with a default edge length of 10.0 meters (Figure 5.5). Important flow-disturbing items like buildings were left blank, as no water flow could happen in these areas. The roughness

data was also already defined by the engineering office, varying between $k_{st}=5$ and $k_{st}=50$ [$\text{m}^{1/3}/\text{sec}$]. While rigid areas as forests or built-up areas are modelled with lower values, smoother parts like the main road through the village were mapped with higher values (cp. Figure 5.1 and 5.6).

Figure 5.5: *Example of the Mesh-Structure*

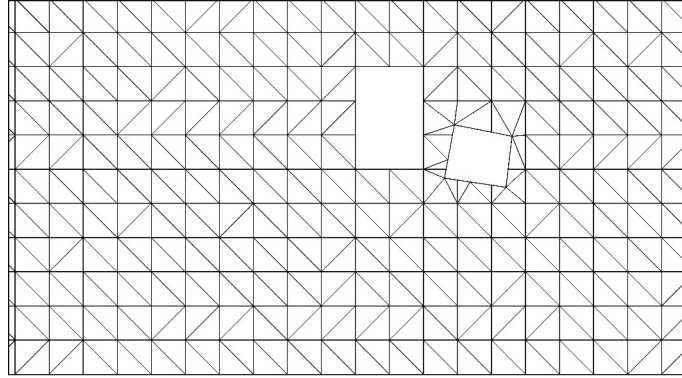
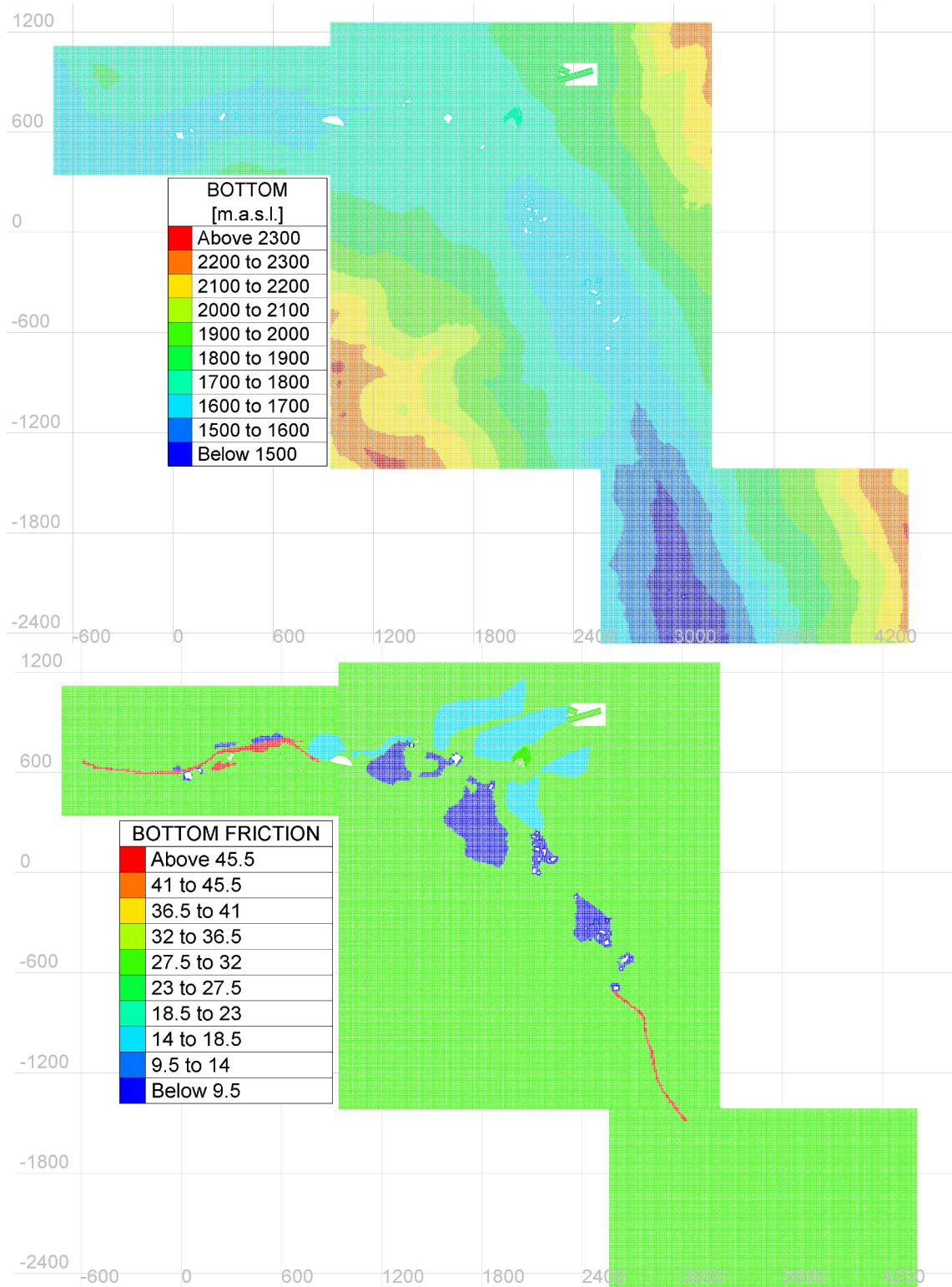


Figure 5.6: *Bottom elevation and bottom friction*

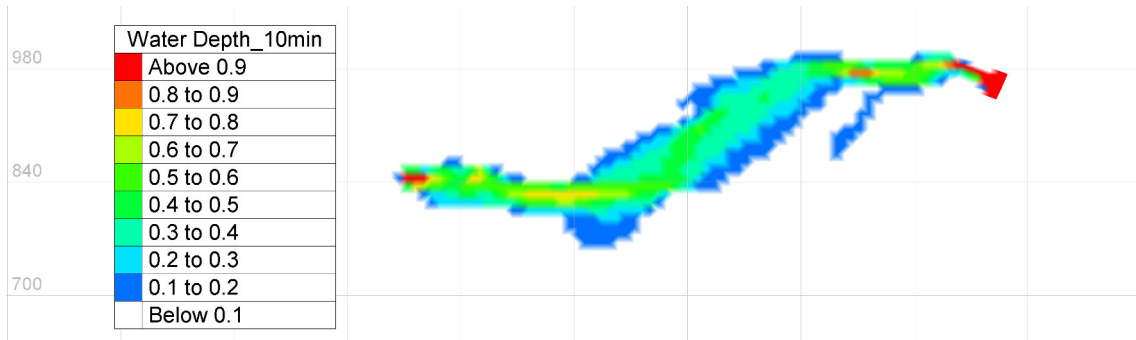
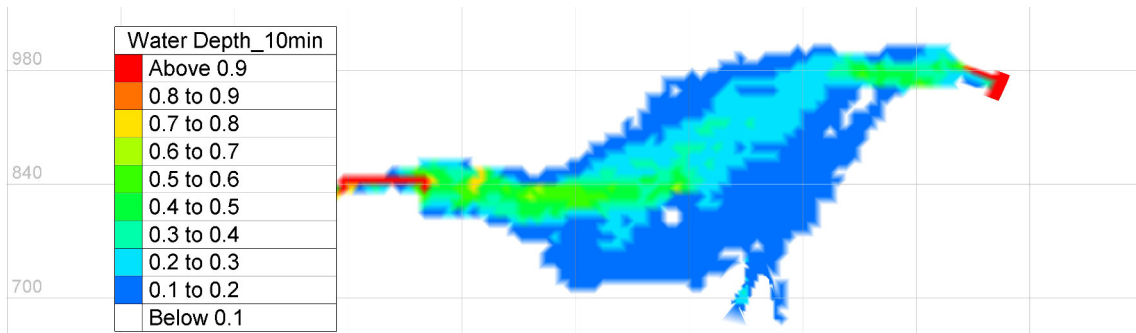
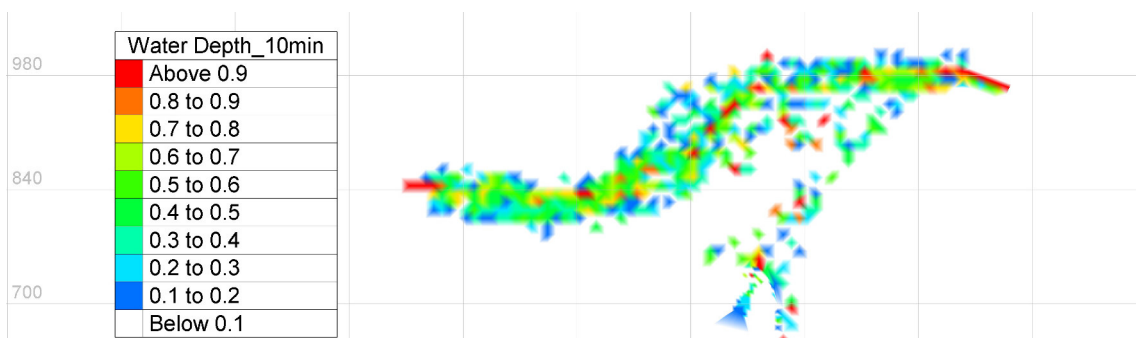


5.2 Scenario A

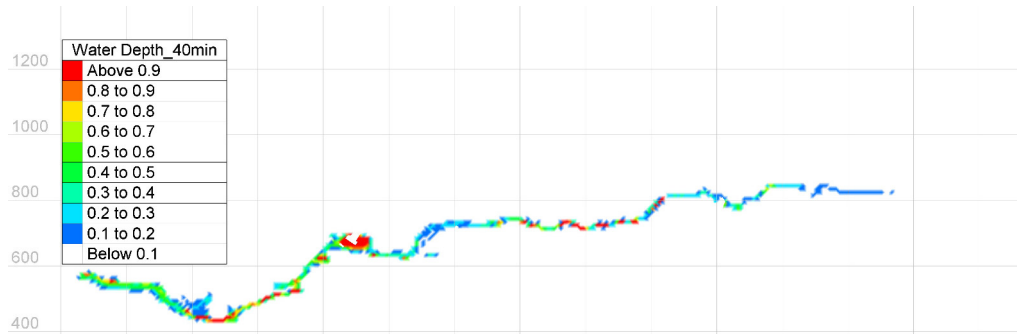
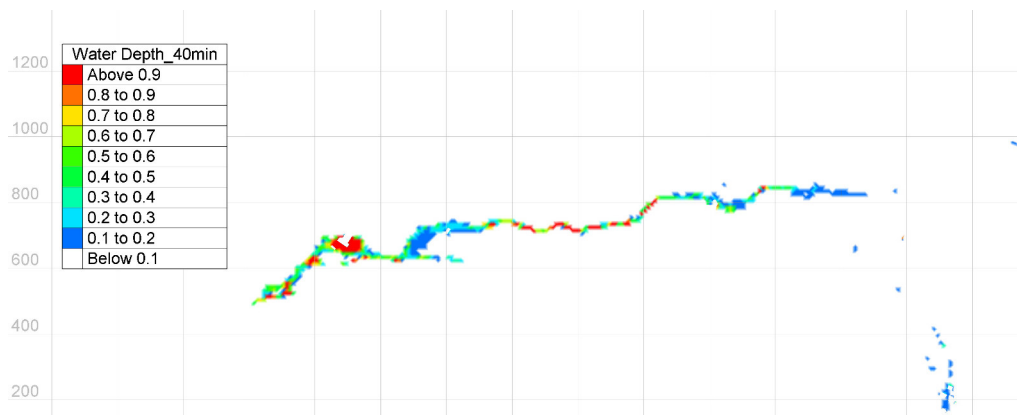
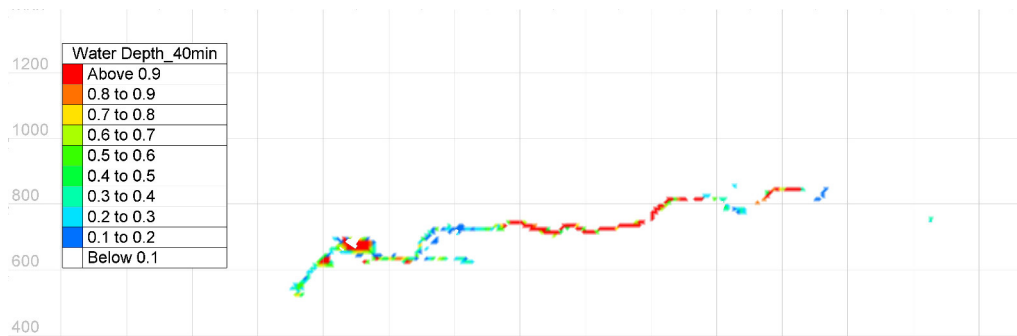
In the A-scenario, the inlet into the model is situated at the North-West of the dam. To create an initial velocity and flow direction, an artificial channel is implemented at the boundary condition. The inflow-discharge is modeled as described before in the section “Boundary Conditions”. The main flow direction (controlled by the inflow channel) accordingly leads the water to the West.

5.2.1 Results from Scenario A - Water Depths

To compare the results with the simulation done by the engineering office, the Water depth at two time steps and the stream power, here defined as the maximum of velocity times the water depth throughout all time steps, will be shown. The computation in Telemac-2D is done once using the Finite Elements Method and once with Finite Volumes. The simulation by the engineering office is also carried out with the Finite Volumes method.

Figure 5.7: *Water Depth after 10 min, Telemac-2D FE, Scenario A***Figure 5.8:** *Water Depth after 10 min, Telemac-2D FV, Scenario A***Figure 5.9:** *Water Depth after 10 min, Basement, Scenario A (questionable results)*

The first series of results compares the water depths after 10 min. The FE- as well as the FV-solution done with Telemac-2D fit well to the one by Basement. The Telemac-2D-FV-solution is spreading more as it wets a wider area.

Figure 5.10: *Water Depth after 40 min, Telemac-2D FE, Scenario A***Figure 5.11:** *Water Depth after 40 min, Telemac-2D FV, Scenario A***Figure 5.12:** *Water Depth after 40 min, Basement, Scenario A*

After 40 minutes, in the FE-solution the water flows faster as in the FV-simulations. It is remarkable, that the more slowly waterflow does not only take place in Basement's FV but also in Telemac-2D's FV calculation.

5.2.2 Results from Scenario A - Stream Power

To illustrate the intensity of a flood wave and its potential of damages, a common way is to show the stream power, here defined as the maximum of the water depth

multiplied by the velocity. With a division of the velocity into U and V, the stream power is calculated with (5.1).

$$\text{Streampower} = \max \sqrt{(U * H)^2 + (V * H)^2} \left[\frac{m^2}{sec} \right] \quad (5.1)$$

Figure 5.13: *Maximum Stream Power, Telemac-2D FE, Scenario A*

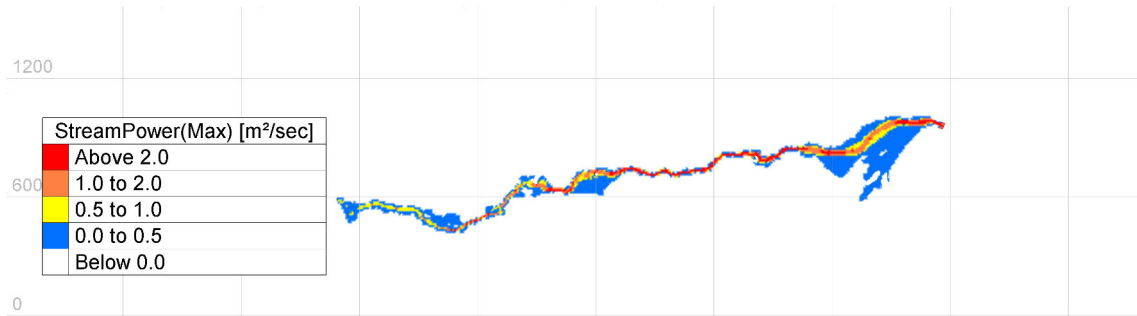


Figure 5.14: *Maximum Stream Power, Telemac-2D FV, Scenario A*

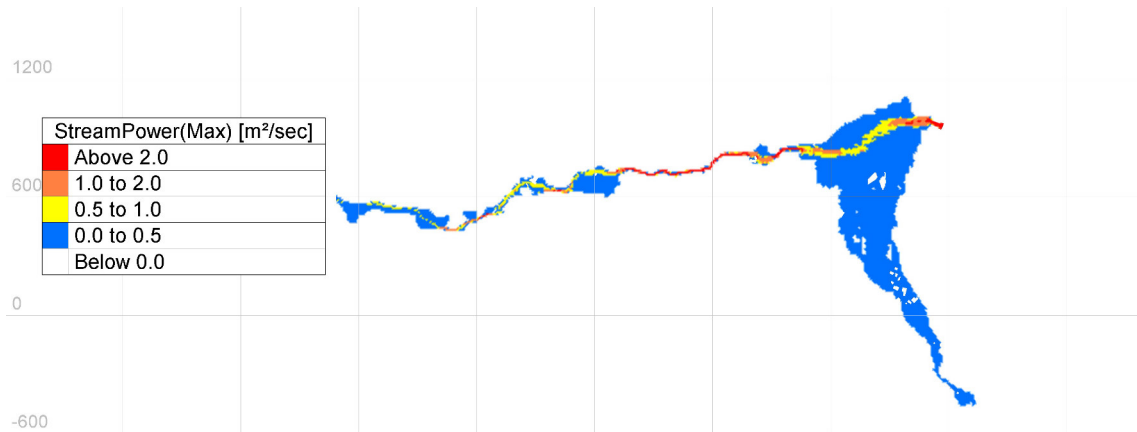
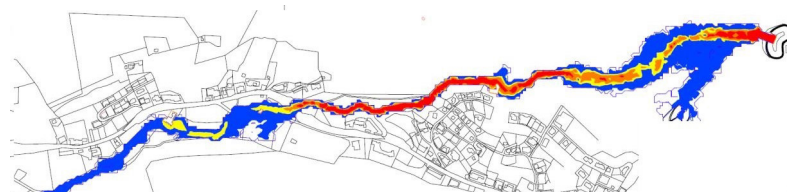


Figure 5.15: *Maximum Stream Power, Basement, Scenario A*



As the results after 10 minutes have already shown, the water in the Telemac-2D simulation is spreading more than in the other simulations. Due to that fact, the

stream power is also more spread in the Telemac-2D-FV solution. Apart from that, the results appear very similar in all of the three simulations and the maximum values coincide in most parts.

5.3 Scenario B

As already mentioned, a successive dam break of the downstream situated storage is probably, as the breach of the dam is located in the South-West in the B scenario and more water flows towards South. Again, the mesh used from the Basement-calculation was used for the Telemac-2D simulations. It has, like in the A scenario, a small pond at the inlet; the inflow channel is trapezoidal and is longer than the one from the A-inlet. In return, the inlet channel from the successive dam break is very limited, as a change in the mesh for creating an inlet channel would significantly disturb the flowing conditions of the from above coming water from the primary storage. The discharge at the secondary inlet was also modeled with a small pond.

5.3.1 Results from Scenario B - Water Depths

Figure 5.16: *Water Depth after 10 min, Telemac-2D FE, Scenario B*

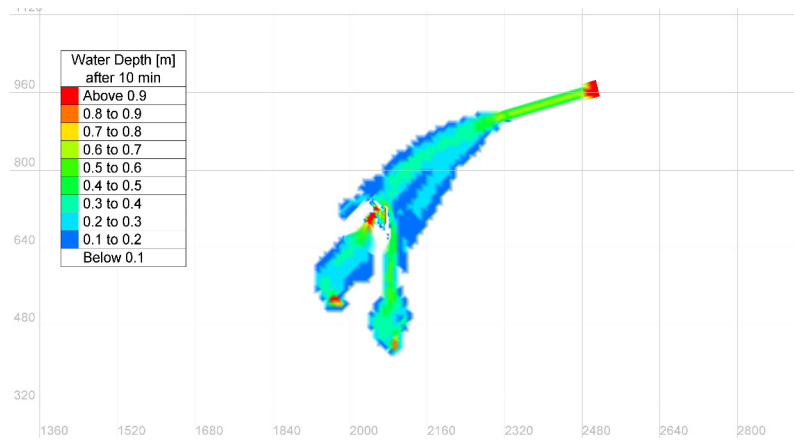


Figure 5.17: *Water Depth after 10 min, Telemac-2D FV, Scenario B*

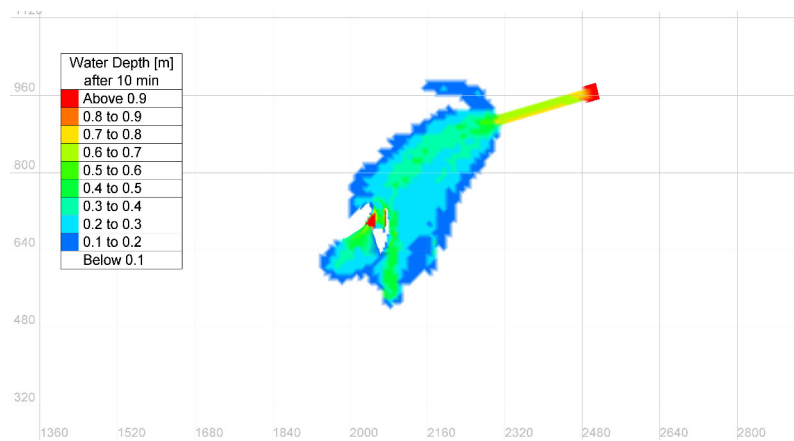
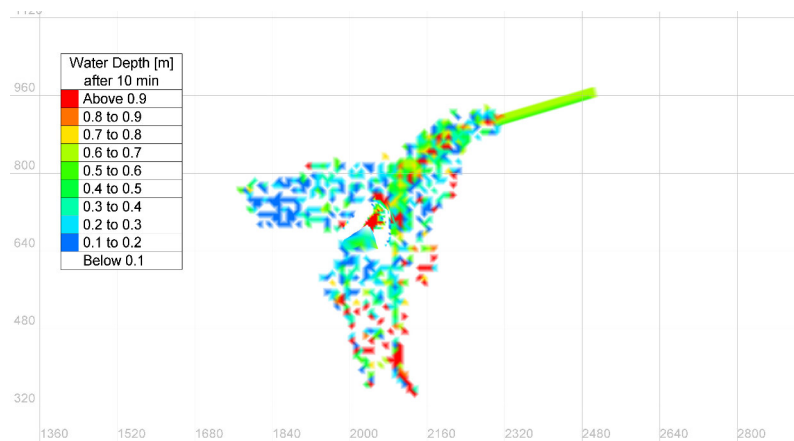
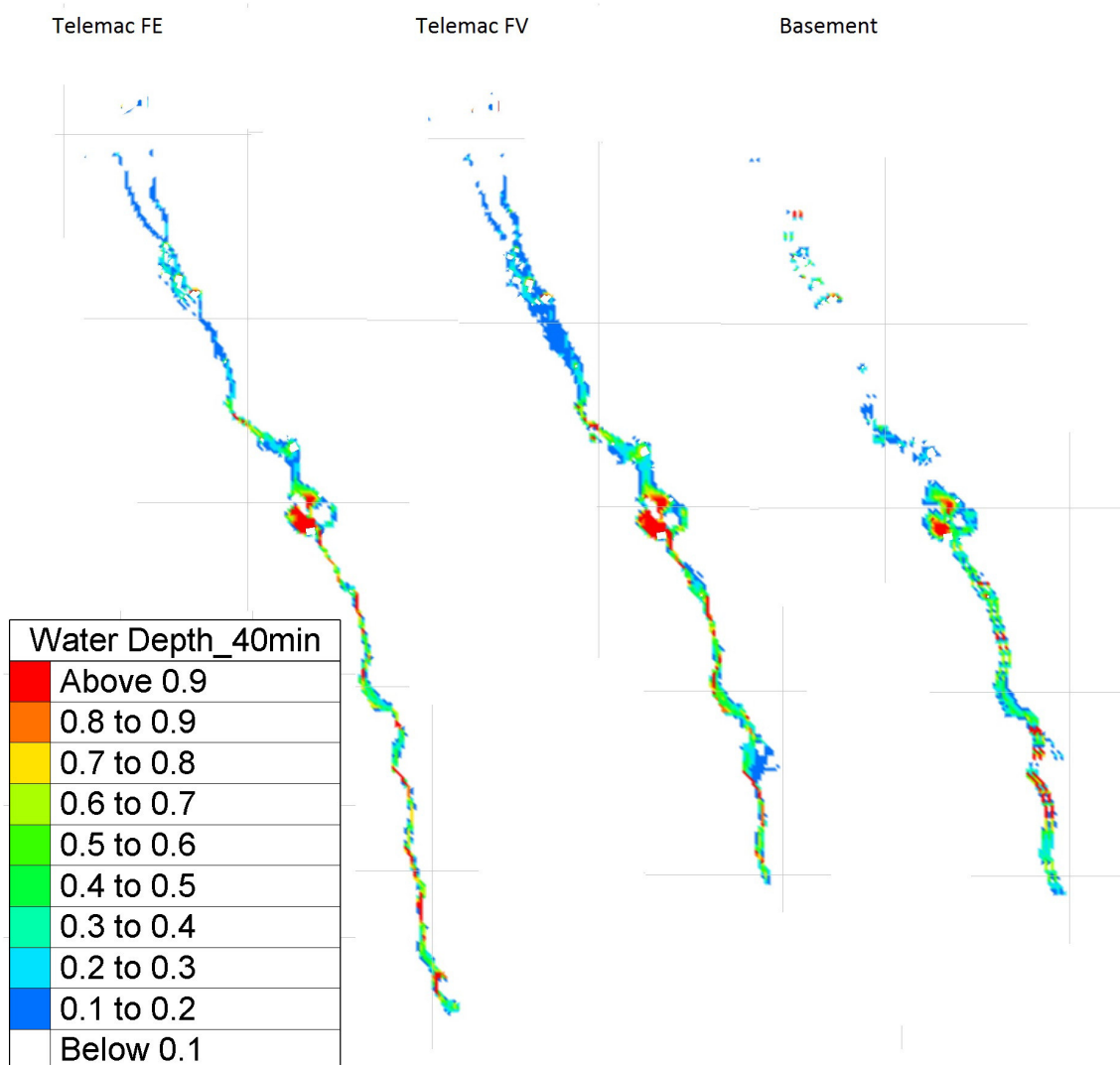


Figure 5.18: *Water Depth after 10 min, Basement, Scenario B (questionable results)*



As in the A-scenario, the water depths after ten minutes are similar in the Telemac-2D simulations and the Basement simulation. Again, the Telemac-2D FV simulation is spreading over a wider area. The start of the inflow from the second dam break is already clearly to see after ten minutes (red part in the center of each 10-min image).

Figure 5.19: *Water Depth after 40 min, Telemac-2D FE, Telemac-2D FV, Basement, Scenario B*

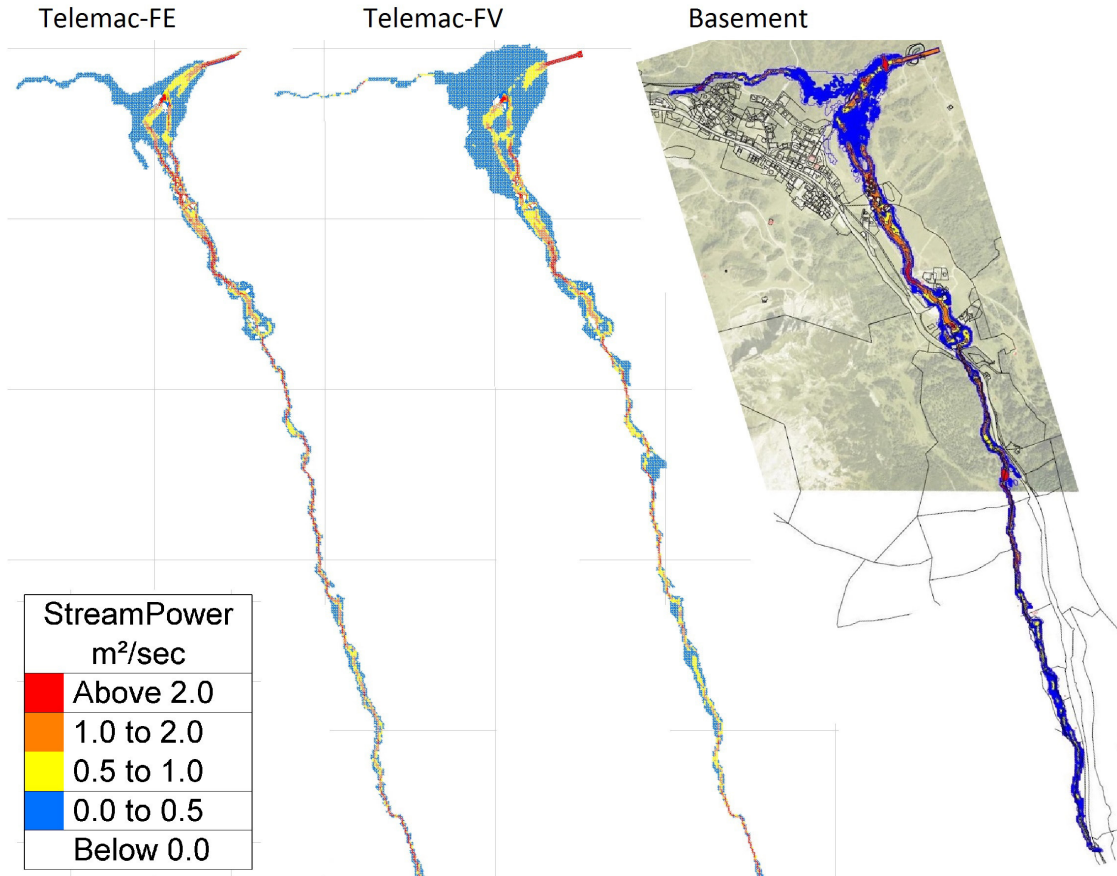


After 40 minutes, the Telemac-2D FE solution – again as in the A scenario – has a higher velocity than the FV simulations. In the Basement FV-calculation, the flood wave stays more compact on a smaller area, while in both Telemac-2D calculations the water rests longer in the flooded areas and streams away later.

5.3.2 Results from Scenario B - Stream Power

Again, the stream power is shown with FE and FV.

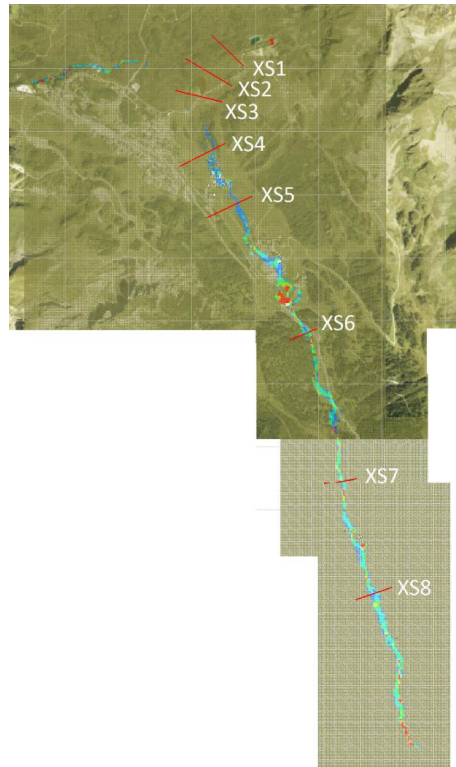
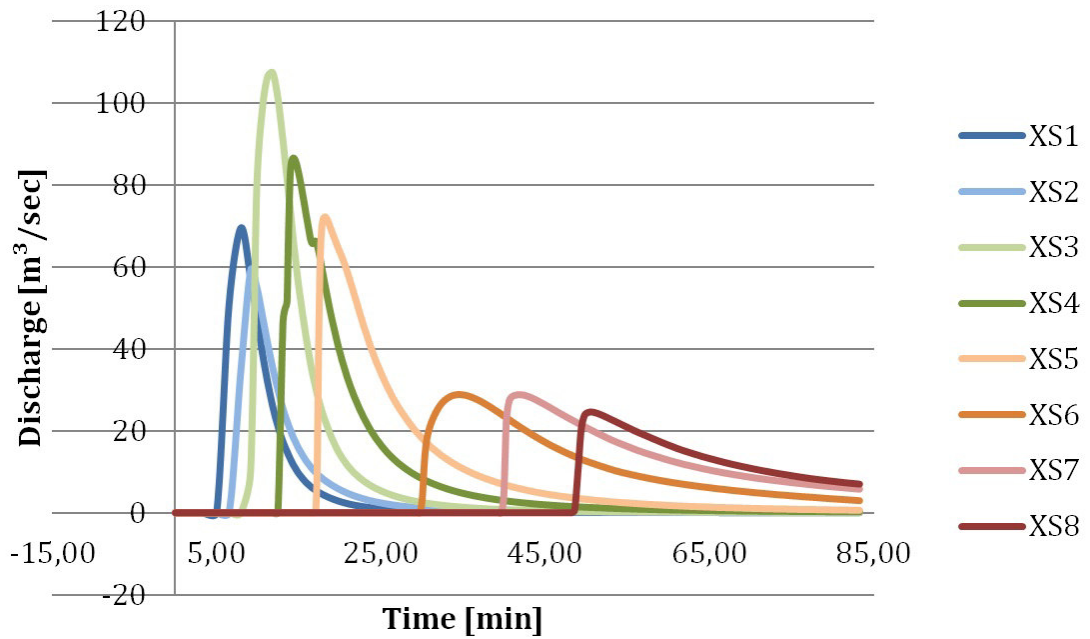
Figure 5.20: *Maximum Stream Power, Telemac-2D FE, Telemac-2D FV, Basement, Scenario B*



The wave intensity is similar in all simulations. In the Telemac-2D FV simulation, a higher stream power is calculated in the area around the inlets, due to the wider water distribution. In the lower part of the valley, the Basement calculation produces lower values, mainly less than $0.5 \text{ m}^2/\text{sec}$, while the Telemac-2D calculations show higher values between 1 and $2 \text{ m}^2/\text{sec}$.

5.3.3 Results from Scenario B - Flood Wave Evolution

To show the attenuation of the discharge-curve during the flow of the water through the valley, an integration of the discharge on different cross sections was done. Therefore, eight cross sections (XS1-XS8) were defined.

Figure 5.21: *Cross Sections for the Flood Wave Evolution***Figure 5.22:** *Flood Wave Evolution, Telemac-2D FV, Scenario B*

The curve from the breach of the storage starts to flat in XS1 and XS2, when in $t=420$ sec the secondary dam failure begins. Accordingly, the discharge curve in XS3 is higher. From XS3 to XS8, the curve flattens as it would be awaited.

5.4 Discussion of the Results

In general it has to be said, that the results from the Basement-simulation appear very similar to those done with Telemac-2D. Still, some specialities occur. In the figures shown for the time $t=40$ min, it is observable, that the water in the FE simulation is already flown farer than in both FV simulations (Telemac-2D and Basement). As no FE-simulation from Basement or any other program is present, it is not possible to say, if FE-calculations generally produce faster propagations than FV-calculations do (compare Figure 5.19).

Another observation is the, in means of the wetted area, wider spreading of the water in the Telemac-2D FV simulations after 10 min (compare Figure 5.8). Thus, regarding the before mentioned faster propagation of water through the valley in the FE-simulations, it can be said, that in FV-simulations the water is spreading over a larger area, while in FE-simulations the water propagates faster towards downstream. In other words, in FV-simulations, the water tends to spread transverse to the main flow direction, whereas in FE-simulations it tends to spread faster along the main flow direction. This development is confirmed by the stream power maps, which accord very well in other respects in all simulations.

5.5 Computation Times

Table 5.1: *Computation Times*

Scenario	FV	FE – $t_s=1$ sec	FE – $t_s=2$ sec
A	23 min	14 min	7 min
B	45 min	14 min	7 min

(All calculations were done in parallel mode with four processors. The used computer has a Intel Core i5-3320M CPU with 2.60 GHz.)

Due to the fact that the variable time step chosen by the Finite Volume Method is usually smaller than the prescribed time step in the Finite Elements Method, the duration of the calculation is significantly longer than with the FE Method. The FV-Method only requires the input of a maximum Courant number by the user, and then decides itself which time step is chosen. In the present case, a Courant number of 0.95 was defined.

The FV-Method in Telemac-2D adapts the calculation matrix every time step. If fewer nodes are wetted, the matrix is smaller. According to that, the A-scenario needs less time for computation, as the flowing area is smaller and thus a smaller

matrix has to be solved. In return, the B scenario wets more nodes and needs more time for computation.

To optimize the calculation time in the FE-method, the time step was raised to 2 sec. As awaited, the calculation time is reduced to the half, but the results are not as stable as with a time step of 1 sec. Oscillations in the water surface occur especially in the area downstream of the second inlet as well as in some lower parts of the valley. Still, the results of the water depths are very similar to those from the calculation with a time step of 1 sec in most parts and thus are still usable.

6 Summary

Although during the design, the construction and the operation of a dam project, great importance is placed on the security of the dam, a small residual risk remains, and for these infrequent situations the affected parties have to be prepared.

Many dam failures in history, accompanied with large damages and dangers for humans, caused by overtopping show, that research on the breaching process and the flood wave propagation is needed. People living downstream of a dam have to be able to live in security and therefore it is required to know, how a dam breaks and which region is affected.

One possibility of analyzing this process of a dam break is the numerical calculation by means of hydrodynamic models. For the breaching process itself, a sediment transport module has to be connected to the hydrodynamic model. In the present work, the ability of the hydroinformatics finite element and finite volume system Telemac-Mascaret was used for simulations of the breaching process and the flood wave propagation in order to compare the results with a laboratory test or computations of different programs to test the ability and accuracy of the Telemac-system. The simulation of a laboratory test case, which was originally done by Coleman et al., shows, that the calculation with Telemac-2D coupled with the sediment transport module Sisyphé achieves very accurate results. Critics of numerical simulations might say, that during such variational studies, the investigators change a simulation as long as it fits. Somehow, this might be correct, but it has to be mentioned, that every single simulation of the Coleman-case led to reasonable, realistic results. In other words, none of them was far away from reality. The variation study then showed, that the FE-method as well as the FV-method are able to approximate very close to the measured data from the laboratory case, if some parameters are adjusted and some modifications are done.

In the second part, the breaching process of a dam of a reservoir in a skiing region made for snow making, was simulated. The outflow hydrographs are presented for FE and FV, both with and without the modifications found in the first part. The comparison was done with a hydrograph produced by the engineering office “Ingenieurbüro Moser GmbH Co KG”.

Two very important modifications were tested in the simulation of the laboratory case and in the breach of the dam of the snowmaking storage, namely the modification of the Meyer-Peter-Müller formula with the approach of Wiberg and Smith (1989) as well as the variable calculation of β in Talmon’s transverse deviation

formula. Both have a significant positive influence on the results in means of an approximation towards the compared data.

Finally, in the third part, the flood wave propagation was computed with Telemac-2D FE and Telemac-2D FV for two scenarios and were compared with a simulation done by the before mentioned office with Basement. According to the water depths, all results are similar, although some specialities in the water spreading were observed.

7 Outlook

Regarding the simulation of dam breaches, further investigation should be done relating to the evolution of the cross sections, as these still do not fully agree to the measured data. The influence of a cohesion could be tested.

Furthermore, the erosion process of a non-uniform grain size distribution should be simulated and validated. During this project, the ability to compute breaching processes with uniform material was tested, but as the erosion is much more complex with mixed grain sizes, there is still a high potential of investigation.

In the B-scenario of the flood wave propagation, a secondary dam break was simulated by simply defining the influx via hydrographs at boundary conditions at every dam. Another experiment could be the combination of the simulation of the breaching process with the computation of the flood wave propagation. Thus, the water from the first dam break (with its simulated breaching process) would flow towards the second reservoir and create the secondary dam break – as in reality – by overtopping of the crest. More simulations would be necessary to find out if this chain effect can be simulated properly.

Concerning the calculation of flood wave propagations, the simulations worked well and the durations of calculation are already low. Thus, for the simulation of two-dimensional free surface flow, the possibilities are unbounded. For example, much larger regions with more complex in- and outlets could be modelled.

Bibliography

- ETH Zurich Basement. Basic Simulation Environment for computation of environmental flow and natural hazard simulation, 2014. URL <http://www.basement.ethz.ch/>.
- Bed-Load-Analyzer. BED LOAD ANALYZER- Software zur Berechnung von hydraulischen und sedimentologischen Parametern in gegliederten Querschnitten-REFERENZHANDBUCH. *Reference Manual*, Release 2.0:24–26, 2013.
- H. Chanson. EMBANKMENT OVERFLOW PROTECTION SYSTEMS AND EARTH DAM SPILLWAYS. *Dams: Impacts, Stability and Design*, pages 101–132.
- S. E. Coleman, D. P. Andrews, and M. G. Webby. Overtopping Breaching of Noncohesive Homogeneous Embankments. *JOURNAL OF HYDRAULIC ENGINEERING*, Sept-2002:829–838, 2002.
- Dr. Broich Deich. Parameter-model for calculation of outflow and breach of a dam, 2014. URL <http://www.ib-broich.de/ibb-produkt-deich.htm>.
- W. Lammerer. Sicherheit und Versagensmechanismen von Talsperren. *Diplomarbeit*, pages 1–168.
- B. Lehmann, H. H. Bernhart, and F. Nestmann. Hydraulik naturnaher Gewaesser. *Forschungsbericht FZKA-BWPLUS*, page 118.
- H. E. Minor. Numerische Modellierung von Fliessgewaessern. *Script-ETH Zurich*, 1:63–66, 2005.
- S. R. Sabbagh-Yazdi and M. Jamshidi. Depth-Averaged Hydrodynamic Model for Gradual Breaching of Embankment Dams Attributable to Overtopping Considering Suspended Sediment Transport. *JOURNAL OF HYDRAULIC ENGINEERING*, 139:580–592, 2013.
- P. E. M. Schoonen. Transverse slope effects on widely graded sediment. *Delft University of Technology*, 1:5–99, 2006.
- Sisyphé. Sisyphé v6.3 User’s Manual. *User Manual*, Release 6.3:6–26, 2014.
- A. M. Talmon, N. Struiksma, and M.C.L.M. Van Mierlo. Laboratory measurements of the direction of sediment transport on transverse alluvial-bed slopes. *Journal of Hydraulic Research*, 33:495–517, 1995.

- Telemac-2D. TELEMAC MODELLING SYSTEM-TELEMAC-2D Software-OPERATING MANUAL. *User Manual*, Release 6.2:11–15, 2013.
- P. L. Wiberg and J. D. Smith. MODEL FOR CALCULATING BED LOAD TRANSPORT OF SEDIMENT. *Journal of Hydraulic Engineering*, 115, 1989.
- J. U. Wiesemann, P. Mewis, and U. C. E. Zanke. Downslope Transport (Transverse Sediment Transport). *Third Chinese-German Joint Symposium on Coastal and Ocean Engineering*, 1:1–16, 2006.
- G. Zenz and M. Goldgruber. BENCHMARK WORKSHOP ON NUMERICAL ANALYSIS OF DAMS - Proceedings. *ICOLD proceedings*, pages 1–410.
- L. M. Zhang, Y. Xu, and J. S. Jia. *ISGSR2007 First International Symposium on Geotechnical Safety Risk*.

List of Figures

2.1	Dam Failure: Dam Types (Zhang et al.)	4
2.2	Percentages of causes for earth dam failures (Zhang et al.)	5
2.3	Subcauses of Quality Problems (Zhang et al.)	5
2.4	Example of a dam failure caused by Overtopping: Glashütte dam, Germany, 2002 (Chanson)	8
2.5	Discharges in the shallow water equations according to their direction (Minor [2005])	9
2.6	Error of the shallow water equations	10
2.7	Comparison of Sabbagh-Yazdi's results	10
2.8	Components of numerical simulations	11
2.9	Shields Diagram (Bed-Load-Analyzer [2013])	14
2.10	Forces applied on the sediment grain on a transverse sloping bed (Wiesemann et al. [2006])	15
2.11	Various calculations of Talmon's beta	17
3.1	Experimental Setup by Andrews (Coleman et al. [2002])	19
3.2	Longitudinal profiles along the developed breach channel centerline for medium sand (Coleman et al. [2002])	20
3.3	3D-View of the Mesh	21
3.4	Mesh-Detail of the Pilot Channel, 3D and Plan View	21
3.5	Free Surface at t=0 and the rigid bed (red)	25
3.6	3D-View of water surface (left) and velocities (right) after 100 sec	26
3.7	Non-coinciding area A_{error} at an example longitudinal profile	27
3.8	Results for the default hydrodynamic simulation, t=72 sec	28
3.9	Results for the default hydrodynamic simulation, t=100 sec	28

3.10	Results for FE-PSI Scheme, $t=72$ sec (Sim. A)	31
3.11	Results for FE-PSI Scheme, $t=100$ sec (Sim. A)	31
3.12	Results for FV-HLLC Scheme, $t= 72$ sec	32
3.13	Results for FV-HLLC Scheme, $t= 100$ sec	33
3.14	Comparison of hydrodynamic simulations at $t=100$ sec	34
3.15	Results for a modified friction angle of 28° , $t=72$ sec (Sim. B)	37
3.16	Results for a modified friction angle of 28° , $t=100$ sec (Sim. B)	37
3.17	Results for Koch/Talmon, $t=72$ sec (Sim. E)	38
3.18	Results for Koch/Talmon, $t=100$ sec (Sim. E)	39
3.19	Breaching process without (left) and with (right) slide effect, $t=100$ sec	39
3.20	Results for Porosity=0.3, $t=72$ sec (Sim. I)	40
3.21	Results for Porosity=0.3, $t=100$ sec (Sim. I)	41
3.22	Results for the modified MPM-formula, $t=72$ sec (Sim. H)	42
3.23	Results for the modified MPM-formula, $t=100$ sec (Sim. H)	42
3.24	Results for $\beta =0.4$, $t=72$ sec (Sim. J)	43
3.25	Results for $\beta =0.4$, $t=100$ sec (Sim. J)	44
3.26	Results for HLLC with MPMmod, $t=72$ sec (Sim. L)	45
3.27	Results for HLLC with MPMmod, $t=100$ sec (Sim. L)	45
3.28	Results for HLLC with MPMmod and beta.mod, $t=72$ sec (Sim. M)	46
3.29	Results for HLLC with MPMmod and beta.mod, $t=100$ sec (Sim. M)	47
3.30	Comparison of Sim. J, all Time Steps (FE's best)	48
3.31	Comparison of MPM versions and different beta-values at $t=100$ sec	49
3.32	Comparison of HLLC with modified Parameters, all Time Steps (Sim. M) FV's best	50
3.33	3D-View of various timesteps of the breaching process in Sim. J	51
3.34	Channel Cross Sections, $t=72$, $t=155$, $t=260$ sec (Sim. J)	52
3.35	Channel Cross Sections, $t=100$, $t=187$, $t=302$ sec (Sim. J)	52
3.36	Comparison of the discharge Q	53
4.1	Example cross section of the storage	56
4.2	Mesh of the Breach Simulation with waterline and rigid bottom level	59

4.3	Comparison of various calculations of the Dam Break Hydrograph . . .	60
4.4	3D-View of various timesteps from the modified FE-simulation	62
4.5	Velocity UV [m/s] at t=10 min	63
4.6	Froude-Number at t=10 min	63
4.7	Influence of Method and Modification on Breaching Velocity	64
5.1	3D-View of the Mesh	67
5.2	Elevation model of the region	68
5.3	Longitudinal section of the bottom elevations along the main flow directions	68
5.4	3D View of the inlet channel for Scenario A with inlet-basin at t=0 sec	69
5.5	Example of the Mesh-Structure	70
5.6	Bottom elevation and bottom friction	71
5.7	Water Depth after 10 min, Telemac-2D FE, Scenario A	73
5.8	Water Depth after 10 min, Telemac-2D FV, Scenario A	73
5.9	Water Depth after 10 min, Basement, Scenario A (questionable results)	73
5.10	Water Depth after 40 min, Telemac-2D FE, Scenario A	74
5.11	Water Depth after 40 min, Telemac-2D FV, Scenario A	74
5.12	Water Depth after 40 min, Basement, Scenario A	74
5.13	Maximum Stream Power, Telemac-2D FE, Scenario A	75
5.14	Maximum Stream Power, Telemac-2D FV, Scenario A	75
5.15	Maximum Stream Power, Basement, Scenario A	75
5.16	Water Depth after 10 min, Telemac-2D FE, Scenario B	77
5.17	Water Depth after 10 min, Telemac-2D FV, Scenario B	77
5.18	Water Depth after 10 min, Basement, Scenario B (questionable results)	77
5.19	Water Depth after 40 min, Telemac-2D FE, Telemac-2D FV, Base- ment, Scenario B	78
5.20	Maximum Stream Power, Telemac-2D FE, Telemac-2D FV, Base- ment, Scenario B	79
5.21	Cross Sections for the Flood Wave Evolution	80
5.22	Flood Wave Evolution, Telemac-2D FV, Scenario B	80

List of Tables

1	Acknowledgement	iii
2.1	Examples of embankment dam failures (Chanson)	7
3.1	Material Properties (Coleman et al. [2002])	20
3.2	Mesh Data	21
3.3	Selected parameters for hydrodynamic modelling	23
3.4	Selected parameters for sedimentologic modelling	24
3.5	Default hydrodynamic settings	26
3.6	Overview of hydrodynamic simulations	29
3.7	Chosen hydrodynamic settings	34
3.8	Default Sedimentary Parameters	35
3.9	Overview of the Sedimentary Simulations	36
3.10	A_{error} of important simulations	50
3.11	Computation Times	55
4.1	Data of the Snowmaking-Storage	57
4.2	Dam Material for the Breach Development	57
4.3	Overview of Simulations for the Dambreak-Hydrograph	60
4.4	Computation Times	65
5.1	Computation Times	81

Appendix

7.1 Laboratory Test Case Steering Files

7.1.1 *Telemac-2D CAS-file for Sim. M*

```
/-----  
/ T2D Steering file  
/ Coleman case Sim. M  
/-----  
  
PARALLEL PROCESSORS           =4  
  
COUPLING WITH                 ='SISYPHE'  
  
SISYPHE STEERING FILE        ='SIS_Coleman.cas'  
  
COUPLING PERIOD FOR SISYPHE   =1  
  
/-----  
/ INPUT-OUTPUT, FILES  
/-----  
  
BOUNDARY CONDITIONS FILE      ='BOTTOM_BC_UP_short.cli'  
  
GEOMETRY FILE                 ='ColeMesh_new_UP_short.slf'  
  
FORTRAN FILE                  ='princi_Coleman_case_effpnt.f'  
  
RESULTS FILE                  ='ColeMesh_res_FE.slf'  
  
/COMPUTATION CONTINUED       = YES  
  
/PREVIOUS COMPUTATION FILE = 'ColeMesh_res_FE.slf'  
  
/-----  
/ INPUT-OUTPUT, GRAPHICS AND LISTING  
/-----
```

```

ORIGINAL DATE OF TIME          =0;0;0 / otherwise BlueKenue 1D bug

LISTING PRINTOUT PERIOD        =200 /

VARIABLES FOR GRAPHIC PRINTOUTS = 'U,V,B,H,S,F,L' / 'U,V,B,H,S,F,L,US'

MASS-BALANCE                   =YES

GRAPHIC PRINTOUT PERIOD        =1000 / 100 fÅEr FV

/-----
/ NUMERICAL PARAMETERS - FE
/-----

FREE SURFACE GRADIENT COMPATIBILITY =0.9

TIDAL FLATS                    =YES

TREATMENT OF NEGATIVE DEPTHS    =1

MASS-LUMPING ON H              =1.0 / must for treatment of neg. depths = 2
/ faster and stabilizing but smoothens the results

TYPE OF ADVECTION              =6;5 /

SUPG OPTION                     =0;1 /upwinding, try :0;1

CONTINUITY CORRECTION          =true

TIME STEP                      =0.001

NUMBER OF TIME STEPS           =302000

TREATMENT OF THE LINEAR SYSTEM  =2

/-----
/ EQUATIONS
/-----

LAW OF BOTTOM FRICTION          =3 / 3 = Strickler      5

FRICTION COEFFICIENT           =92 / 0.0005

/TURBULENCE MODEL FOR SOLID BOUNDARIES =2 / 1 = default = smooth, 2: rough
/LAW OF FRICTION ON LATERAL BOUNDARIES =3
/ROUGHNESS COEFFICIENT OF BOUNDARIES  =120

TURBULENCE MODEL               =1 / 1 = default = const. eddy visc.

```

```
VELOCITY DIFFUSIVITY          =1.E-6 / default = 1.E-6 = laminar

/-----
/ EQUATIONS, BOUNDARY CONDITIONS
/-----

VELOCITY PROFILES             =1 / 4:  propor. to sqrt(g*h), here not relevant

PRESCRIBED ELEVATIONS         =0.3 /

INITIAL CONDITIONS : 'PARTICULAR' /like ritter case

OPTION FOR LIQUID BOUNDARIES =1

/-----
/ NUMERICAL PARAMETERS, SOLVER
/-----

SOLVER                        =1 / =7 if TREATMENT OF THE LINEAR SYSTEM = 1

/-----
/ FINITE VOLUME OPTIONS
/-----

EQUATIONS                     ='SAINT-VENANT VF'

FINITE VOLUME SCHEME          =5 / HLLC

VARIABLE TIME-STEP            =true

DURATION                      =302 / Seconds

DESIRED COURANT NUMBER        =0.95 / or smaller

/ NEWMARK TIME INTEGRATION COEFFICIENT =1.0
/ 1.0: explicit Euler, 0.5: second order in time!

/-----
/ PHYSICAL CONSTANTS
/-----

WATER DENSITY =1000. / default!
```

7.1.2 *Sisyphé CAS-file for Sim. M*

```

/-----
/ Sisyphé Steering file
/ Coleman case Sim. M
/-----

PARALLEL PROCESSORS           =4

/-----
/ INPUT-OUTPUT, FILES
/-----

BOUNDARY CONDITIONS FILE      ='BOTTOM_BC_UP_short.cli'

GEOMETRY FILE                 ='ColeMesh_new_UP_short.slf'

RESULTS FILE                  ='ColeMesh_res_SIS.slf'

/COMPUTATION CONTINUED      = YES

/PREVIOUS SEDIMENTOLOGICAL COMPUTATION FILE = 'ColeMesh_res_SIS.slf'

/-----
/ INPUT-OUTPUT, GRAPHICS AND LISTING
/-----

LISTING PRINTOUT PERIOD      =200

GRAPHIC PRINTOUT PERIOD      =1000

VARIABLES FOR GRAPHIC PRINTOUTS =
'H,S,F,B,TOB,MU' /'H,S,F,M,E,B,QSBL,1A*,QS*,R,D50,TOB,MU'

MASS-BALANCE                 =YES

/-----
/ SISYPHE NUMERICAL ALGORITHMS
/-----

MASS-BALANCE                 = YES
/ TIDAL FLATS                 = YES / = default
/ OPTION FOR THE TREATMENT OF TIDAL FLATS = 1 / = default
ZERO                         = 1e-12 / default = 1.E-6
TETA                         = 0.5 / default = 0.0 I
SOLVER ACCURACY              = 1.E-8 / default = 1.E-7
MINIMAL VALUE OF THE WATER HEIGHT = 1.E-4 / = default
MASS-LUMPING                 = YES / = default,
OPTION FOR THE TREATMENT OF NON ERODABLE BEDS = 3 / = default

```

```

/ MASS-LUMPING                                = NO / = default

/-----
/ SEDIMENTOLOGICAL PARAMETERS
/-----

NUMBER OF SIZE-CLASSES OF BED MATERIAL        = 1

SEDIMENT DENSITY                             = 2630.0

SEDIMENT DIAMETERS                           = 0.0005

INITIAL FRACTION FOR PARTICULAR SIZE CLASS   = 1.0
/ turn off if provided externally!

/ SHIELDS PARAMETERS                          = 0.047;0.03 /

/ NON COHESIVE BED POROSITY = 0.4            / = default

/-----
/ SEDIMENT TRANSPORT OPTION AND CORRECTIONS
/-----

SLOPE EFFECT                                 = YES / = default

FORMULA FOR SLOPE EFFECT                      = 2 / 1= Koch et Flokstra, 2

FORMULA FOR DEVIATION                        = 2 / 1= Koch et Flokstra, 2

PARAMETER FOR DEVIATION                      = 0.4 / 0.85= default,

BETA                                          = 1.3 / = default,

SKIN FRICTION CORRECTION                     = 1 / 1:flat bed

RATIO BETWEEN SKIN FRICTION AND MEAN DIAMETER = 3.0 /skin roughness = rati

SEDIMENT SLIDE                               = YES / =default

FRICTION ANGLE OF THE SEDIMENT               = 32.0 /

/ HIDING FACTOR FORMULA                      = 0 / =default.
/ HIDING FACTOR FOR PARTICULAR SIZE CLASS    = 1.;1.;1.;1.;1.

/ HIDING FACTOR FORMULA                      = 1 / Egiazaroff

```

```

CONSTANT ACTIVE LAYER THICKNESS          = YES / =default /NO: automatic
ACTIVE LAYER THICKNESS                   = 10000 / =default = no stratifi

/-----
/ BED LOAD TRANSPORT
/-----

BED LOAD = YES

BED-LOAD TRANSPORT FORMULA                = 1 / Meyer-Peter Mueller
MPM COEFFICIENT                           = 8.D0 / =default, Meyer-Peter M

/-----
/ SUSPENDED LOAD TRANSPORT
/-----

/ SUSPENSION = NO

```

7.2 Flood Wave Propagation Steering Files

7.2.1 *Telemac-2D CAS-file for FE, Scenario A*

```

/-----
/ T2D Steering file
/ Snowmaking Storage FE, Scenario A
/-----
/ INPUT-OUTPUT, FILES
/-----
PARALLEL PROCESSORS =4

BOUNDARY CONDITIONS FILE ='Storage_Moser_BC.cli'

LIQUID BOUNDARIES FILE ='Dambreak_Hydrograph_onlyQ.txt'

PREVIOUS COMPUTATION FILE = 'Storage.slf'

COMPUTATION CONTINUED          =YES
INITIAL TIME SET TO ZERO       =YES

GEOMETRY FILE                  ='Storage_Moser.slf'

RESULTS FILE                   ='Storage_res_FE_1sec.slf'

/-----
/ INPUT-OUTPUT, GRAPHICS AND LISTING
/-----

```

```

ORIGINAL DATE OF TIME          =0;0;0 /
LISTING PRINTOUT PERIOD       =60 /
VARIABLES FOR GRAPHIC PRINTOUTS = 'U,V,B,H,S,F,L,Q,E,M' / 'U,V,B,H,S,F,L,US'
MASS-BALANCE                  =YES
GRAPHIC PRINTOUT PERIOD       =30 /

/-----
/ NUMERICAL PARAMETERS
/-----

FREE SURFACE GRADIENT COMPATIBILITY =0.9
TIDAL FLATS                    =YES
TREATMENT OF NEGATIVE DEPTHS    =1
MASS-LUMPING ON H              =1.0 / must for treatment of neg. depths
TYPE OF ADVECTION              =1;5 /try :14;5 try 14 for dam-break fl
SUPG OPTION                    =0;1 /
CONTINUITY CORRECTION          =true
TIME STEP                      =2.0
NUMBER OF TIME STEPS           =5000
TREATMENT OF THE LINEAR SYSTEM =2

/-----
/ EQUATIONS
/-----

LAW OF BOTTOM FRICTION         =3 / 3 = Strickler
FRICTION COEFFICIENT           =92 / 0.0005

/ TURBULENCE MODEL FOR SOLID BOUNDARIES =2 / 1 = default = smooth, 2: rough
/ LAW OF FRICTION ON LATERAL BOUNDARIES =3
/ ROUGHNESS COEFFICIENT OF BOUNDARIES =120

```

```

TURBULENCE MODEL                =1 / 1 = default = const. eddy viscos

VELOCITY DIFFUSIVITY            =1.E-6 / default = 1.E-6 = laminar

/-----
/ EQUATIONS, BOUNDARY CONDITIONS
/-----

VELOCITY PROFILES                =1;4 / 4:  propor. to sqrt(g*h), here not relevan

/-----
/ NUMERICAL PARAMETERS, SOLVER
/-----

SOLVER                          =1 / =7 if TREATMENT OF THE LINEAR SYSTEM

/-----
/ PHYSICAL CONSTANTS
/-----

WATER DENSITY =1000. / default!

```

7.3 Excerpt from the Fortran Subroutines Defining the Modification of thend the Implementation of Van Rijn's Approach for Transverse Deviation

```

C Van Rijn's approach for Talmon:
  DO I=1,NPOIN
    BETA_NEW=9.0D0*(DM/MAX(HN%R(I),1.D-06))**0.3
!    implement condition to prevent overflow?
    SURBETA2=1.D0/BETA_NEW
    C = (XMVS-XMVE)*GRAV*DM*SURBETA2**2
    TT1=SQRT(C/MAX(TOB%R(I),1.D-10))
    AA=STETA%R(I)-TT1*DZFDY%R(I)
    BB=CTETA%R(I)-TT1*DZFDX%R(I)
    NORM=MAX(SQRT(AA**2+BB**2),1.D-10)
    SALFA%R(I)=AA/NORM
    CALFA%R(I)=BB/NORM

C MPM- mod by Wiberg and Smith:

  DO I=1,QSC%DIM1
    QSC%R(I)=C2*9.64D0*(TETAP%R(I))**0.166
&          *SQRT(MAX(TETAP%R(I)-ACP%R(I)*HIDING%R(I),0.D0))**3
  ENDDO

```

